AN ANALYSIS OF OPTICAL AND ELECTRON SPIN RESONANCE SPECTRA OF METAL-AMINE SOLUTIONS

Thesis for the Degree of M. S.

MICHIGAN STATE UNIVERSITY

Jay Dean Rynbrandt

1966

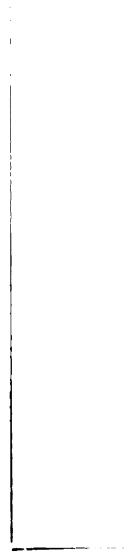

ABSTRACT

AN ANALYSIS OF OPTICAL AND ELECTRON SPIN RESONANCE SPECTRA OF METAL-AMINE SOLUTIONS.

by Jay Dean Rynbrandt

The electron spin resonance (ESR) hyperfine splitting value of potassium in ethylamine-ammonia mixtures is highly dependent upon the temperature and the ammonia content. A rapid equilibrium between two species (atoms and monomers) is proposed to explain this behavior. Using a computer program which employs an iterative procedure, the equilibrium model is shown to quantitatively describe the change in hyperfine splitting. The free energy of solution of metal atoms is calculated which, combined with the free energy of formation of the gaseous atom yields $\Delta G^{\circ} = -5.2$ kcal mole $^{-1}$ for the solvation process

$$K\ (g) \quad = \quad K\ (solv.)$$

ESR spectra resulting from overlap of a potassium four line hyperfine pattern with a broad single absorption have been separated into the contributions from each. A correlation was observed between the linewidth of the extra line and the potassium hyperfine splitting value. Two types of computer programs used in making the separation are described.

The variation of linewidth for the eight line hyperfine pattern of cesium in ethylamine is fit to a polynomial in powers of the nuclear spin quantum number, m_I. Graphs of the coefficients of a third order fit are given as a function of 1 / T for three different samples along with the program used to make the calculation. A program is also described which makes second order corrections to the field positions in ESR spectra having large hyperfine splittings.

A new variable-temperature spectrophotometer has been assembled to measure the optical spectra of solutions in ESR sample tubes. This spectrophotometer can be used over the temperature range from -150 to 30°C.

AN ANALYSIS OF OPTICAL AND ELECTRON SPIN RESONANCE SPECTRA OF METAL-AMINE SOLUTIONS.

By

Jay Dean Rynbrandt

A THESIS

Submitted to

Michigan State University

in partial fulfillment of the requirements

for the degree of

MASTER OF SCIENCE

Department of Chemistry

1966

To my Parents

ACKNOWLEDGMENTS

The author wishes to express his sincere appreciation to Professor James L. Dye for his guidance and assistance throughout the course of this investigation.

He also wishes to extend his appreciation to Mr. Russell Geyer for his advice and to a colleague, Mr. Larry R. Dalton for his assistance in the experimental work.

Financial aid from the Atomic Energy Commission is gratefully acknowledged.

****

TABLE OF CONTENTS

TABLE OF CONTENTS - Continued

LIST OF TABLES

LIST OF FIGURES

I. INTRODUCTION

The behavior of metal solutions is not easily explained. Their blue color has intrigued workers since 1864, when Weyl discovered that alkali metals dissolve in ammonia (1). Progress has been made in identifying the source of this color, but even today there is considerable difference of opinion regarding the structure of these solutions. The possibility that a species, very similar to that found in metal ammonia solutions, is an important agent of radiation damage to biological systems (2), has provided a new impetus for the explanation of metal solutions.

The optical and electron spin resonance spectra of metal-ammonia solutions are deceivingly simple: a single absorption occurs in each case (47,48). However when alkyl amines are added to these systems, both spectra become more complicated. Two additional optical bands begin to appear, until, in solutions of high amine content, three separate absorption bands are present. The ESR spectrum of metal-amine solutions also becomes more complex, with at least two different species being detected.

It now seems that no ESR signal is intense enough to be solely responsible for any of the optical absorption bands. However, because all species in the solution interact with each other, optical and ESR measurements are interrelated and correlations between them should be valuable. With the spectrophotometer described in this thesis, optical

and ESR measurements can be made on the same sample under similar experimental conditions.

As the description of metal solutions becomes more quantitative, more exact and extensive date are required. Often these new data cannot be obtained directly from either the optical or ESR spectra and must be calculated by separating the factors contributing to a spectrum or by considering trends among large quantities of data. Another part of this thesis describes some techniques developed to use high speed computers for solving these problems.

II. HISTORICAL

The first quantitative information about metal-ammonia solutions came from the conductance studies of Kraus (3). He proposed that the solvation process involved the separation of an electron from the metal (4-6), according to

$$M = M^+ + e^- . \qquad (1)$$

The state of the electron was described by an equilibrium between free and solvated species (7). Gibson and Argo, on the basis of spectral studies, concluded that few free electrons existed and extended their work to amines by obtaining optical spectra of solutions of metals in methylamine as well as in ammonia. Although these studies were limited to the visible region, they were able to differentiate between the visible band, V, at 650 mu and the tail of the infrared band, IR, seen in ammonia solution (8). The V band was attributed to undissociated metal atoms, M (8). It is now clear that these early proposals do not adequately explain the behavior of metal solutions.

The range of wavelengths investigated and the variety of solvents used have since been extended. The maximum in the IR band occurs in ammonia at 1400-1500 mu and an intermediate red (R) band is also observed for potassium, rubidium and cesium with a maximum at 910 to 1040 mu depending upon the metal and temperature. A summary of metal-amine optical results is given in Table I. The similarity in the behavior of a given band for the different alkali metals strongly suggests that it is due to the same type of chemical species (9,10). For this reason the chemistry of the three species will be first considered individually with an

Table I. Absorption Maxima of Metals in Amine Solvents.

Solvent	Metal	Temperature °C	Absorption Max. mμ	Absorbance	Cell Path Length mm	Reference
NH_3	Li	-70	1500	2.43	0.1	(11)
	Na	-62	1470	2.57	1.0	(11)
	K	-71	1480		0.1	(11)
	Cs		1500			(51)
CH_3NH_3	Li	-55	1320	0.73	0.1	(11)
	Na	-40	650[a]			(8)
	Na	-30	650	0.45	1.0	(11)
	Na		690			(12)
+20%NH_3	Na		690[b] 1320			(12)
+40%NH_3	Na		1250			(12)
	K	-67	660 800		1.0	(11)
	K		650[a]			(8)
	Cs		650[a]			(8)
	Ca	-60	1280	0.8	0.1	(8)
$CH_3CH_2NH_2$	Li	-40	1420	2.14	0.1	(11)
	Li	RT	1300 700	1.3	0.2	(10)
	Na		680			(12)
+30%NH_3	Na		700 1300			(12)
+50%NH_3	Na		1250			(12)

Table I. Continued.

Solvent	Metal	Temperature °C	Absorption Max. mμ	Absorbance	Cell Path Length mm	Reference
$CH_3CH_2NH_2$	K	-64	650	1.66		(11)
	K	RT	675	1.2	10	(10)
	Rb	RT	930 630	1.6	10	(10)
	Rb	-80	650[c]		10	(10)
	Cs	RT	1040 710 1300	0.8	10	(10)
	Cs	-80	675[c] 940			(10)
$NH_2(CH_2)_2NH_2$	Li	RT	660 1280	0.9 1.2		(13)
	Na	RT	660 1280	2.0 0.03		(13)
	Na	RT	670[d]			(14)
	Na		650	1.5	1.0	(15)
	K	RT	845 650 1300		0.1	(13)
	K	RT	660 840 1300		1.0	(13)
	K		670[d]			(14)
	K		650 800[c]	1.0 0.8	0.1	(15)
	Rb	RT	890 1280 650[e]	1.0 0.5		(13)

Table I. Continued.

Solvent	Metal	Temperature °C	Absorption Max. mμ	Absorbance	Cell Path Length mm	Reference
$NH_2(CH_2)_2NH_2$	Rb		700 900	1.3 1.5	0.1	(15)
	Rb		700[f] 900	0.7 0.4	0.1	(15)
	Cs	RT	1030 1250	1.35	0.1	(13)
	Cs	RT	1280[f]		0.1	(13)
$NH_2CH(Me)CH_2NH_2$	Na	RT	600[d]			(14)
	K	RT	670[d] 870			(14) (14)

[a] Limited to visible region

[b] Absorption maxima listed in order of decreasing magnitude unless otherwise noted

[c] Samples diluted by decomposition

[d] Limited to below 1000 mμ

[e] Seen only after some decomposition

[f] After some decomposition

emphasis on the trends among the various metals and solvents.

1. The IR band. This is the only optical absorption seen in metal-ammonia and metal-deuteroammonia solution (16). This absorption has been shown to obey Beer's law (17-19) and to have a temperature dependence of $-14.3 cm^{-1} deg^{-1}$ (16) in deuteroammonia and a slightly lower value in ammonia (18,11,20). However Burrow and Lagowski point out that ammonia possesses an intense absorption band at 1532 mμ which may cause the ammonia results to be somewhat ambiguous (16).

An IR absorbing species is produced when pure ammonia, ethylamine, propylamine, ethylenediamine and 1,3 propanediamine are exposed to short pulses of high energy electrons (21). This IR absorption in ethylenediamine has the same shape in the region studied as the IR band for metal solutions in this solvent (22,13). When fresh or faded metal solutions in ethylamine were flashed with pulses of high intensity light, an immediate increase of the IR absorption was noted (23,24,10).

The IR band tends to become more predominant relative to the V and R band absorptions in better solvents for ionic species. The ESR hyperfine splitting appears to correlate with solubility in the larger alkyl amines showing the greatest hyperfine splitting, lowest IR absorption, and lowest solubility (25-27). The metal used also affects the relative size of the IR band. It is predominant in fresh lithium solutions and becomes less predominant as the metal solubility decreases in the order Li > Cs > Rb > K > Na. Dewald's work with cesium and lithium in ethylenediamine indicated that the cesium IR band decomposes more slowly than the R band, and that the lithium IR band is less stable than the V band (22,13).

The IR absorption band is attributed to the solvated electron. ESR results indicate that in fresh, saturated solutions of the larger alkyl amines the electrons probably exist primarily as the paired species (28,29). A possible pairing reaction is

$$2e^- = e_2^{--} . \qquad (2)$$

The low dielectric constants of the amines would also tend to favor ion pairing of the electrons with metal cations (9) according to

$$e_2^{--} + 2M^+ = M^+ . e_2^{--} + M^+ = M^+ . e_2^{--} . M^+ . \qquad (3)$$

Alternatively, the paired species might exist as ion triples and quadrupoles. The presence of different absorption bands indicates that the electrons can also interact in other ways with the metal to give rise to species not present in ammonia.

2. The R band. This absorption is observed only in amine solutions of potassium, rubidium and cesium. The absorption maxima for these metals in ethylenediamine at room temperature occur at 840, 890 and 1020 mμ respectively and at 910, 930 and 1040 mμ in ethylamine (22,10). The similarity in temperature dependence of the band maximum, $-11.3\ cm^{-1}\ deg^{-1}$ for cesium and rubidium in ethylamine supports assignment of the R band to the same chemical species for the different metals (10,9). It is generally agreed that this species is dimeric (9,10). The peak positions of potassium, rubidium and cesium in ethylenediame correlate well with the intense $^1\Sigma_u \leftarrow {}^1\Sigma_g$ transitions of gaseous dimers listed in Herzberg (30,9). However the potassium R band absorption in ethylenediamine occurs

at a higher energy (840 mμ at room temperature) than the dimer transition in the gas phase (860 mμ) (30,9). Solvation would be expected to lower the energy of this transition. The position of maximum absorption shifts to even higher energies as the temperature is lowered (10). Work in this laboratory (31), indicates that the absorption should probably be assigned to the $^1\pi \leftarrow {}^1\Sigma_g$ transition. In the gas phase dimers, this is a comparatively narrow absorption occurring near 660 mμ in rubidium and 770 mμ in cesium. This absorption is presumed to broaden and shift to longer wavelengths as a result of solvation.

Dye and Dewald, using thermodynamic arguments, have predicted the concentrations of metal dimers in ethylenediamine using the rubidium concentration and absorbance as a standard (9). These calculations agree well with the observed absorbances and indicate that lithium and sodium solutions should have no R band absorption, in agreement with experiment. Less polar amines seem to favor this band. It is also more predominant at high metal concentrations. The cesium R species sppears to be the least stable of those giving optical absorption; in decomposing cesium solutions in ethylenediamine, this band decays most rapidly (13).

3. The V band. The behavior of this band (650-750 mμ) is somewhat paradoxical. Its presence or absence is dependent upon the metal used but the position of its maximum absorbance is only slightly - if at all - metal dependent. It is not observed in metal-ammonia spectra but is more prominent in strongly solvating amines than in the less polar amines. When compared to the relative intensity of the R band, the V band is favored by low temperatures and by dilute solutions where these tests have been made (13,22,10). Under similar conditions, the lighter alkali metals

favor the V band in comparison with the R band.

Tuttle and co-workers found that in decomposing solution, the ratio of the square of the V band absorption to that of the R band was constant for solutions of both potassium and rubidium in ethylamine (32,24). The relative intensities of the V and R band were not however, reproduced in regenerated solutions (32). A graph of log absorbance at 650 mμ versus the log absorbance at 850 mμ for the data of Tuttle and co-workers showed a slope slightly greater than 1/2. Data obtained in this laboratory, when plotted on the same graph, had a slope of nearly one (25,29). The non-reproducibility of the decomposition data indicates mainly that these results are not good criteria on which to base proposed models. The qualitative dilution observations remain useful however. A correlation between the V band optical absorption and the ESR signal in a decomposing potassium ethylamine solution, along with other ESR studies in mixtures of amines and the optical decomposition results, have led Tuttle and co-workers to conclude that this absorption is due to a Becker-Lindquist-Adler monomer (33,32,28). In this laboratory, using reference standards of known spin concentration, it has been shown that there is no correlation between the number of spins in the potassium hyperfine pattern and the V band optical absorption (25,29).

4. Interconversion studies. Studies of the interconversion of different optically absorbing species have given interesting results. The absorptions at 660 mμ and at 1280 mμ in lithium ethylenediamine solutions decayed at different rates (13). The IR absorption decayed more rapidly

and, when it had disappeared, the decay rate of the V band increased (22,13). The decomposition rate of the sum of the V and IR band absorbances was continuous implying that the IR absorbing species acts as a buffering agent for the V species (13). In another study, a lithium ethylenediamine solution showing only V band absorption was removed from contact with its decomposition products. The V band continued to decay but as it did an IR absorption slowly built up and finally both peaks decayed (22,13). The slow interconversion of the lithium V and IR bands implied the breaking of a covalent bond. On this basis, an $M_2^+.e^-$, molecule-ion was proposed as the V species (9).

Recent flash photolysis studies by Linschitz and co-workers (10,24,23) of metal-ethylamine solutions over a range of temperatures and concentrations seem pertinent to the understanding of the interconversion of the V, R and IR bands. Briefly these investigators flashed the solutions with light of known wavelength and then observed the change in absorbance at various wavelengths as a function of time. Flashing at wavelengths below 480 mμ initially gave rise to an increased absorbance in the IR region and a bleaching of both the V and R bands. Following photobleaching of the V band, a rapid second order build-up of the R species was noted. No absorbance was observed in the region scanned (410-1000 mμ) whose decrease matched the rapid build-up of the R absorbance. The increased IR absorption from this flash decayed at about the same first order rate as a second, slower, first order build-up of the R band noted in cesium solutions. The R species then decayed in a first order reaction to give the V species. The rate constant of the first order build-up of the V band (except for a fast initial build-up amounting to 10% of the total

recovery) is the same as that of the R band decay. The IR species obtained when the R band in rubidium solutions was flashed behaved differently from that resulting from flash photolysis of the V band. This IR species decays in a rapid second order process which matches the build-up of the R band, implying that the two IR species undergo different reactions as the system returns to equilibrium (10).

III. EXPERIMENTAL AND RESULTS

A. Optical and Electron Spin Resonance Spectra.

Many data have recently been obtained in this laboratory from ESR and optical studies of potassium solutions in ethylamine-ammonia mixtures and from similar studies on other metal-amine systems. In order to extract additional information from these data and to process data in different ways, computer techniques were required. This section provides a background for the theories and methods used in these calculations. While the author has participated in all phases of solution preparation, and in some of the measurements, this thesis deals primarily with the treatment of the ESR and optical spectra. In addition, the construction of a new spectrophotometer is described. Earlier publications have described in detail the preparation of the solutions used (34,13,29).

1. Optical spectra of potassium solutions in ethylamine-ammonia mixtures. These spectra are strongly dependent upon the ammonia concentration. In agreement with the observation of Kraus (35) potassium formed no blue solution in high purity ethylamine. At ammonia concentrations up to 4.5 mole percent, the V band is predominant with a temperature shift of $-11\ cm^{-1}\ deg^{-1}$. At higher temperatures and 7 to 14 mole percent ammonia, all three absorption bands were observed. The IR band is present in all solutions in this concentration range and the ratio of R to V band absorption was very temperature dependent, again favoring the R band at higher temperatures. For example, at 15 mole percent ammonia and 25°C the

visible absorption appeared only as a shoulder on an intense R absorption and the solution showed strong IR absorption. However, at -38°C and below, the V band was the strongest absorption, the R band was not observed and only a small IR absorption was apparent. For the same temperatures, the position of the V band shifted to longer wavelengths with increased ammonia concentration. Comparing the sample containing 4.5% ammonia with that containing 9.9% ammonia, this change was approximately 400 cm^{-1}. The IR band became more predominant with higher ammonia content until in a sample containing 32.5% ammonia, both the V and R bands were absent (29).

2. ESR studies of metal-amine solutions. These studies have produced much new information pertaining to these systems. Metal-ammonia solutions show only a single narrow ESR absorption. Most metal-amine solutions however give hyperfine splitting. Hyperfine splitting of an electron by a nucleus is related to the fraction of the time the electron spends at this nucleus. The change in hyperfine splitting with temperature and solvent composition provides valuable information regarding the nature of the hyperfine species. ESR linewidths, g values and spin concentrations are also useful because they relate respectively to the relaxation time, the orbital angular momentum and the concentration of the unpaired electrons in question. Some ESR spectra of metal-amine solutions indicate that two or more species with unpaired electrons are simultaneously present in the solutions (29,36).

The structure of the hyperfine pattern observed in lithium-ethylamine solutions is different from that seen for the other metals in this solvent. At room temperature a single ESR absorption is seen which at

-40°C converts to a nine line pattern with peak intensities suggesting splitting by four nitrogen nuclei (I = 1) (37,27). This pattern becomes clearer as the temperature is lowered and is well resolved at the freezing point of the solvent. Below the freezing point the nine line pattern converts back to a single absorption (27). This nitrogen splitting in lithium solutions was first observed by Tuttle (28), but the low signal-to-noise ratio made it advisable to confirm this observation. In all other metal-amine solutions showing hyperfine structure, the splitting is attributed to a metal nucleus.

Potassium solutions have been most extensively studied, particularly solutions of potassium in ethylamine-ammonia mixtures. At room temperature, fresh potassium-ethylamine solutions with low ammonia content give a well-resolved four line potassium hyperfine splitting pattern as seen in Figure 1. This observation was first reported by Tuttle and has since been confirmed by other investigators (28,29). The hyperfine splitting value decreases markedly with increased ammonia concentration as illustrated in Figures 2 and 3. A striking change in hyperfine splitting also resulted from changes in the temperature of given samples. Between -60°C and 20°C the hyperfine splitting increased moderately with temperature but above 40°C the temperature dependence of the hyperfine splitting changed markedly as shown in Figure 4. Extrapolation of log contact density versus 1/T to infinite temperature gives a value close to that of the free atom (29). By considering the hyperfine splitting to arise from a rapid equilibrium between a species with the magnetic properties of free atoms and one or more species having a lifetime greater than the rotation time of a solvent molecule, the temperature and ammonia dependence of the hyperfine splitting

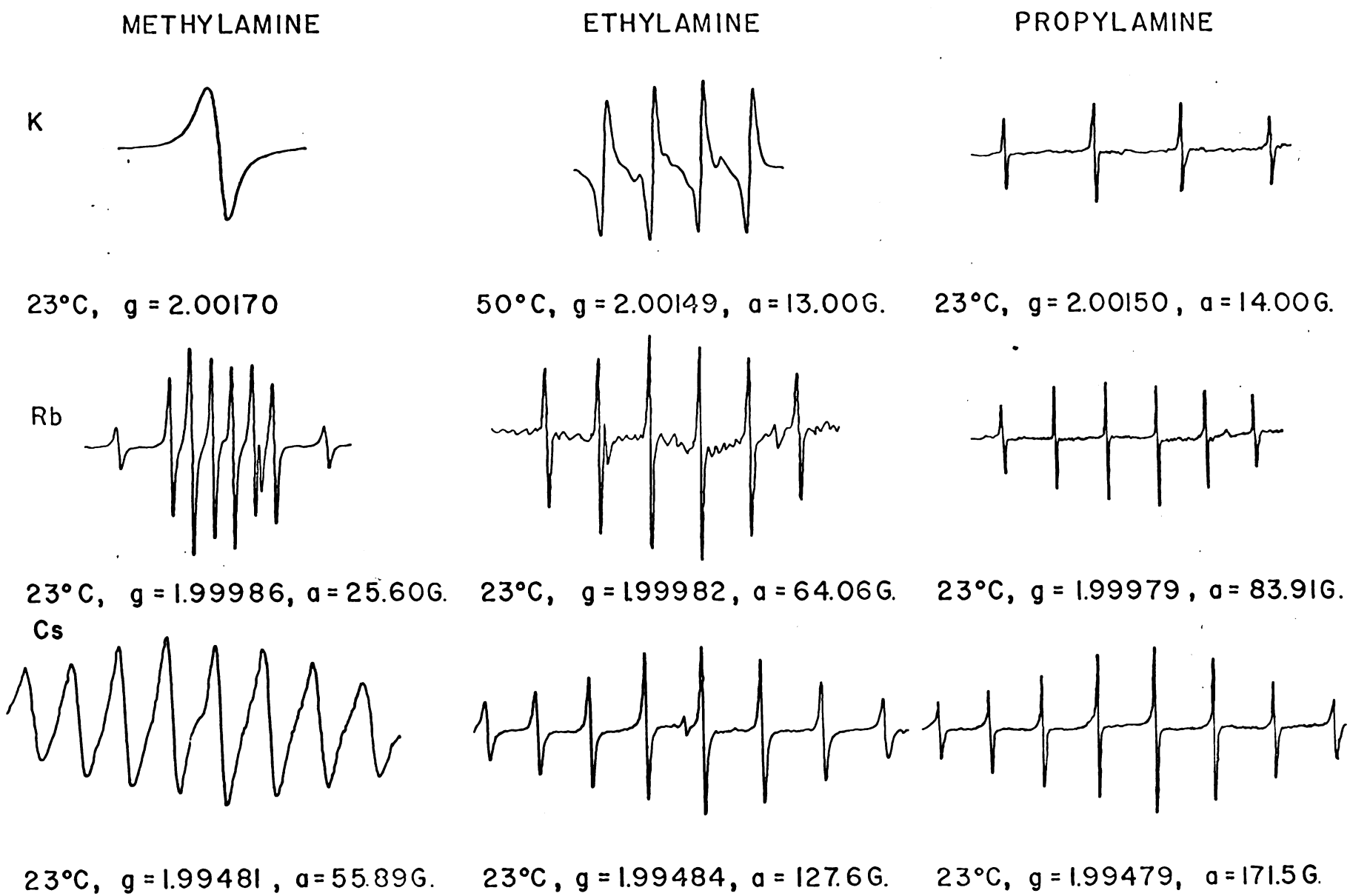

Figure 1. ESR spectra of alkali metals in some amines; data given are for ^{39}K, ^{85}Rb and ^{131}Cs.

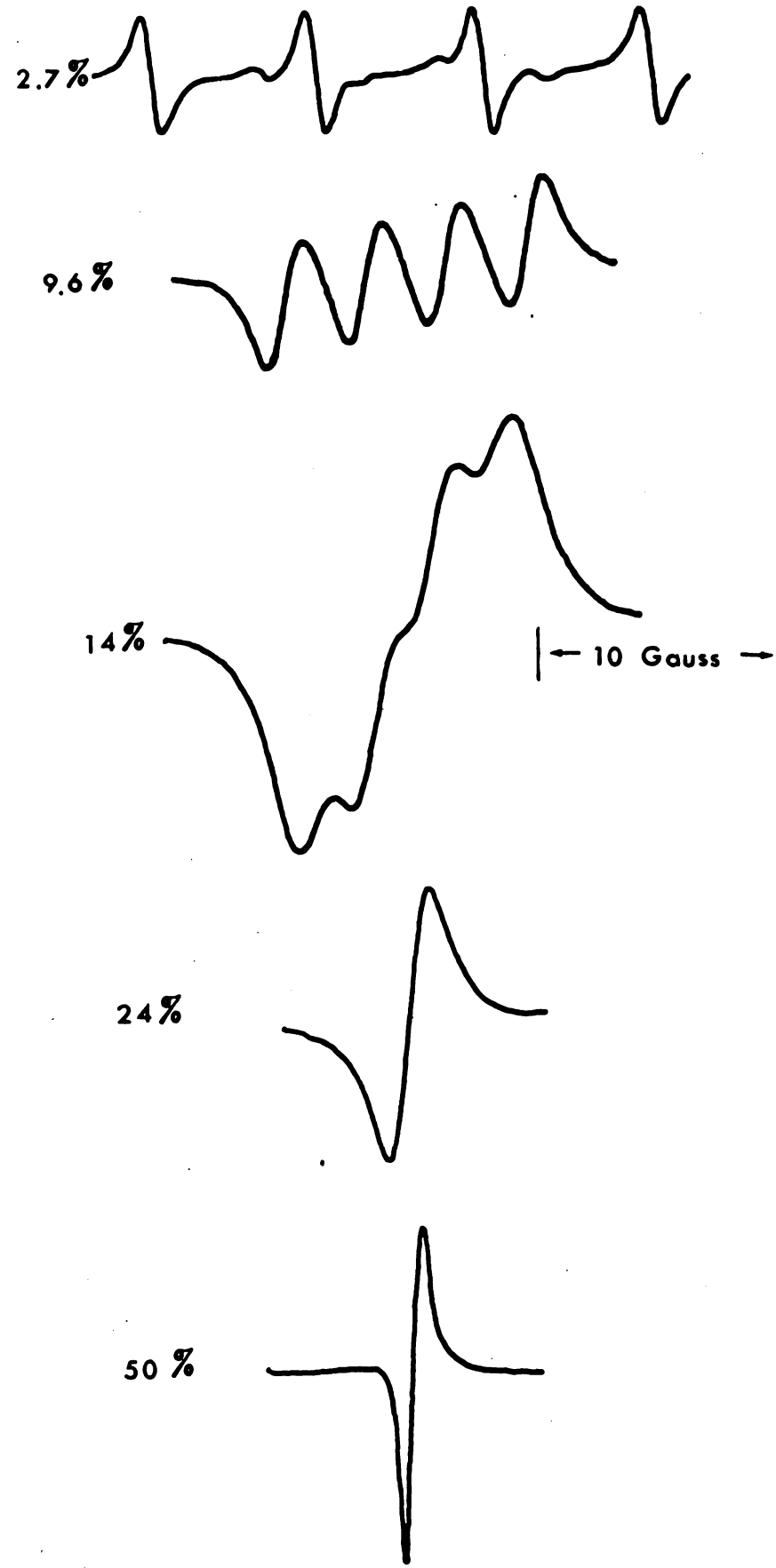

Figure 2. Qualitative ammonia dependence of the ESR spectra.

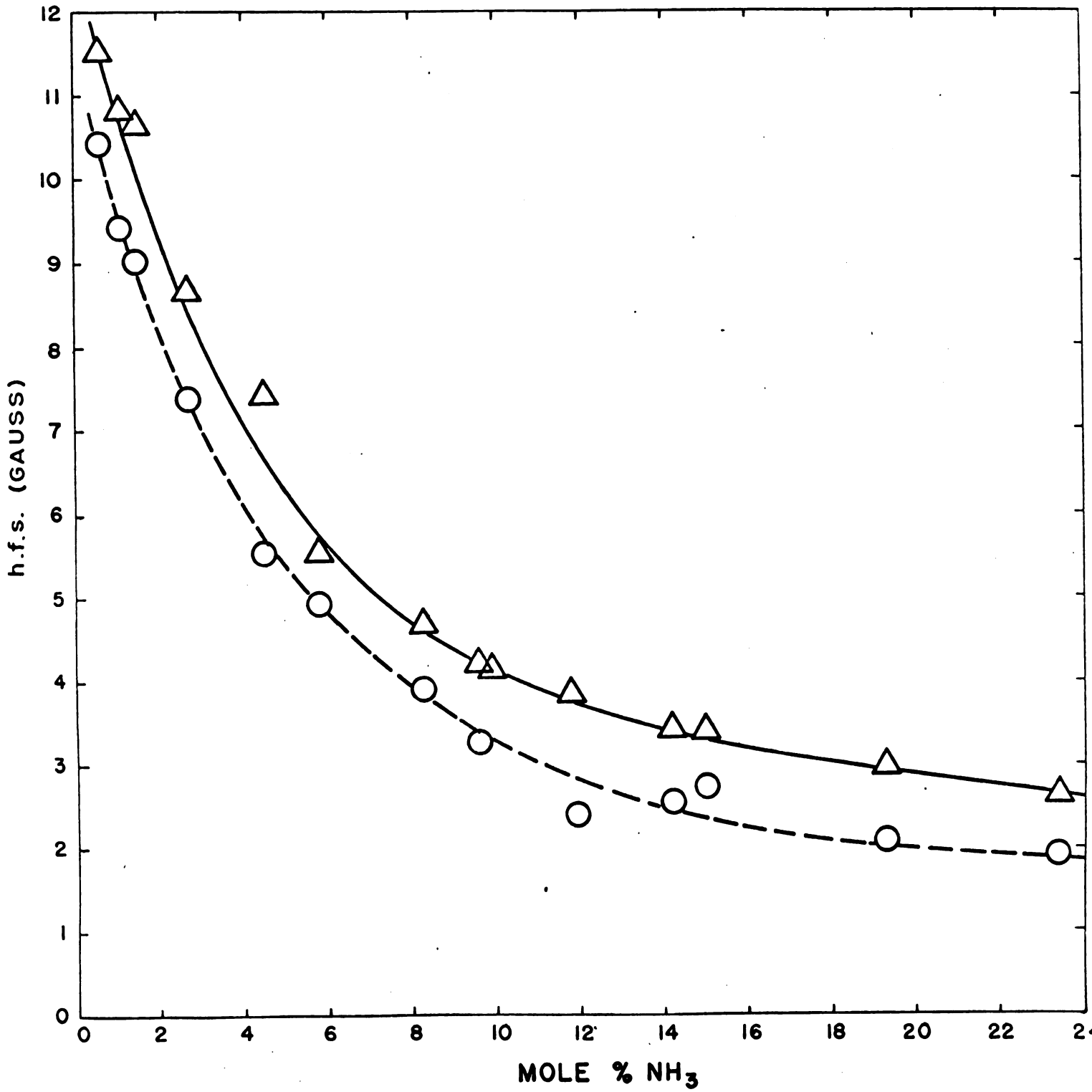

Figure 3. Dependence of the hyperfine splitting upon ammonia concentration. Triangles are for a temperature of 25°C; circles, for -40°C.

Figure 4. Temperature dependence of the hyperfine splitting.
, 1.2; , 2.7; , 5.8; , 9.6 mole % ammonia.

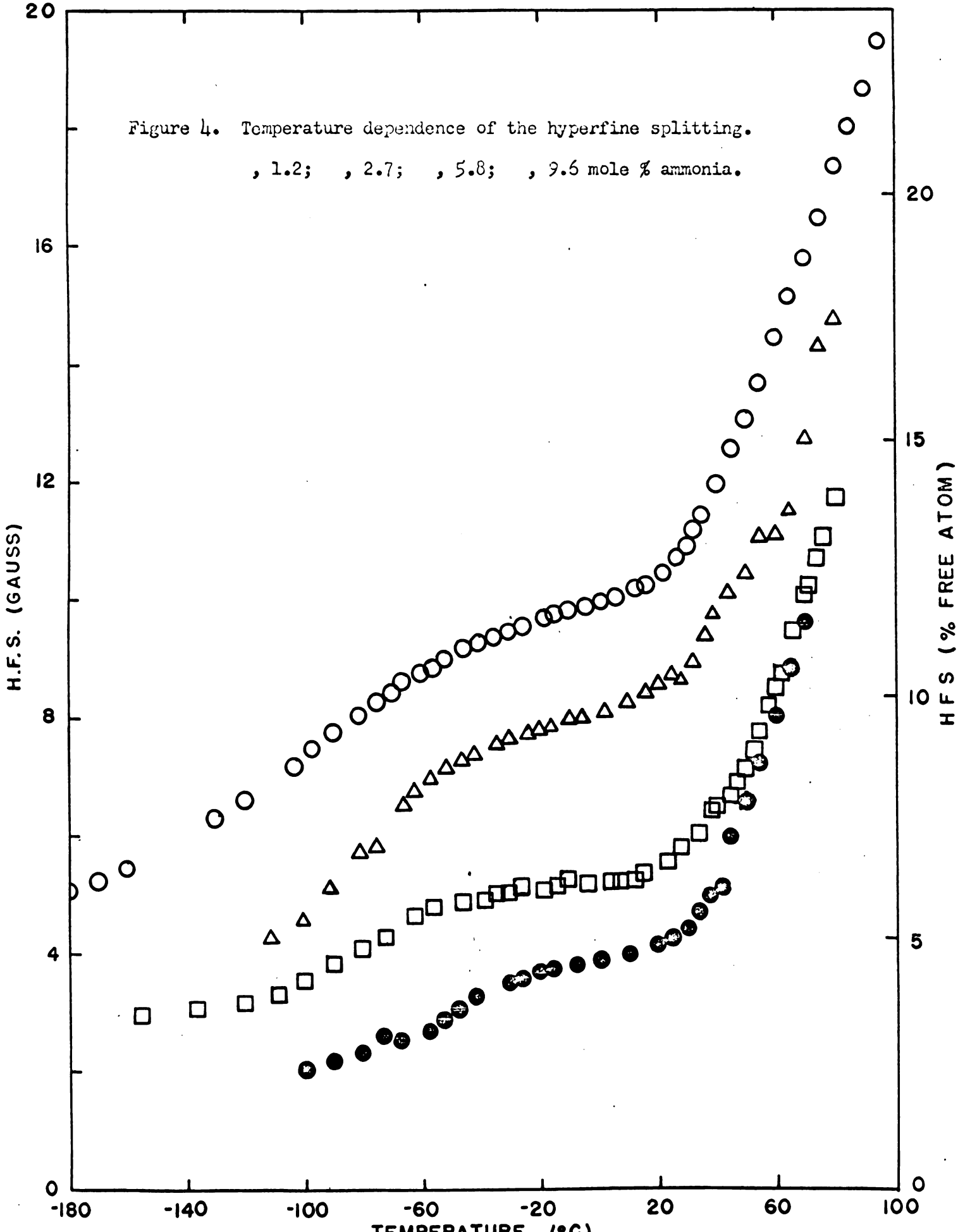

could be quantitatively described. The program used to separate the contributions to hyperfine splitting from an atom and monomer is described later.

Along with the four line potassium hyperfine splitting pattern, at least one additional single line absorption was noted. In older potassium solutions with low ammonia concentration, the single line was quite narrow, centered near the free electron g value and related to the degree of decomposition. Symons and co-workers have observed an extra absorption in unsaturated solutions. The absorption of the species they describe correlates with the intensity of the four line species and implies the equilibrium (36)

$$M = M^+ + e^- . \qquad (4)$$

This may well be the same species observed in this laboratory in saturated solutions of higher ammonia content. In solutions with 9.6 to 14.2 mole percent ammonia, a broad extra line was observed underlying the four line hyperfine pattern (29). Two programs, (ESR FT and GEN LS), were written to separate the observed spectra into contributions from the ^{39}K and ^{41}K hyperfine patterns and these from a broad single absorption. These programs are described later in this section. At 33 mole percent ammonia, the hyperfine structure is no longer discernable.

ESR spectra of rubidium-amine solutions are a superposition of hyperfine patterns from ^{85}Rb and ^{87}Rb as can be seen in Figure 1. A narrow single absorption was also noted in these solutions. The hyperfine splitting in many Rb amine solutions was large enough to warrant performing second and third order corrections in order to obtain the g value and hyperfine splitting more accurately.

Amine solutions of cesium have the largest ESR hyperfine splitting and therefore also require second order corrections. As will be noted in Figure 1, the linewidth of the eight line cesium hyperfine pattern shows marked dependence upon the nuclear spin, m_I (26). Recent results in this laboratory indicate that the variation of linewidth with nuclear spin is greater in 1, 2 propanediamine than in ethylamine whereas the hyperfine splitting value is smaller in 1, 2 propanediamine than in ethylamine (27). An explanation and treatment of the variation of linewidth is described later in this section. In addition to the hyperfine pattern, a single line was noted with a g value near that of the free electron. The magnitude of this line seemed related to the degree of decomposition as in the potassium solutions.

B. Programs and Results.

All programs described in this section were written in Fortran 3600 for use with the Michigan State University Control Data 3600 computer.

1. Program A M EQ. This program was used to separate the hyperfine splitting of potassium ethylamine-ammonia solutions into contributions from the atom, A, and two solvated monomeric species, B and C, which are considered to be M $(EtNH_2)_x$ and M $(EtNH_2)_{x-1}(NH_3)$. The following scheme describes the equilibra involved:

$$A = B \qquad K_a = (B)/(A) \tag{5}$$

$$B + NH_3 = C + EtNH_2$$

$$K_1^{(c)} = ((C) / (B))((1 - X) / X).$$

in which X is the mole fraction of ammonia. The measured hyperfine splitting

A_F is related to the concentration of these species and their respective splittings by

$$A_F = (n_A A_A^\circ + n_B A_B^\circ + n_C A_C^\circ) / n \qquad (6)$$

in which $n = n_A + n_B + n_C$.

If the solutions are assumed to be saturated, the concentration of atoms would be expected to vary according to

$$\ln (A) = \frac{-\Delta H^\circ}{RT} + \frac{\Delta S^\circ}{R} \qquad (7)$$

in which ΔH° and ΔS° are the molar enthalpy and molar entropy of solution of the metal to give atoms. The strong dependence of A_F upon temperature above 40°C indicates that the temperature variation of atom concentration is much greater than that of the other two species. This permits an approximate separation of the splitting due to atoms from that due to the species B and C by extrapolation of the low temperature behavior. The separation is accomplished by using the approximation

$$n_A^\circ = n (A_F^\circ - A_M^\circ) / (A_A^\circ - A_M^\circ) , \qquad (8)$$

in which A_M° represents the splitting expected to be observed in the absence of atoms and includes the contributions from species B and C

$$A_M^\circ = (n_B A_B^\circ + n_C A_C^\circ) / (n_B + n_C) . \qquad (9)$$

A_M° was obtained for the low temperature region by calculating a least squares line through the A_F values as a function of temperature assuming no contribution from atoms to the observed splitting. The high temperature

value of A_M° was then estimated from a linear extrapolation into this region. Using n_A calculated from Equation (3) as a measure of the concentration of atoms, a least squares line was calculated through a plot of ln (n_A) vs. 1 / T to evaluate ΔH° and ΔS° in Equation (7) with a standard state of one mole per liter. The points on this line were weighted to place greater emphasis on those for higher temperature which are less affected by errors resulting from the extrapolation of A_M° into this region. The atom concentrations in the low temperature region were then calculated from the extrapolation of the high temperature ln (n_A) vs. 1 / T plot. These calculated atom concentrations were then combined with the experimental splitting to give new values of A_M° using the expression

$$A_M^\circ = (nA_F - n_A A_A) / (n - n_A) \qquad (10)$$

in the low temperature region. These new values of A_M° were extrapolated into the high temperature region and new values of n_A were calculated. This procedure was repeated five times to give consistent results. These results are reported in Table II. Calculated and experimental splittings are compared in Figure 5a for a 2.7 mole percent ammonia solution.

It is seen from Table III that the value of ΔG° is reasonably independent of ammonia concentration as are ΔH° and ΔS° at lower concentrations. This lends support to the treatment used, especially in light of the large variation of A_F and n with ammonia concentration. The average value of ΔG°, combined with the free energy of formation of the gaseous atom yields $\Delta G^\circ = -5.2$ kcal mole^{-1} for the solvation process

$$K\ (g) = K\ (\text{solution}) \qquad (11)$$

Table II. Least-Squares Slopes and Intercepts from Computer Analysis of Atom-Monomer Equilibria.

Mole percent ammonia	Monomer[a] slope	Monomer[a] intercept	Atom[b] slope	Atom[b] intercept
1.2	0.00277	9.5337	-4192.3	42.940
2.7	0.00765	7.7905	-4928.2	45.079
5.8	-0.00042	4.9918	-4601.9	44.224
9.6	0.00538	3.7188	-6512.4	50.663
11.8	0.01093	2.8433	-7326.3	54.285
14.2	0.00709	3.0427	-7607.6	55.607

[a]The slopes and intercepts given are for the linear function used to evaluate the contribution to the total hyperfine splitting arising from the concentration of monomers in solution. It is well to remember that the intrinsic splittings of the monomer and atom units may or may not be temperature dependent.

[b]Slope and intercept of the exponential function used to evaluate the contribution arising from atoms in concentration units of spins per cc. The slope and intercept must be multiplied by R to obtain the correct units.

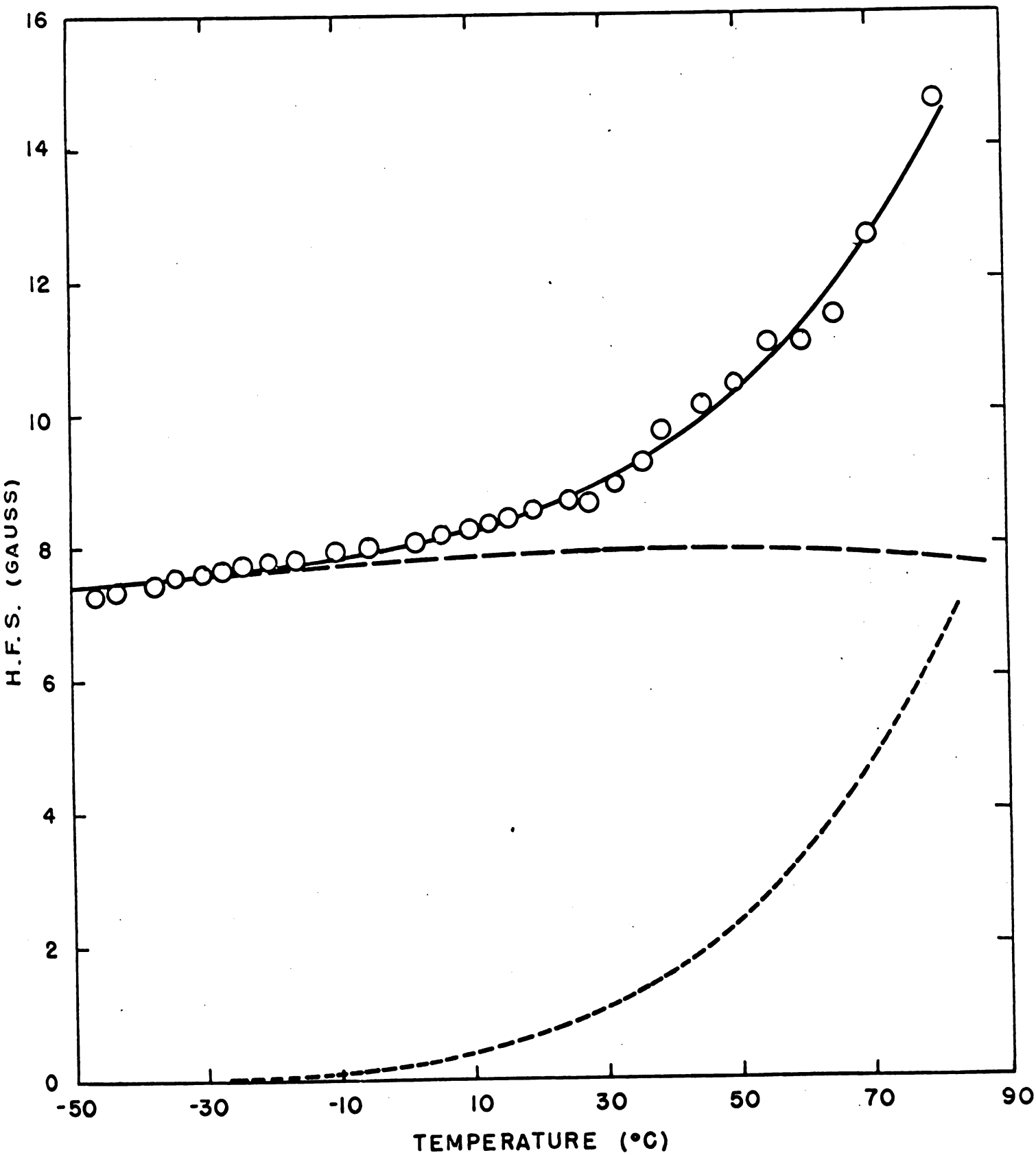

Figure 5a. Separation of hyperfine splitting into atomic and monomeric contributions, , experimental; _____, calculated; _ _, monomer contr.; ----, atom contr.

Table III. Thermodynamic Parameters for Solvation of the Gaseous Potassium Atom.

Mole percent ammonia	Parameters of Eq. 7		
	ΔH° (kcal)	ΔS° (cal/degree)	ΔG°(25°C) (kcal)
1.2	8.3	-9.3	11.2
2.7	9.8	-5.5	11.4
5.3	9.1	-7.2	11.9
9.6	12.9	5.6	11.3
11.3	14.6	12.8	10.8
14.2	15.1	15.4	10.5

using standard states of 1 mole / liter for both the gas and the solution. Results for the three lowest ammonia concentrations yield $\Delta H^{\circ} = -12.4$ kcal mole $^{-1}$ and $\Delta S^{\circ} = -24.2$ cal mole^{-1} deg^{-1} for this process. Because of the limited studies above ambient temperatures at higher ammonia concentrations and possible unsaturation of the solutions, the values of ΔH° and ΔS° especially in the high ammonia region, are subject to considerable uncertainty (29).

2. Program K ESR. The ESR spectra of potassium in ethylamine-ammonia mixtures between 9.9 and 14.5 mole percent in ammonia were difficult to interpret because of overlap of a four line hyperfine pattern with a broad extra line (29). To be certain that the pattern did not simply result from broadening of the hyperfine lines, a program was written to calculate and plot the expected spectra for a given splitting value as the lines broadened. This program could use both Gaussian and Lorentzian line shapes and included the pattern from both ^{39}K and ^{41}K. Neither line shape could give spectra similar to those observed. The problem was then one of separating the observed spectra into contributions from a single and a four line pattern.

A program, K ESR, was written to generate a spectrum which would duplicate as closely as possible those observed and is described and listed in the appendix. An observed spectrum was read into the computer as a series of X - Y points. Using initial estimates for splitting, g value, linewidth and intensity parameters, the computer calculated a composite spectrum. The parameters were then adjusted individually until the sum of squares of the deviations from the observed spectrum was minimized. Each time a parameter other than intensity was changed, the intensity was adjusted to give the best fit. During adjustment of one parameter the

contribution of the other pattern was kept constant. The relative intensities of the two patterns depended on which was adjusted first. After approximately fifteen iterations however, the relative intensities reached values which were in most cases nearly independent of the order of adjustment. Table IV lists the results obtained when various spectra were fit using this program with Gaussian shape functions; Figure 5b illustrates the type of pattern fit and the degree of fit obtained. If more spectra were fitted by this method, a new program should be written similar to IR, FIT, to be described later. This shorter and more flexible program has the advantage of permitting independent adjustment of intensities. By adjusting the intensities of both patterns from the start, the other parameters would not be forced to compensate for the initial absence of one pattern. The other parameters could then be adjusted and, would presumably converge more quickly to the best value.

3. Program GEN LS. Many of the problems resulting when the parameters were individually adjusted, were eliminated by using the method of generalized least squares (38,39) to fit the spectra. This method is more rigorous, more accurate and requires less computer time. The program, GEN LS, utilizing this method requires the same kind of information described previously. The program, described in detail in the appendix, uses matrix techniques to find corrections to the estimated parameters. The matrices are generated from partial derivatives of the spectral function evaluated at each point being considered. The corrected parameters are then used as new estimates in repeated cycles. Usually constancy better than the precision of the data is reached after three iterations. There are,

Table IV. EPR Parameters of hfs Pattern and Extra Absorption as Obtained by Computer Analysis[a], Using Program K ESR.

Temp. (°C)	A_F (gauss)	ΔH(hfs) (gauss)	ΔH(extra absorption) (gauss)	n_{extra}/n_{hfs}
Sample K-12		5.8 Mole percent ammonia		
-38	5.08[b]	1.25[b]		
-72	4.24[b]	1.17[b]		
Sample K-11		9.6 Mole percent ammonia		
-7	3.76[b]	2.11[b]	12.1[b]	2.31[b]
-15	3.66	2.18	10.3	1.28
	3.66[b]	2.18[b]	10.2[b]	1.27[b]
-41	3.24	1.76	12.7	4.94
	3.23[b]	1.84[b]	11.8[b]	3.35[b]
Sample K-25		9.9 Mole percent ammonia		
-8	3.52	2.63	9.27	1.74
	3.52[b]	2.64[b]	9.24[b]	1.70[b]
-35	3.39	2.54	8.83	1.78
-68	2.97	2.24	7.87	1.88
	2.97[b]	2.24[b]	7.85[b]	1.73[b]
Sample K-10		11.8 Mole percent ammonia		
-12	2.74	2.31	6.83	4.81
-42	2.36	1.97	5.95	6.45
-75	1.89	1.48	4.69	7.78

Table IV. (continued)

Temp. (°C)	A_F (gauss)	Δ H(hfs) (gauss)	Δ H(extra absorption) (gauss)	n_{extra}/n_{hfs}
Sample K-9		14.2 Mole percent ammonia		
-10	2.94	2.50	7.45	4.77
-41	2.54	2.16	6.51	4.31
-69	2.21	1.77	5.68	3.19

[a]Spectra were fit by the superposition of two absorption patterns. One of these was the Gaussian hyperfine pattern arising from electronic interaction with the ^{39}K and ^{41}K nuclei. The other was a single absorption of Gaussian shape. The routine alternately adjusted the parameters for both of these patterns. Except as noted, initial adjustment was made on the single absorption.

[b]The hyperfine pattern was adjusted first.

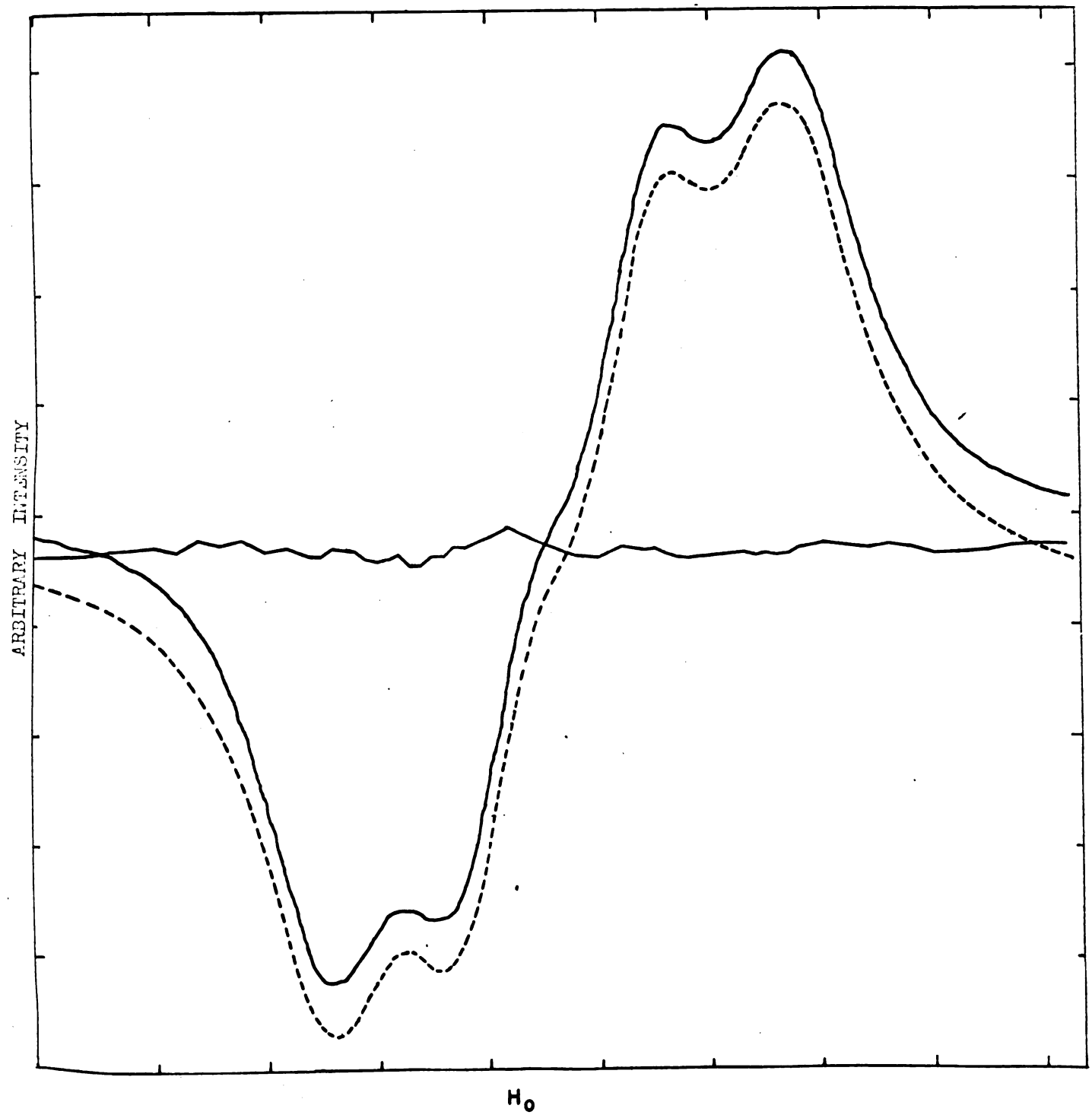

Figure5b. Computer analysis of ESR pattern. Observed spectrum at -42°C for 11.3 mole % ammonia is the solid line. The calculated superposition of a hyperfine pattern and a single line is given (displaced vertically) by the dotted line. The difference (obs - calc.) is shown by the solid line in the center.

however, two disadvantages involved in using this method with a computer. First, it requires that one take the partial derivatives of the function representing the spectrum with respect to each parameter being adjusted. This makes it difficult to adapt the program to new functions. Second, the initial parameters must be known more accurately than for the program which adjusts each parameter individually.

The parameters obtained for each spectrum using the program K ESR were used as the initial estimates for program GEN LS. The results using this method generally agreed well with those obtained earlier. Those cases which had yielded two sets of parameters depending upon which pattern had been adjusted first now converged on the same set of parameters from either starting point as seen in Table V. These parameters are considered to be more accurate than those given in the previous Table. A striking correlation was found between the linewidth of the extra line and the hyperfine splitting of the four line potassium pattern as illustrated in Figure 6. The correlation was much better than that between the linewidths of the two patterns shown in Figure 7. The linewidths and splittings in these Figures are in arbitrary units. The implications of this correlation are not yet fully understood.

4. Program POLY FT. A detailed theoretical treatment based upon the McConnell model (50) of an asymmetric species has been derived by Kivelson (49) and co-workers to describe the variation of linewidth with nuclear spin, m_I. On the basis of this model, the variation of linewidth with m_I seen in

Table V. ESR Parameters of hfs Pattern and Extra Absorption as Obtained by Computer Analysis, Using Program GEN LS.

Temp. (°C)	A_F (gauss)	Δ H(hfs) (gauss)	Δ H(extra absorption) (gauss)	n_{extra}/n_{hfs}
Sample K-11		9.6 Mole percent ammonia		
-7	3.76	2.36	10.13	1.03
-15	3.66	2.32	9.65	0.90
-41	3.24	2.03	9.70	1.61
-67	2.58	1.65	6.74	1.50
Sample K-25		9.9 Mole percent ammonia		
-8	3.52	2.66	9.13	1.62
-35	3.39	2.58	8.69	1.67
-68	2.97	2.25	7.73	1.61
Sample K-10		11.8 Mole percent ammonia		
-12	2.74	2.36	6.79	4.48
-42	2.36	2.01	5.96	6.27
-46	2.45	2.14	6.07	4.92
-75	1.89	1.46	4.74	8.52
-86	1.84	1.38	4.50	3.74
Sample K-9		14.2 Mole percent ammonia		
-10	2.94	2.55	7.45	4.63
-41	2.54	2.18	6.46	4.21
-69	2.21	1.79	5.64	3.05

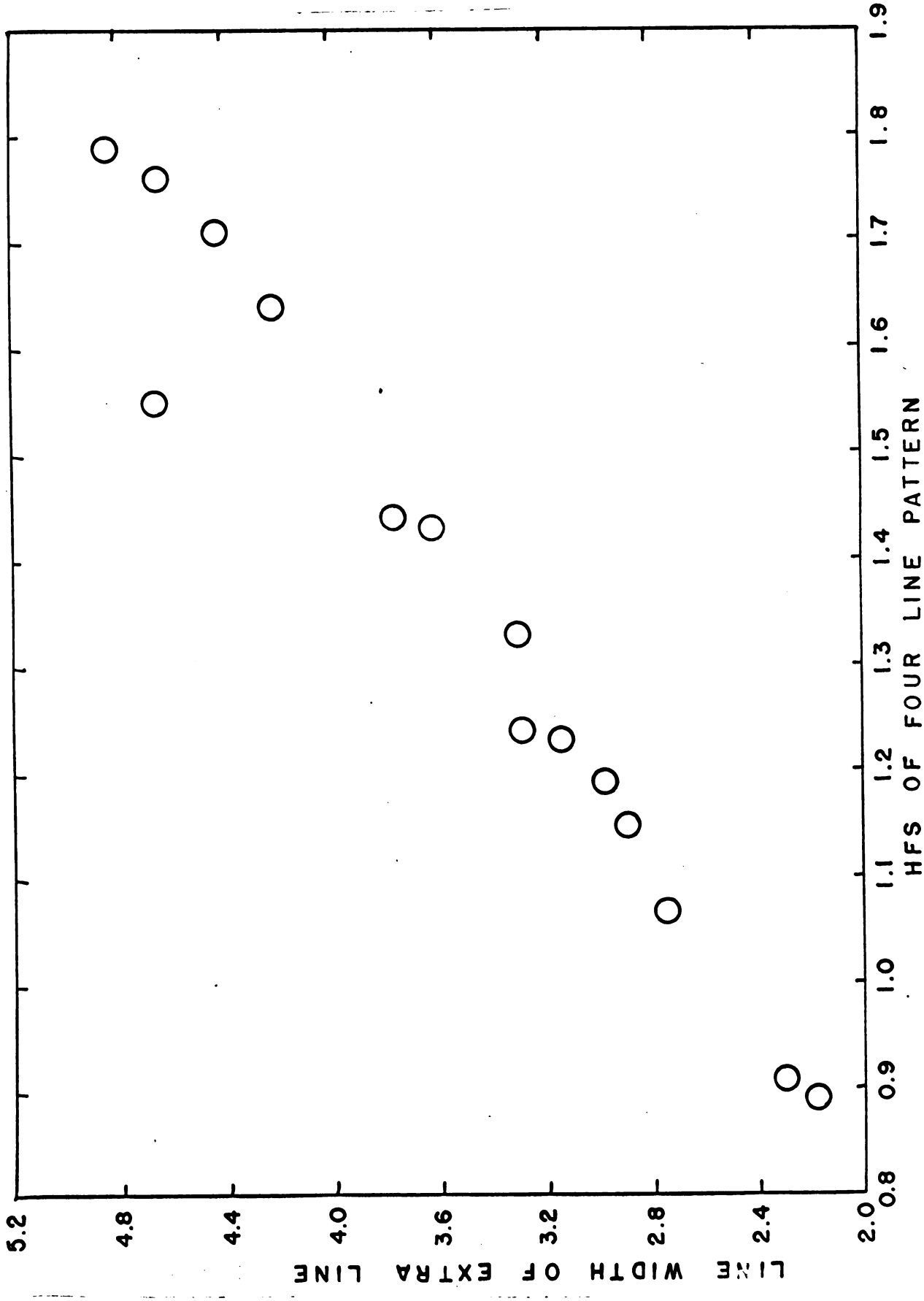

Figure 6. Correlation of linewidth of extra line and hyperfine splitting of monomer for potassium.

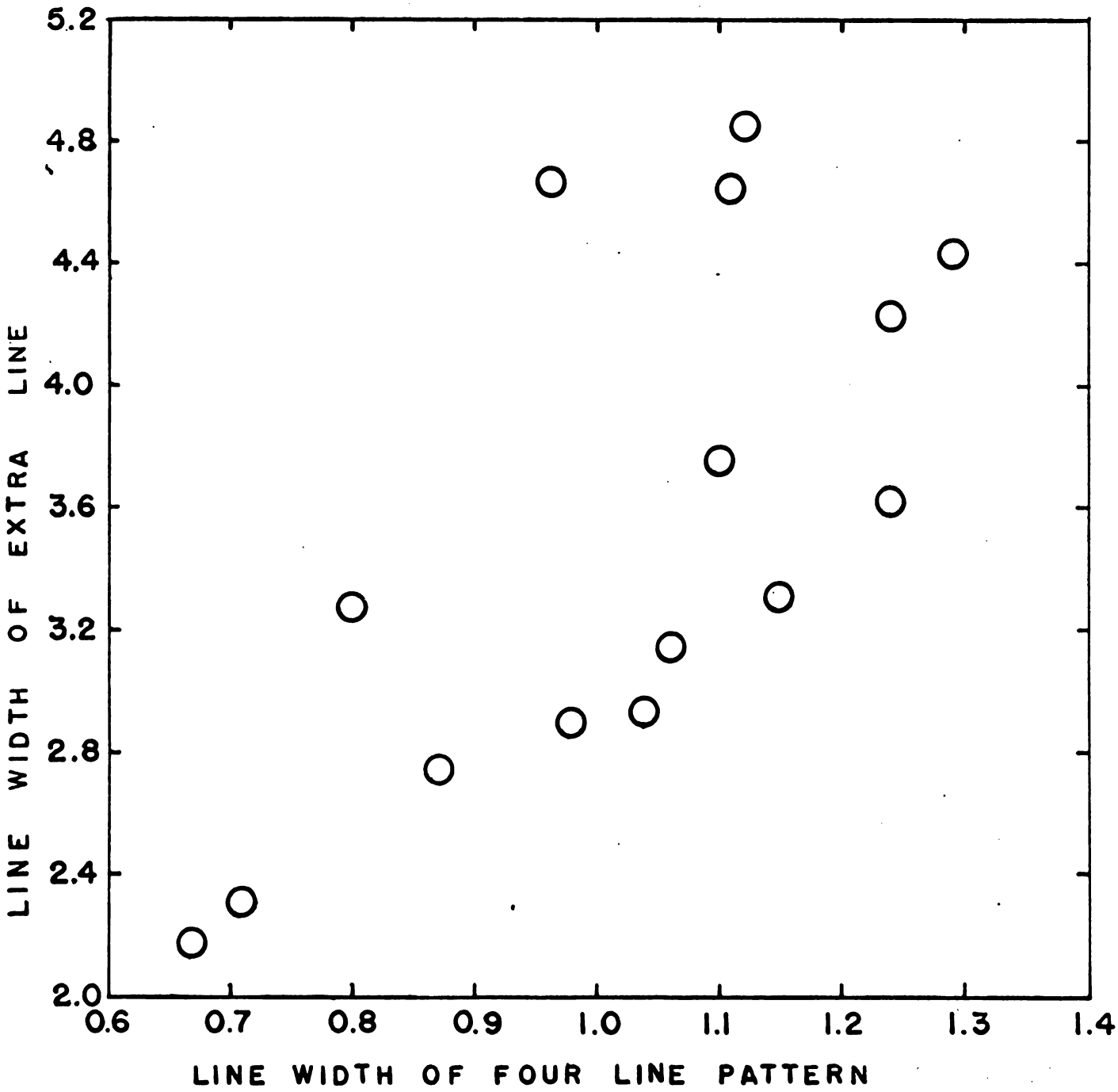

Figure 7. Correlation of the linewidth of the extra line with that of the hyperfine pattern for potassium.

cesium solutions should be described by the polynomial

$$\text{linewidth} = C_0 + C_1 m_I + C_2 m_I^2 + C_3 m_I^3 \ldots \quad . \qquad (12)$$

The ratio of coefficients of the various powers of m_I can be calculated from a knowledge of certain properties of the species giving rise to the absorption. Hopefully, knowing the behavior of the ratios, more precise assignments can be made with regard to the absorbing species. A program, POLY FT, was written to fit a least-squares polynomial in m_I to the varying linewidth. In this program the heights were used as a measure of the linewidth and one of the eight lines was more closely examined and used as a standard in calculating the linewidths of the others. A modified library least-squares polynomial fitting subroutine (co-op identification: E2 UCSD LSQPOL) was used to calculate the curve through the points. Figures 8,9,10,11 illustrate the behavior of the coefficients of a third order fit on three different cesium-ethylamine samples as a function of 1 / T. The program is listed and described in the appendix.

5. Program IR FIT. The overlap between peaks in the optical spectra of metal amine solutions often makes it difficult to know the absorbances of the various species. The technique developed for fitting ESR spectra by summing the contributions of two patterns seemed well suited to separating the optical spectra into their V, P and IR bands. To accomplish this, a more general program of the ESR FT type was written. This program uses one subroutine to minimize the sum of squares of deviations and a second to monitor the adjustment of a specific parameter. The main program determines the sequence of parameters adjusted and the number of iterations over the set of parameters available to fit a spectrum. To date, this

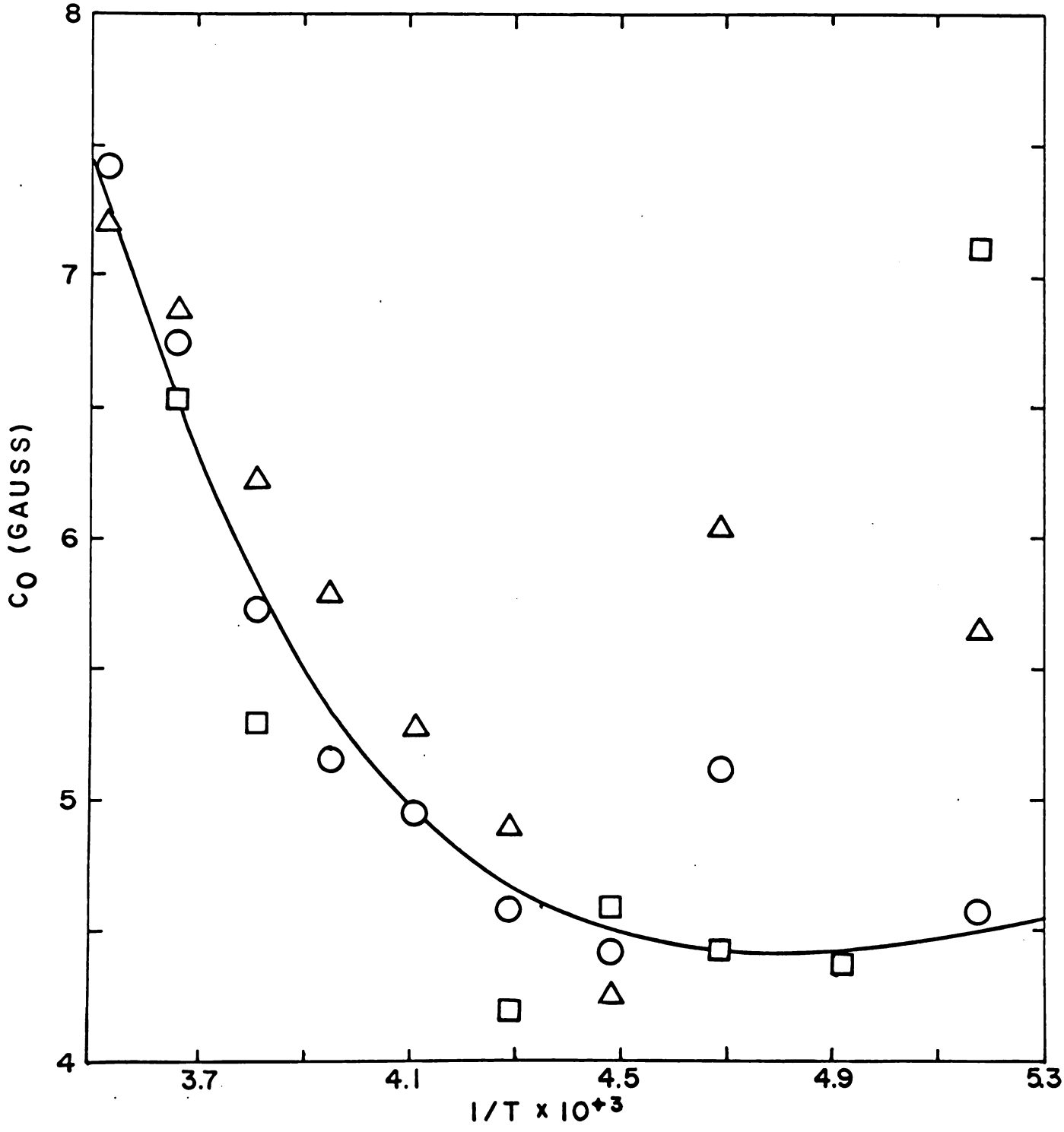

Figure 8. Variation of the coefficient of m_I, (C_0) with 1/T: Cs in ethylamine. Results are shown for three different sample preparations.

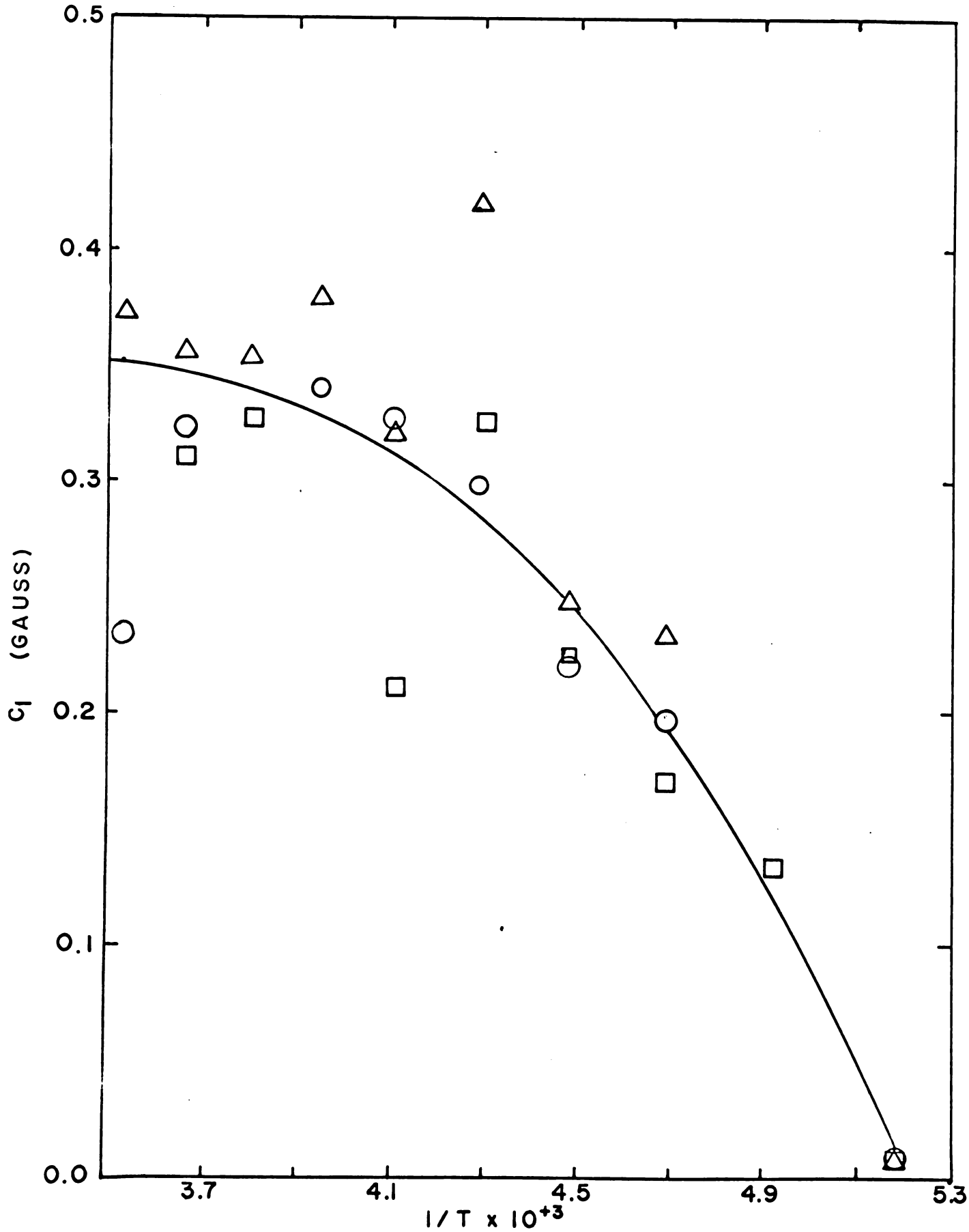

Figure 9. Variation of the coefficient of m_I, (C_1) with 1/T: Cs in ethylamine. Results are shown for three different sample preparations.

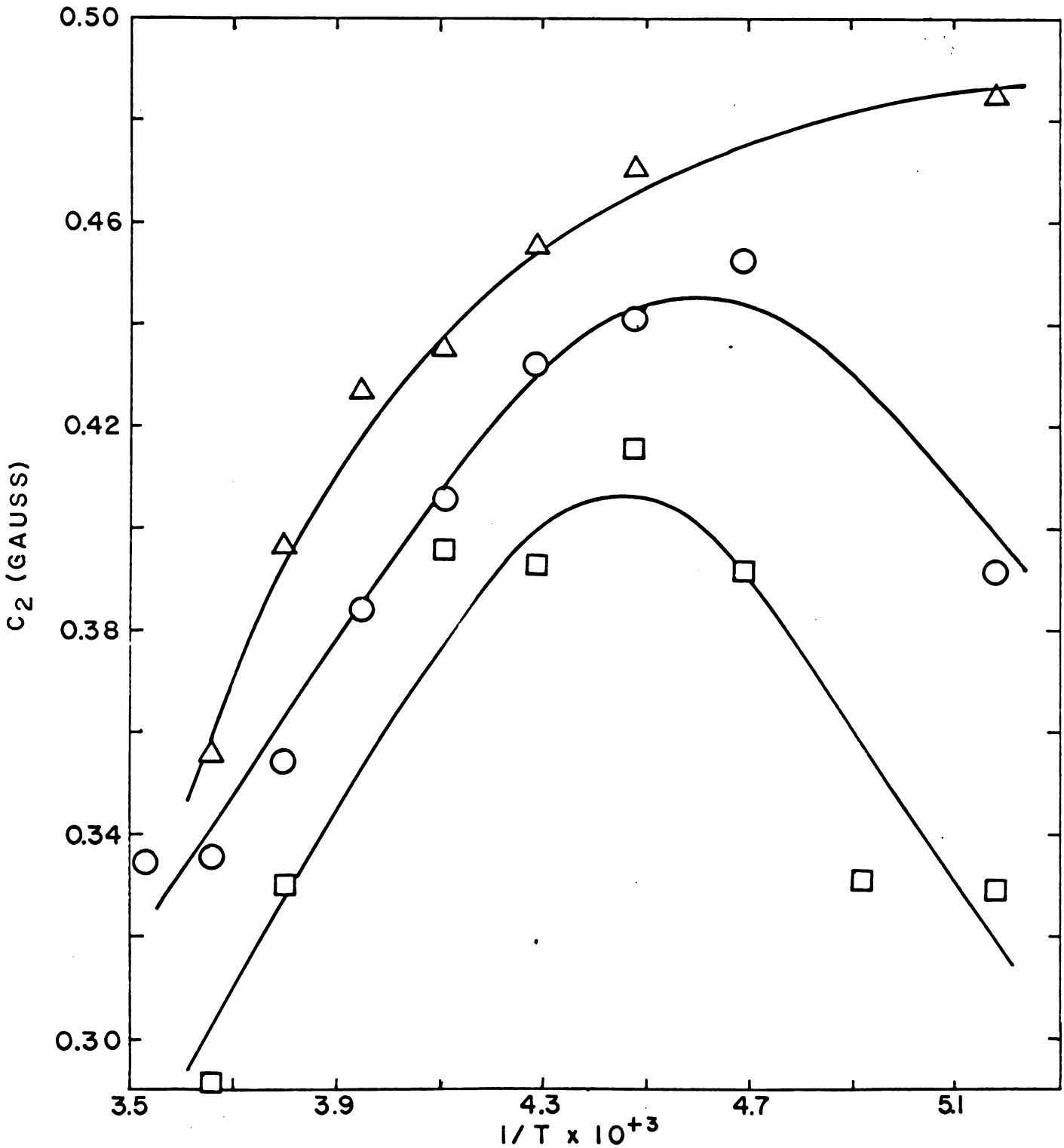

Figure 10. Variation of the coefficient of m_I, (C_2) with 1/T: Cs in ethylamine. Results are shown for three different sample preparations.

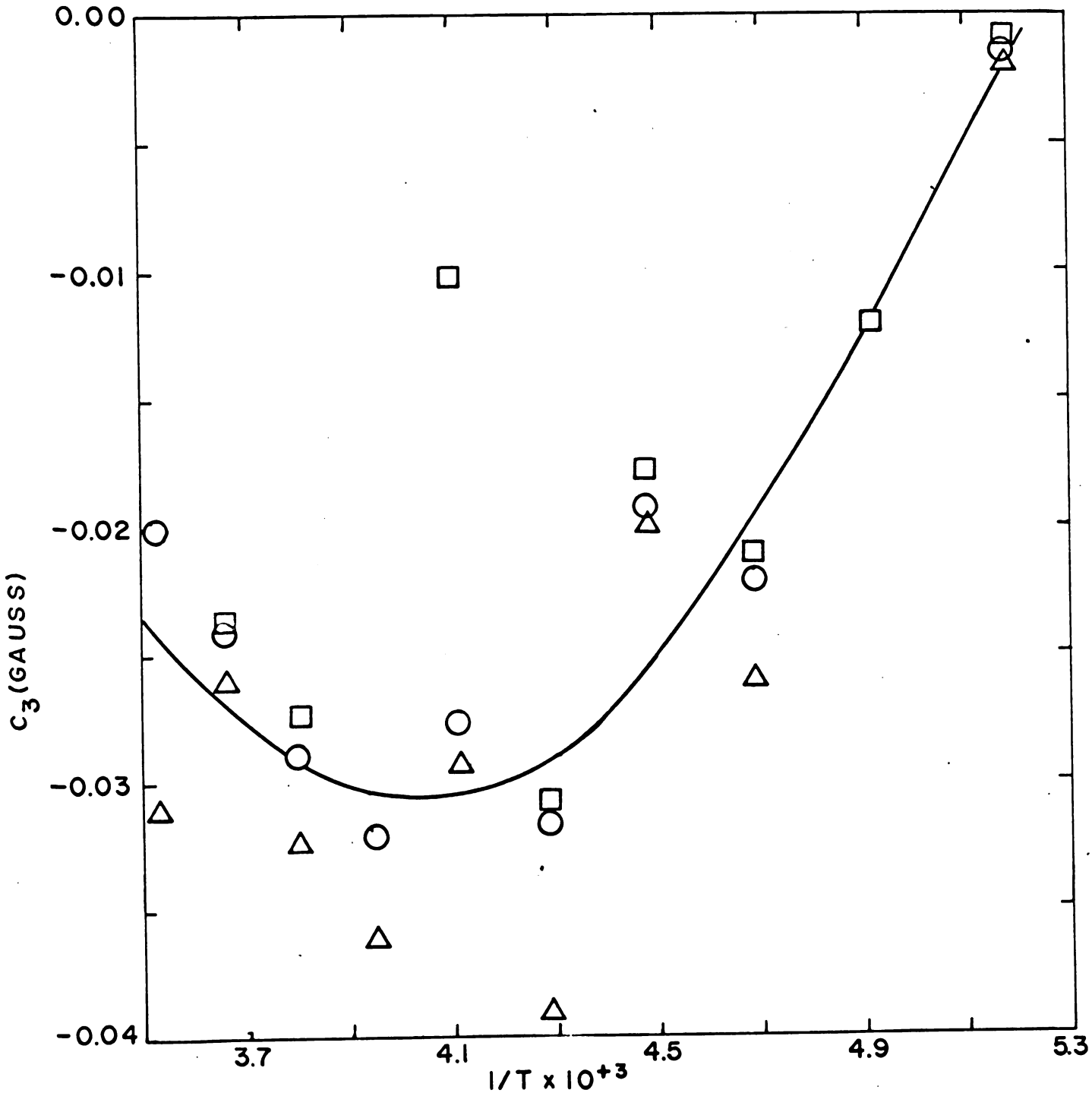

Figure 11. Variation of the coefficient of m_I, (C_3) with 1/T: Cs in ethylamine. Results are shown for three different sample preparations.

program has been used to find a function capable of fitting the IR peak with the minimal number of parameters. It seems to require at least four parameters to describe this absorption; they relate to the center (C), the intensity (I), the width (W) and the asymmetry (S) of the peak in question. Approximately ten Gaussian or Lorentzian functions with different asymmetry properties have been used in attempting to fit the curve representing the absorption. This curve was plotted on the basis of either a wave length or wave number scale. In both cases the function

$$\text{Absorption } (\lambda \text{ or } \bar{\nu}) = I\,(1 + S \cdot R) \,/\, (1 + (R/W^2)$$

in which $R = (\lambda \text{ or } \bar{\nu}) - C$, gave the most satisfactory results. The degree of fit in the region of interest is nearly identical for the wave length and wave number fit, with agreement within 0.02 of an absorption unit for a peak with a maximum absorption of one. Of course the constants required in the two representations are different.

6. Program SEC OC. Perturbation methods are usually used to treat the hyperfine splitting of electronic energy levels resulting from contact with atomic nuclei (40). The magnetic field, H_o, at which the transition would occur in the absence of the perturbation is given by (41)

$$H_o = H_m + A \cdot m + A^2 \cdot (I\,(I + 1) - m^2) \,/\, 2H_m + A^3 \,/\, 4H_m^2 \qquad (13)$$

in which H_m is the observed field position for the hyperfine component with nuclear spin quantum number m, I is the total nuclear spin, and A is the hyperfine splitting. In this Equation, the perturbation treatment is carried through third order. Because of the large values of A for rubidium and cesium in amines, these higher order corrections are required and the

hyperfine splittings cannot be taken directly from the spectra.

A program, SEC OC, described and listed in the appendix, was written to make second and third order corrections to the peak positions and from these to calculate hyperfine splittings and g values. This program calculates the quantity $H_c - Am$ by subtracting the second and third order contributions from the observed field position. This calculation for various values of m can be used to evaluate H_o and A. The process is repeated until constant values are obtained. The center of the spectrum, H_o, is taken as the average of values calculated for each peak using Equation (2). Finally the g value is calculated from the expression (42)

$$g = h\nu / \beta H_o \qquad (14)$$

where h is Planck's constant, ν the klystron frequency and β the electronic Bohr magneton.

C. A New Variable-Temperature Spectrophotometer.

The desirability of measuring optical spectra under conditions used for ESR measurements prompted the construction of a temperature controlled optical cell compartment. Previously it was necessary to attach an Aminco optical cell to the ESR tube. Difficulty in cleaning the sample tubes, the large surface to volume ration of the optical cells and the cumbersome temperature control unit restricted the measurements which could be made. Obviously, if the ESR tubes themselves could be used for optical measurements over the entire ESR temperature range, some of these problems would be eliminated.

The stopped-flow system assembled in this laboratory (43) employing

a Perkin-Elmer model 108 rapid scanning monochromator was adapted to take static spectra by replacing the flow cell with a temperature controlled cell compartment which held the ESR cells in a fixed position. The monochromator, using a fused quartz prism, is able to scan the spectral region from 0.2 to 12.5 μ with appropriate light sources. To date this instrument has been used over a range of 0.4 to 1.1 μ with a Bausch and Lomb tungsten-iodine source. A stacked mirror beam splitter, with appropriate focusing mirrors, divides the emergent light from the monochromator into two beams and focuses the slit image approximately 8 cm from the monochromator. After passing through the sample and reference cells, the two light beams strike photomultipliers whose anode current output is fed into a Philbrick differential amplifier and log circuit rendering output voltages which are proportional to absorbance from 0.01 to 2.0 absorbance units.

A Textronix type 564 storage oscilloscope, with types 2A63 differential amplifier and 3B4 time base plug-in units, recorded the spectra. The spectra were photographed with a C-12 camera attachment using Polaroid type 146-L red sensitive film to give transparancies with good contrast between the spectrum and background. In order to insure that the horizontal positions on the screen during successive scans would represent the same wavelength, a triggering circuit was devised which fired each time a slot in a rotating sector disc within the monochromator allowed light from a small neon lamp to strike a cadmium sulfide photocell. The principle difference between this spectrophotometer and that used in the flow system is the temperature-controlled cell compartment.

This unit employs a Varian V-4557 Variable temperature accessory as the temperature controller. It operates by heating a stream of precooled

nitrogen to the desired temperature with stability sufficient to maintain a $\pm$ 1°C maximum temperature variation at the sensor. Two thermocouples were placed at the bottom of the cell compartments as a added check on the temperatures. This was necessary because the sensor is approximately two inches from the samples and because of the comparatively large spaces which required cooling. The sample and reference cell compartments can accommodate either conventional one centimeter optical cells or round ESR cells.

In order to position the round ESR-optical cells reproducibly, the cell holder illustrated in the appendix was designed. A point, groove and plane locating system for the cell holders proved to be quite functional. When the cells were in these holders, their position could be adjusted to allow proper alignment in the light beam. Quartz rods were used to connect the cell holder to the adjustment system. The low coefficient of thermal expansion of quartz minimizes changes in the cell position with changing temperature. The quartz rods were attached to the upper and lower cell holder plates with epoxy cement. The point, groove and plane of the locating system for the cell holder were set as far as possible from the cell compartments to lessen the effect of any distortions in their positions as the temperature changed. The cell compartments and light tubes were constructed of black Plexiglas to reduce light and heat leaks.

Double windows were required to keep the cold nitrogen gas in the cell compartment and to prevent frosting. The centers of thick pieces of black plastic were drilled out to make the light tubes. Originally quartz flats (American Thermal Fused Quartz Co.) were sealed with epoxy cement to the ends of the light tubes. Upon cooling, the inner quartz flats cracked because of the difference in the thermal expansion coefficient of the quartz and Plexiglas. Next a plastic bracket screwed to the main body

of the light tube was used to press the quartz flats and a thin Teflon gasket to the tube body. When this unit cooled, the windows frosted even though dry nitrogen was blown into the light tubes during assembly. The moisture may have entered the light tubes when the cooling lowered the pressure inside the tubes and impaired the sealing quality of the Teflon. The frost was eliminated by blowing a small stream of dry nitrogen through the light tubes while the temperature controlling unit was in operation. If this unit were to be rebuilt, it would be advisable to substitute evacuated one-piece quartz or quartz faced light tubes for those now in use.

When conventional one centimeter optical cells were used in the spectrometer, good spectra were obtained. However when the solutions used in the one centimeter cells were transferred to round ESR-optical cells, certain anomalies in their spectra became obvious. The problem was eliminated by carefully masking the front side of the cell holder to prevent light from striking the side of the round cell and being refracted around it without having passed through the sample. A one millimeter slit positioned in front of and very near the sample provided the desired masking effect.

IV. CONCLUSIONS

The computer program, A M EQ, has permitted the equilibrium model to be tested quantitatively. A satisfactory description of the dependence of the hyperfine splitting and spin concentration on temperature and ammonia content has resulted. Although stationary-state models can qualitatively describe the nature of this dependence, they have not yet permitted a quantitative description of the ESR results. Symons and co-workers have recently proposed an additional equilibrium with diamagnetic species to explain the broadening of the four-line potassium pattern with increased cation concentration (36).

The appearance of a broad extra absorption underlying the potassium four line hyperfine pattern in ethylamine-ammonia mixtures between 9.9 and 14.5 mole percent ammonia has been confirmed by a quantitative fit of the spectra. The surprising correlation between the linewidth of this extra absorption and the hyperfine splitting of the four line pattern strongly suggests that the species giving rise to the broad extra absorption is also interacting with one or more metal nuclei. It should be noted that the spectra analyzed by the computer were in the low-temperature range. At these temperatures atom concentration predicted by the equilibrium model is negligible. The factors which influence the width of the extra line are therefore those which also influence the monomer hyperfine splitting. The change of the linewidth of the extra line into the higher temperature region should be examined to see whether the presence of atoms destroys

this correlation.

Both of the fitting programs developed are useful in synthesizing spectra for comparison with experiment. The ER FIT type which adjusts each parameter individually is very easily modified for use with different functions. It can be used effectively to develop and test fitting functions or in cases where only a few spectra are to be analyzed. Where many similar spectra are to be treated, programs of the GEN LS type take less computer time and are probably more accurate. If some of the parameters to be used in fitting the spectra are not reasonably well known, the generalized least-squares method may not converge. In such cases a combination of the two types of programs should be a powerful technique. The least well known parameters couldbe adjusted individually before they were all simultaneously corrected. The ability to obtain data not otherwise accessible suggests that this method would be useful for other systems where merger of several patterns makes analysis difficult.

The second order correction program, SEC OC, illustrates the use of computers in efficiently treating large quantities of information. Over two hundred spectra have been treated with this program.

It is difficult at this time to draw any definite conclusions from the dependence of the cesium linewidth on m_I. It can only be said that the major contributions to the linewidth come from the coefficients of the zero and second-power terms in the polynomial and that these coefficients showed more consistency from one sample to another than did the other two coefficients.

The new temperature-controlled spectophotometer enables us to measure optical spectra on all solutions used for ESR measurements, pro-

vided the absorbance is small enough. The conditions present when ESR measurements are made can be duplicated in this instrument. As the description of metal-amine solutions becomes more quantitative it will be increasingly necessary to correlate results from different areas of study. This instrument should prove to be a valuable asset in obtaining data for correlation of optical and ESR spectra.

V. A MODEL FOR THE V BAND

There is general agreement among workers in this field on the assignment of the species giving rise to the IR and R absorption bands as has been discussed in the historical section. The temperature dependence of the hyperfine splitting is adequately explained by an equilibrium between atoms and monomers. This section will deal with the species giving rise to the broad single ESR absorption and the V species.

The absorption in the region of 650 mμ (V band) is assigned to e_2^{--} species whose potential has been lowered by a partially solvated metal cation at the cavity center giving a species of stoichiometry M^-. This is a symmetrical species to be differentiated from M^- in ammonia (44-46) which is assumed to exist mainly in an ion pair between e_2^{--} and M^+. The assignment of the V species is based primarily on the flash photolysis results of Linschitz and is supported by the changes in intensity relative to the R band which occur upon dilution and cooling (10,13,22). The species which result from photo bleaching of the V band must be capable of combining in a rapid second order reaction to form dimers (R species). The proposed reactions are

$$M^-(V) \xrightarrow{h\nu} M + e^-(IR) \qquad (15)$$

$$2M \longrightarrow M_2(R)$$

The increased IR absorption observed immediately following V band photolysis is attributed by the author to electrons, implying their

removal from the V species. The R species can then produce the V species by the reaction

$$M_2(R) = M^-(V) + M^+ . \qquad (16)$$

This reaction will also occur upon dilution. The increased relative intensity of the V band at low temperatures implies a species favored by low concentrations and/or by a more highly structured solvent, both of which support this assignment. The apparent low V band absorption for rubidium and cesium may arise because they are too large to fit easily within the cavity. The explanation of the slow interconversion of the lithium V species to the IR band (22) according to this model is admittedly weak. It is attributed to the high activation energy brought about by the required solvent reorganization since a symmetric species M^- goes to species with the charges separated.

The broad extra ESR absorption observed in certain solutions of potassium in ethylamine-ammonia mixtures is attributed to an unpaired electron. The high metal concentrations present when this phenomenon is observed would allow the solvated electron to pair with and separate from a number of metal cations rapidly enough to give a single line. It is believed that simultaneous interaction with several nuclei occurs since a single metal nucleus would not be capable of broadening the electron ESR line to a width greater than the splitting observed for the monomer.

The greater asymmetry of the cesium hyperfine pattern compared with potassium and rubidium could result from a slower atom-monomer equilibrium and/or the increased hyperfine splitting by the cesium nucleus. Although

the former may be true, the major effect appears to be the increased hyperfine splitting.

Clearly much work remains before models are developed which are capable of quantitatively describing all facets of the behavior of metal solutions. The instrumentation and computer programs described in this thesis should help to develop and test such models.

REFERENCES

1. E. J. Hart, "Solvated Electron" in Advances in Chemistry Series 50, R. F. Gould, Ed., American Chemical Society Pub., vii (1965).

2. L. Ebert and A. J. Swallow, "Solvated Electron" in Advances in Chemistry Series 50, R. F. Gould, Ed., American Chemical Society Pub., 209 (1965).

3. C.A. Kraus, J. Am. Chem. Soc., 36, 864 (1914).

4. C. A. Kraus, J. Am. Chem. Soc., 29, 1557 (1907).

5. C. A. Kraus, J. Am. Chem. Soc., 30, 1197 (1908).

6. C. A. Kraus, J. Am. Chem. Soc., 30, 653 (1908).

7. C. A. Kraus, J. Am. Chem. Soc., 30, 1323 (1908).

8. G. E. Gibson, and W. L. Argo, J. Am. Chem. Soc., 40, 1327 (1918).

9. J. L. Dye and R. R. Dewald, J. Phys. Chem., 68, 135 (1964).

10. M. Ottolenghi, K. Bar-Eli and M. Linschitz, J. Chem. Phys., 43, 206 (1965).

11. H. Blades and J. W. Hodgins, Can. J. Chem., 83, 411 (1955).

12. G. Hollstein and V. Wannagat, Z. Anorg. Chem., 288, 193 (1956).

13. R. R. Dewald, Ph.D. dissertation, Michigan State University, (1963).

14. G. W. A. Fowles, W. R. McGregor and M. C. R. Symons, J. Chem. Soc., 1957, 3329.

15. S. Windwer and B. Sundheim, J. Phys. Chem., 66, 1254 (1962).

16. D. F. Burow and J. J. Lagowski, "Solvated Electron" in Advances in Chemistry Series 50, R. F. Gould, Ed., American Chemical Society Pub., 125, (1965).

17. W. L. Jolly, C. J. Hallada and M. Gold, Metal Ammonia Solutions, G. Le Poutre and M. J. Sienko, Ed., Benjamin, New York, 174 (1964).

18. R. C. Douthit and J. L. Dye, J. Am. Chem. Soc., 82, 4472 (1960).

19. M. Gold, W. L. Jolly and H. S. Pitzer, J. Am. Chem. Soc., 84, 2264 (1962).

20. M. Gold and W. L. Jolly, Inorg. Chem., 1, 818 (1962).

21. L. R. Dalton, J. L. Dye, E. M. Fielden and E. J. Hart, J. Phys. Chem., in press.

22. R. R. Dewald and J. L. Dye, J. Phys. Chem., 68, 121 (1964).

23. M. Ottolenghi, K. Bar-Eli and H. Linschitz, J. Am. Chem. Soc., 87, 1309 (1965).

24. M. Ottolenghi and H. Linschitz, "Solvated Electron" in Advances in Chemistry Series 50, R. F. Gould, Ed., American Chemical Society Pub., 149 (1965).

25. J. L. Dye, L. R. Dalton and E. M. Hansen, Abstracts, 149th National Meeting of the American Chemical Society, April 1965, 455.

26. J. L. Dye and L. R. Dalton, Symposium on Electron Spin Resonance, East Lansing, Michigan, August 1966.

27. L. R. Dalton and J. L. Dye, results to be published.

28. K. Bar-Eli and T. R. Tuttle,Jr., J. Chem. Phys., 40, 2508 (1964).

29. L. R.Dalton, J. D. Rynbrandt, E. M. Hansen and J. L. Dye, J. Chem. Phys., 44, 3969 (1966).

30. G. Herzberg, Spectra of Diatomic Molecules, D. Van Nostrad Co., New York (1950).

31. A. Hess and J. L. Dye, unpublished results.

32. M. Ottolenghi, K. Bar-Eli and H. Linschitz, J. Chem. Phys., 40, 3729 (1964).

33. E. Becker, R. H. Lindquist and B. Alder, J.Chem. Phys. 25, 971 (1956).

34. J. L. Dye, R. F. Sankuer and G. E. Smith, J. Am. Chem. Soc., 82, 4797 (1960).

35. C. A. Kraus, Metal Ammonia Solutions, G. Le Poutre and M. J. Sienko, Ed., Benjamin, New York, 9 (1964).

36. R. Catterall, L. C. R. Symons and J. W. Tipping, private communication.

37. N. F. Ramsey, Nuclear Moments, John Wiley and Sons, Inc., New York, 89 (1953).

38. W. E. Wentworth, J. Chem. Ed., 42, (2), 96 (1965).

39. W. E.Wentworth, J. Chem. Ed., 42,(3), 162 (1965).

40. R. P. Kohin, Ph. D. dissertation, University of Maryland (1961).

41. H. A. Kuska, Ph. D. dissertation, Michigan State University (1965).

42. J. R. Morton, Chem. Rev., 64, 453 (1964).

43. J. L. Dye and L. Feldman, Rev. Scientific Instr., 37, (2), 154 (1966).

44. E. Arnold and A. J. Patterson, J. Chem. Phys., 41, 3089 (1964).

45. L. C. R. Symons, L. J. Blandamer, R. Catterall and L. Shields, J. Chem. Soc., 1964, 4357.

46. W. H. Brendly and E. C. Evers, "Solvated Electron" in Advances in Chemistry Series 50, R. F.Gould, Ed., American Chemical Society Pub., 111 (1965).

47. H. C. Clark, A. Horsfield and M. C. R. Symons, J. Chem. Soc. 1959, 2478.

48. R. Catterall, J. Carset and M. C. R. Symons, J. Chem. Phys. 38, 272 (1963).

49. R. Wilson and D. Kivelson, J. Chem. Phys., 44, 154 (1966).

50. H. M. McConnell, J. Chem. Phys., 25, 709 (1956).

51. ... Gold, W. L. Jolly and K. S. Pitzer, J. Am. Chem. Soc., 84, 2264 (1962).

APPENDICES

APPENDIX A

1. ATOM-MONOMER EQUILIBRIUM

A. IDENTIFICATION

Title: Atom-Monomer Equilibrium

Category: Separation of effects

Programmer: Jay D. Rynbrandt

Date: July 29, 1966

B. PURPOSE

Given the variation of potassium hyperfine splitting in ethylamine-ammonia mixtures with temperature, calculate the contributions of atoms and monomers to this splitting.

C. USAGE

1. Arguments

JL, KL are integers defining the low field region for each data set.

JH, KH are integers defining the high field region for each data set.

PC is the mole percent ammonia.

C is the array name of the temperature in degrees centigrade.

A is the array name for the hyperfine splitting in Gauss.

S is the array name for the total number of spins.

T is the array name for the temperature in degrees Kelvin.

X is the array name stored in common and used to transfer the independent variables into the least squares subroutine.

Y is the same as X but for dependent variables.

AT is the array name for the calculated number of atom spins.

MA is the array name for the weighting factors. (NOTE: A more

recent least squares subroutine than that used with this program is listed. This subroutine can use non-integer weighting values.)

KA, JA are the integers defining the first and last points to be used in the least squares subroutine.

SAC, SMC are the calculated contributions to the splitting of the atom and monomer.

SPA, SPM are the atom and monomer splittings calculated another way.

PA, PM are the percent atom and monomer contributions to the splitting.

TS, DS are the total splitting and its difference from the observed value.

AM is the calculated monomer splitting.

YB is the splitting from atoms.

YA is the number of spins due to atoms.

2. Print-Outs: All arrays on each iteration.

3. Output Formats: See listing.

4. Timing: Roughly one minute for all operations described here.

5. Accuracy: Depending on data and number of iterations.

6. References: L. R. Dalton, J. D. Rynbrandt, E. M. Hansen and J. L. Dye, Journal of Chemical Physics 44, 3969, 1966 and J. D. Rynbrandt, MS Thesis, Michigan State University.

D. METHOD

The contributions of either of two species to the total hyperfine splitting are calculated in one temperature range and extrapolated

into another, to be used in the calculation of the contribution from the other species. An iterative procedure is then applied to reach constant contributions from each. For the details of the calculation see the references.

Program A M EQ

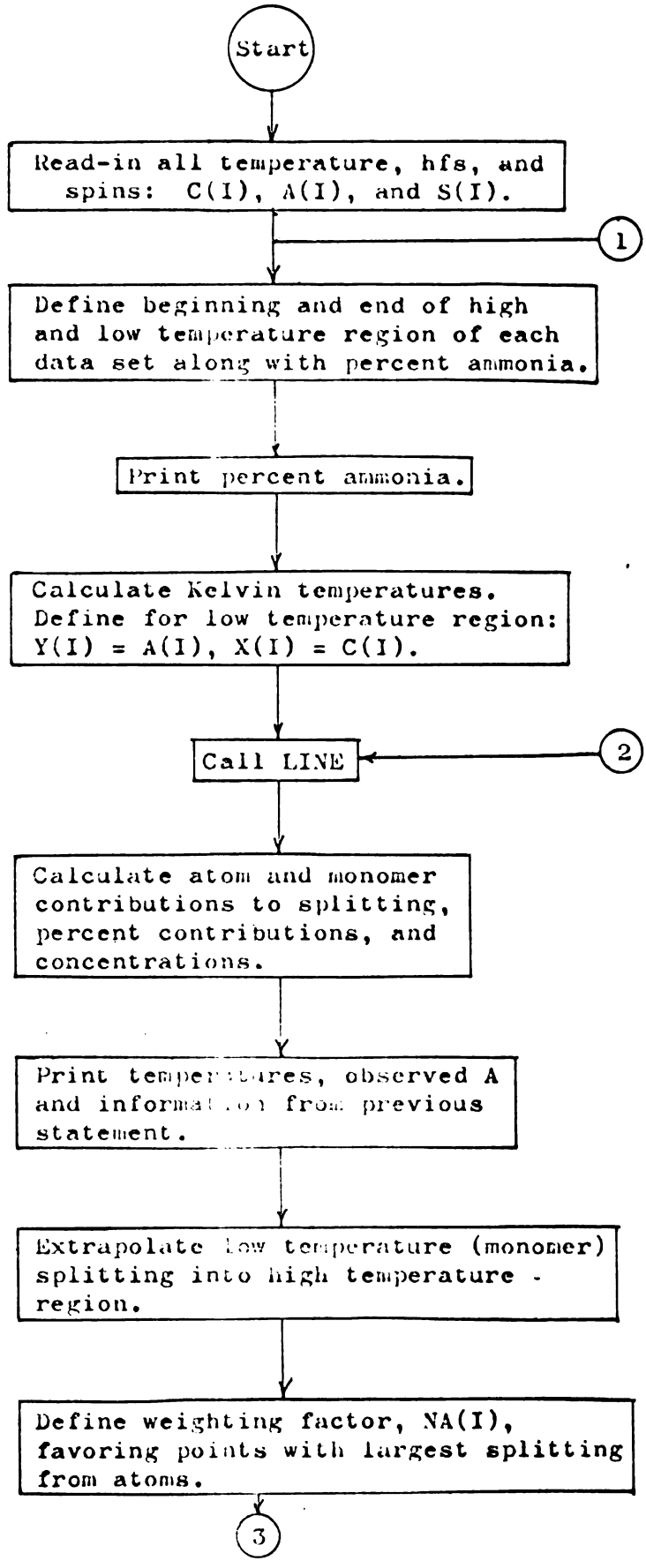

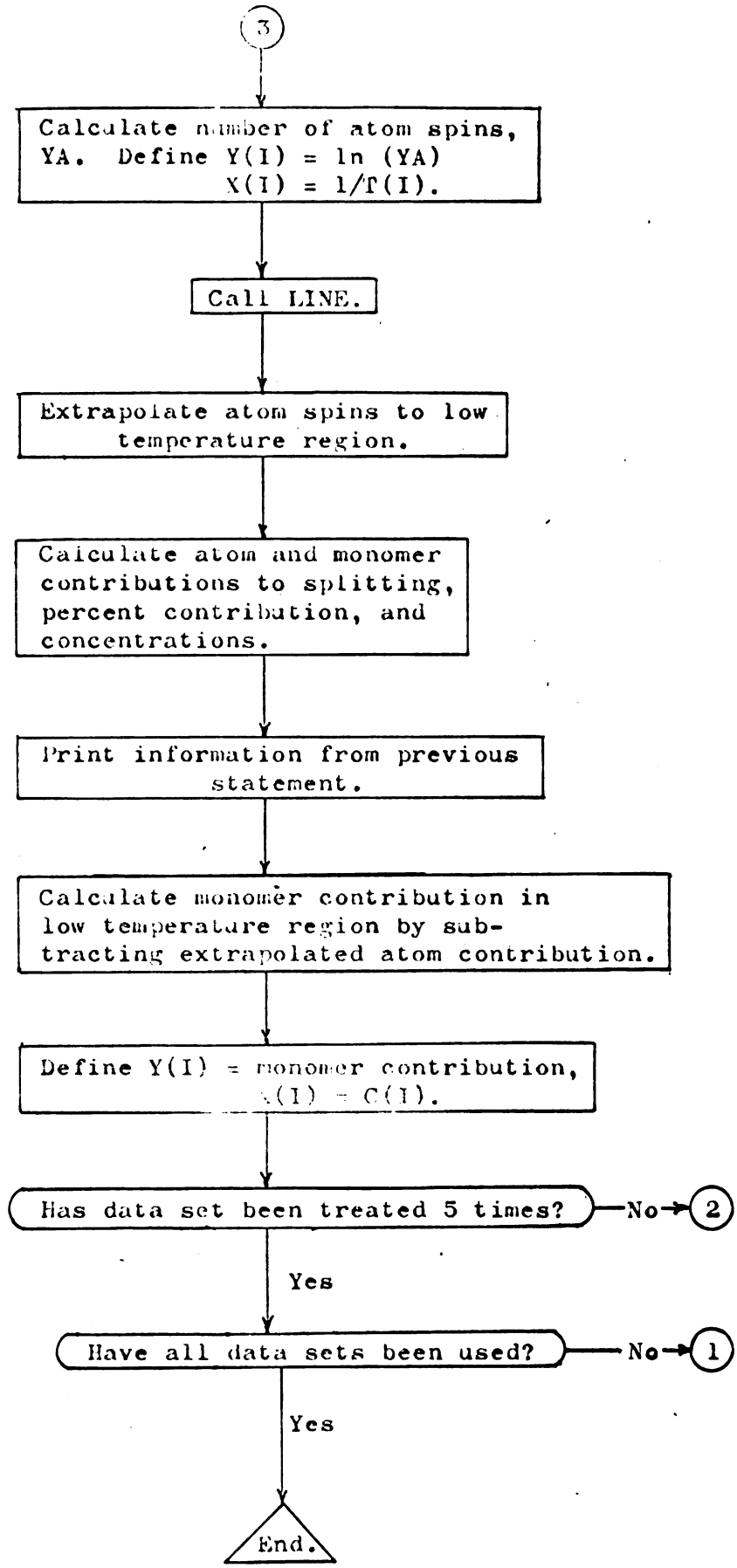
3
Calculate number of atom spins, YA. Define Y(I) = ln (YA)
X(I) = 1/T(I).
Call LINE.
Extrapolate atom spins to low temperature region.
Calculate atom and monomer contributions to splitting, percent contribution, and concentrations.
Print information from previous statement.
Calculate monomer contribution in low temperature region by subtracting extrapolated atom contribution.
Define Y(I) = monomer contribution,
X(I) = C(I).
Has data set been treated 5 times?
No
2
Yes
Have all data sets been used?
No
1
Yes
End.

```
      PROGRAM A M EQ
      COMMON JA,KA,NA,SY,CY,X,Y
      DIMENSION T(200), A(200), S(200), X(200), Y(200), C(200), NA(200)
     1 AT(200)
    1 FORMAT  (2F10.0  ,E10.2)
    2 FORMAT (*1PERCENT NH3 = *F4.1 )
    3 FORMAT (*0    TEMP          A        MON A C      MON A       P MON
     1    AT A C      AT A          P AT       T S      OBS-CALC*/)
    4 FORMAT (*0      TEMP       SPINS       MON S       P MON      AT S C
     1      P AT         */)
    5 FORMAT (10F11.5)
    6 FORMAT (F11.5,2E11.3,F11.5, E11.3,F11.5)
      NB = 165
      READ 1, (C(I), A(I), S(I), I = 1,NB)
      DO 15 MB = 1,6
      BM = MB
      IF (BM-1.0) 20,20,21
   20 CONTINUE
      JL = 1
      KL = 17
      JH = 18
      KH = 35
      PC = 1.6
      GO TO 32
   21 CONTINUE
      IF (BM-2.0) 22, 22,23
   22 CONTINUE
      JL = 36
      KL = 54
      JH = 55
      KH = 66
      PC = 2.7
      GO TO 32
   23 CONTINUE
      IF (BM-3.0) 24,24,25
   24 CONTINUE
      JL = 67
      KL = 85
      JH = 86
      KH = 107
      PC = 5.8
      GO TO 32
   25 CONTINUE
```

```
      IF (BM-4.0) 26,26,27
   26 CONTINUE
      JL = 108
      KL = 118
      JH = 122
      KH = 130
      PC = 9.6
      GO TO 32
   27 CONTINUE
      IF (BM-5.0) 28,28,29
   28 CONTINUE
      JL = 131
      KL = 140
      JH = 143
      KH = 148
      PC = 14.2
      GO TO 32
   29 CONTINUE
      IF (BM - 6.0) 30,30,31
   30 CONTINUE
      JL = 149
      KL = 156
      JH = 159
      KH = 165
      PC = 11.8
      GO TO 32
   31 CONTINUE
   32 CONTINUE
      PRINT 2, PC
      DO 11 I= JL,KH
      T(I) = C(I) + 273.15
      X(I) = C(I)
      Y(I) = A(I)
      AT(I) = 0.0
      NA(I) = 1
   11 CONTINUE
      JA = JL
      KA = KL
      CX = 0.0
      SX = 0.0
      DO 14 MA = 1,5
```

```
      CALL LINE
      PRINT 3
      DO 16 I = JL,KH
      SAC = AT(I)                    *82.4/S(I)
      SMC =(C(I)*SY + CY)*(S(I) - AT(I)) / S(I)
      SPA = A(I) - SMC
      SPM = A(I) - SAC
      PA = 100.0*SAC/A(I)
      PM = 100.0*SMC/A(I)
      TS = SAC + SMC
      DS = A(I) - TS
      PRINT5, C(I), A(I), SMC, SPM, PM, SAC, SPA, PA, TS,DS
   16 CONTINUE
      JA = JH
      KA = KH
      DO 12 I = JA,KA
      AM = SY*C(I) + CY
      YB = A(I) - AM
      NA(I) = YB + 1.0
      YA = YB*S(I) / (82.4 - AM)
      Y(I) = LOGF(YA)
      X(I) = (1.0 / T(I))
   12 CONTINUE
      CALL LINE
      PRINT 4
      DO 17 I = JL,KH
      AT(I)=EXPF(SY/T(I) + CY)
      SAC = AT(I)
      SPM = S(I) - SAC
      PA = 100.0*SAC/S(I)
      PM = 100.0*SPM/S(I)
      TS = SAC + SMC
      DS = S(I) - TS
      PRINT 6, C(I), S(I),       SPM, PM, SAC,       PA
   17 CONTINUE
      KA = KL
      JA = JL
      DO 13 I = JA,KA
      Y(I) = (S(I)*A(I) - AT(I)*82.4) / (S(I) - AT(I))
      X(I) = C(I)
      NA(I) = 1
   13 CONTINUE
   14 CONTINUE
   15 CONTINUE
      END
```

APPENDIX A

2. LEAST SQUARES LINE.

A. IDENTIFICATION

Title: Least Squares Line

Category: Line calculating

Programmer: Jay D. Rynbrandt

Date: July 29, 1966

B. PURPOSE

Given a set of X - Y points, calculate a least squares line through them.

C. USAGE

1. Calling sequence:

CALL LINE (X,Y,YY,DY,S,C,SDB,SDA,TIGS,W,N)

2. Arguments:

X is the array name of the independent variable.

Y is the array name of the dependent variable.

YY is the array name of the calculated dependent variable.

DY is the array name for the difference between Y and YY.

S is the slope.

C is the intercept.

SDB is the standard deviation of the slope.

SDA is the standard deviation of the intercept.

TIGS is the total sum of the squares of DY.

W is the array name of the weighting factors.

N is the number of data points.

3. Print-Outs: All values listed in calling sequences

4. Out-put formats: See listing.

5. Timing: Less than a second for 50 data points.

6. Accuracy: Floating point, single precision.

7. References: B. W. Lindgren and G. W. McElrath, Introduction to Probability and Statistics, The Mac Millan Co., New York (1959).

D. METHOD

$$C = \frac{\Sigma W_i \cdot Y_i \Sigma W_i \cdot X_i^2 - \Sigma W_i \cdot Y_i \cdot X_i \Sigma W_i \cdot X_i}{\Sigma W_i \Sigma W_i \cdot X_i^2 - (\Sigma W_i \cdot X_i)^2}$$

$$S = \frac{\Sigma W_i \Sigma W_i \cdot X_i \cdot Y_i - \Sigma W_i \cdot X_i \Sigma W_i \cdot Y_i}{\Sigma W_i \Sigma W_i \cdot X_i^2 - (\Sigma W_i \cdot X_i)^2}$$

See reference for standard deviation evaluation.

```
      SUBROUTINE LINE (X, Y, YY, DY, S, C, SDB, SDA, TIGS, 6, N)
      DIMENSION X(100),Y(100),W(100),YY(100),DY(100)
    1 FORMAT (*0SLOPE      =*E14.6)
    2 FORMAT (* INTERCEPT =*E14.6)
    3 FORMAT (*0      X               Y           Y CALC         RESIDUE
     1      W*/)
    4 FORMAT (5F14.7)
    5 FORMAT (*0STD DEV SLOPE  =*E14.6)
    6 FORMAT (* STD DEV INTCPT =*E14.6)
      P = N
      SS=0.0
      WS = 0.0
      XS=0.0
      YP=0.0
      YS=0.0
      DO 10  I = 1,N
      W(I) = ABSF(W(I))
      SS = SS + W(I)*X(I)**2
      WS = WS + W(I)
      XS=XS+X(I)*W(I)
      YP =  YP +X(I)*Y(I)*W(I)
      YS=YS+Y(I)*W(I)
   10 CONTINUE
      C = ((XS*YP) - (SS*YS))/((XS**2) - WS*SS)
      S = ((XS*YS) -WS*YP) / ((XS**2) - WS*SS)
      AVX = XS / P
      TIGS = 0.0
      TXS = 0.0
      PRINT 3
      DO 11 I = 1,N
      YY(I) = S *X(I) + C
      DY(I) =  Y(I) - YY(I)
      SIGS = DY(I)**2
      SXS = X(I)*(X(I) - AVX)
      TIGS = TIGS + SIGS
      TXS = TXS + SXS
      PRINT 4, X(I), Y(I), YY(I), DY(I), W(I)
   11 CONTINUE
      STIGS = TIGS/P
      STXS = TXS/P
      VARA = STIGS * (1.0 + AVX**2/STXS)/P
      VARB = STIGS / (P*STXS)
      VARA = ABSF(VARA)
      VARB = ABSF(VARB)
      SDA = SQRTF(VARA)
      SDB = SQRTF(VARB)
      PRINT 1,S
      PRINT 2,C
      PRINT 5, SDB
      PRINT 6, SDA
   13 RETURN
      END
```

APPENDIX B

1. LEAST SQUARES SPECTRA SYNTHESIZING.

A. IDENTIFICATION

Title: Least Squares Spectra Synthesizing.

Category: Curve fitting.

Programmer: Jay D. Rynbrandt

Date: July 29, 1966

B. PURPOSE

Given a spectrum as a series of X - Y coordinates, a shape function capable of fitting the curve and estimates of the parameters involved, more precise values of the parameters are obtained by adjusting them in an iterative process to obtain a best fit as judged by the sum of the squares of the deviation from the observed spectra. This specific program was used to reproduce an optical spectrum consisting of three peaks with four parameters used to describe each peak.

C. USAGE

1. Calling sequence:

Terms are stored and transferred through common.

2. Arguments:

X is the array name of the independent variable. The second subscript, I, is a running index over all points used. The first subscript denotes : 1. the wavelength in mu, 2. the wave number and 3. is an extra array in the event that X must be read in some different units and converted to one of the prior two.

Y is the array name of the dependent variable. The second subscript, I, is a running index over all points used. The first subscript, 1 - 6, designates: 1. the contribution from the IR band

at the point in the spectrum being considered, 2. the contribution from the R band, 3. that from the V band, 4. the observed spectra, 5. the calculated spectra and 6. the difference of the observed and calculated spectra.

W is the array name of the weighting factor which enables certain regions of the spectrum to be emphasized, The first subscript, 1 - 3, representing the peak; the second subscript, the point in question.

P is the array name of the parameters used for each peak. The first subscript, 1 - 3, designates the IR, R and V band, respectively; the second subscript, 1 - 3, relates to the skew factor, the linewidth and the peak center respectively.

B is the array name of the parameters related to the magnitude of the three peaks.

C is the array name of the adjustment increments with subscripts corresponding to those of P.

SO is the sum of the deviation squared.

TRYS is the number of attempts allowed to obtain a best fit by adjusting any particular parameter.

N is the number of points used to represent the spectrum.

J is the integer designating the particular band.

K is the integer ranging over three of the parameters describing each peak.

L represents the fitting function used.

TR is the number of times the program passed through a given point in subroutine SIZE.

3. Storage: 1300

4. Input, Output formats: See listing.

5. Timing:

   a. Compile 20 sec.

   b. Execution 10 sec for 10 iterations over three peaks.

6. Accuracy: Limited by the capacity of the shape function and the number of iterations.

7. References: 3h00/3600 Fortran Reference Manual, Control Data Corporation, Palo Alto, Calif. (1965).

Program IR FIT

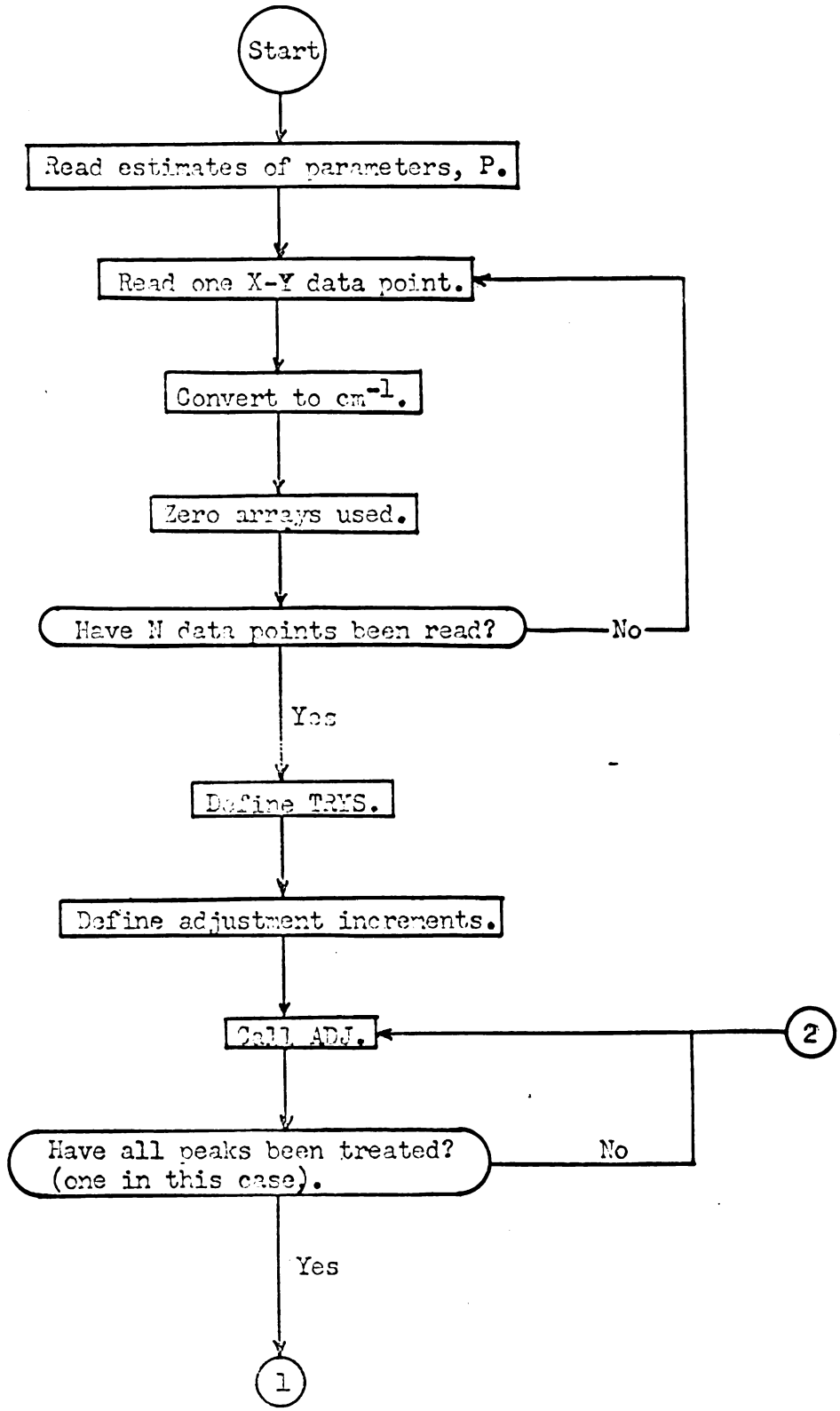

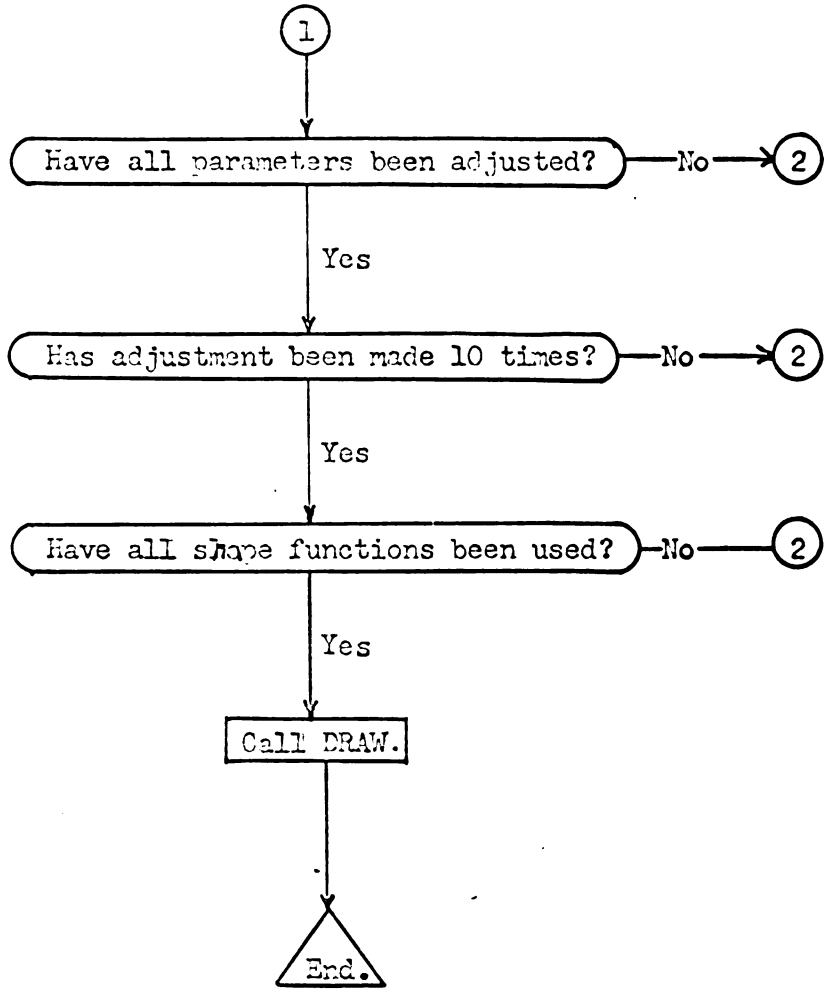
1
Have all parameters been adjusted?
No
2
Yes
Has adjustment been made 10 times?
No
2
Yes
Have all shape functions been used?
No
2
Yes
Call DRAW.
End.

Proposed Flow Chart fot IR FIT

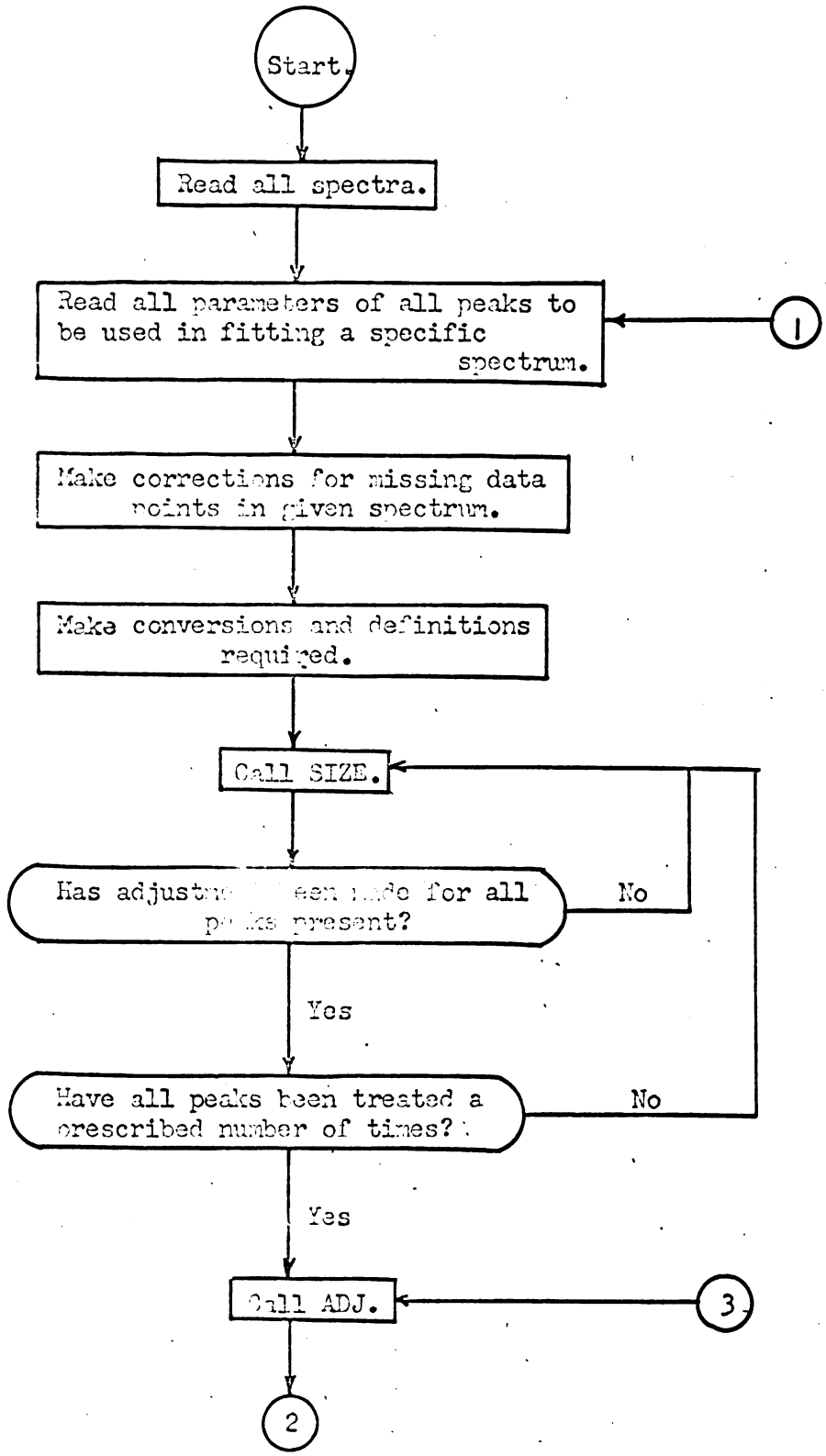

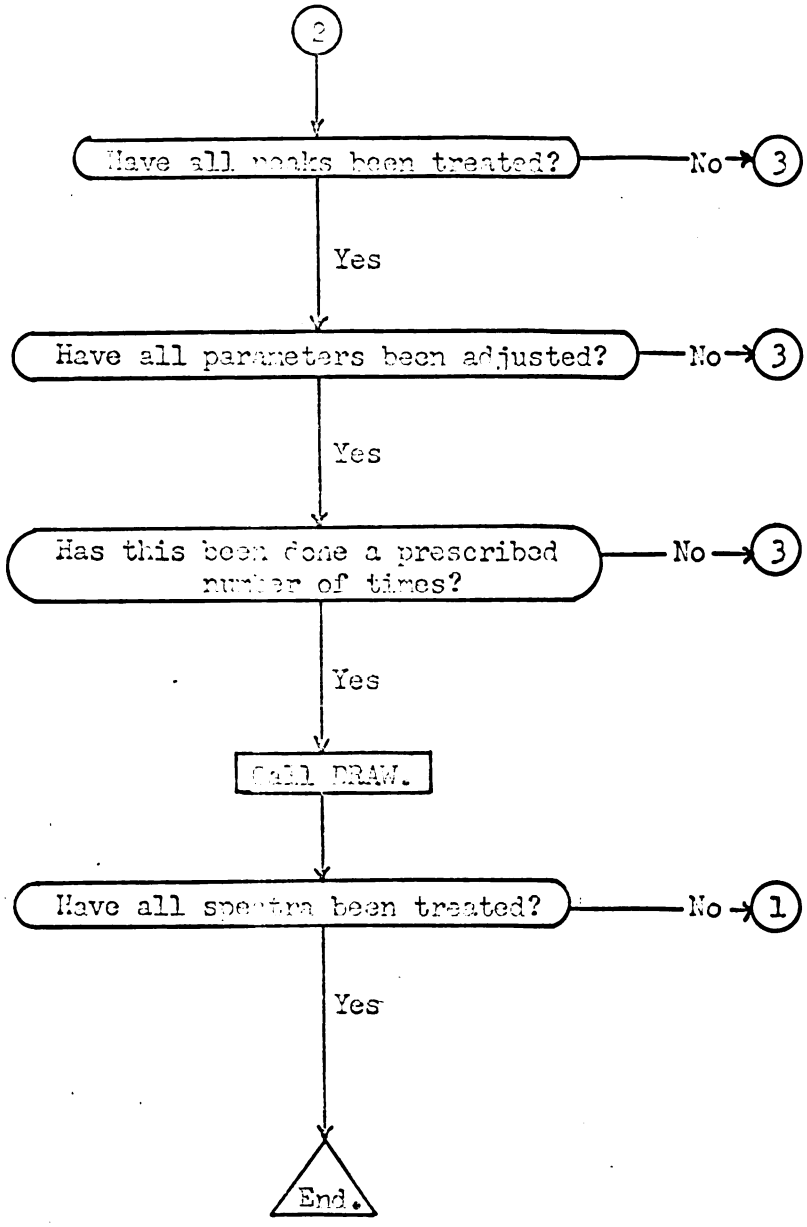
2
Have all peaks been treated?
No
3
Yes
Have all parameters been adjusted?
No
3
Yes
Has this been done a prescribed number of times?
No
3
Yes
Call DRAW.
Have all spectra been treated?
No
1
Yes
End.

```
      PROGRAM IR FIT
      COMMON X, Y, W, P, C, B, SO, TRYS, N, J, K, L, TR, BO
      DIMENSION X(3,100), Y(6,100), W(3,100), P(3,3), C(3,3), B(3)
    1 FORMAT (I2,A8)
    2 FORMAT (2E10.3)
    3 FORMAT (3E10.0)
    4 FORMAT (*1DATA OF SPECTRUM *A8)
    5 FORMAT (*0                              L =*I2)
      READ 1, N,RECORD
      READ 3, P(1,1), P(1,2), P(1,3)
      DO 11 I = 1,N
      READ2, X(1,I), Y(4,I)
      X(2,I) = 10000000.0/X(1,I)
      X(3,I) = 0.0
      Y(2,I) = 0.0
      Y(3,I) = 0.0
      W(1,I) = 1.0
      W(2,I) = 1.0
      W(3,I) = 1.0
   11 CONTINUE
      SO = 1.0
      TRYS = 25.0
      DO 15 L = 1,8
      PRINT 4, RECORD
      PRINT 5, L
      B(1) = 1.0
      BO = 0.4
      C(1,1)=0.1 $ C(1,2)=0.005 $ C(1,3)=0.002
      DO 14 NB = 1,10
      DO 14 J  = 1,1
      DO 14 K  = 1,3
      CALL ADJ
   14 CONTINUE
      CALL DRAW
   15 CONTINUE
      END
```

APPENDIX B

2. ADJUSTMENT MONITOR (ADJ.)

A. IDENTIFICATION

Title:	Adjustment Monitor
Category:	Curve Fitting
Programmer:	Jay D. Rynbrandt
Date:	July 29, 1966

B. PURPOSE

Given a set of parameters of which one is being adjusted, obtain the best value of that parameter.

C. USAGE

See Least Squares Spectra Synthesizing (IR FIT).

Subroutine ADJ

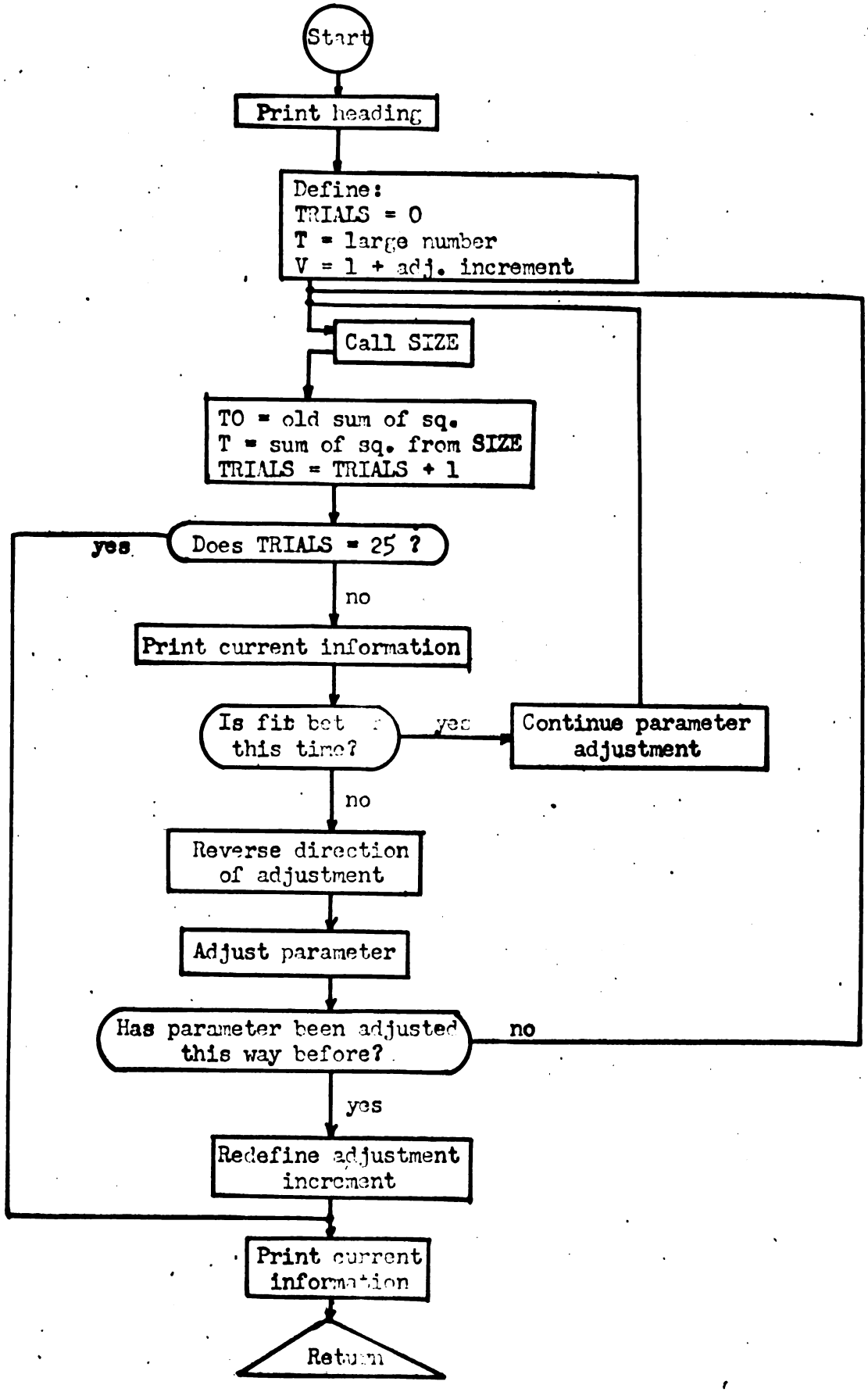

```
      SUBROUTINE ADJ
      COMMON X, Y, W, P, C, B, SO, TRYS, N, J, K, L, TR, BO
      DIMENSION X(3,100), Y(6,100), W(3,100), P(3,3), C(3,3), B(3)
    1 FORMAT (I6, I10, 4X, 4E12.4,2F7.1)
    2 FORMAT(/*     PK NO    CONST NO      CONST          ADJ           INT
     1    SO           TR     TRIALS*/)
      PRINT 2
      TRIALS = 0.0
      T = 999999.9
      V = 1.0 + C(J,K)
      DO 8 N1 = 1,2
    3 CONTINUE
      CALL SIZE
      TO = T
      T = SO
      TRIALS = TRIALS + 1.0
      IF  (TRIALS - TRYS) 5,9,9
    5 CONTINUE
      PRINT 1, J, K, P(J,K), C(J,K), B(J), SO, TR,TRIALS
      IF (T - TO)6,7,7
    6 CONTINUE
      P(J,K) = P(J,K)*V
      GO TO 3
    7 CONTINUE
      C(J,K) = -C(J,K)
      V = 1.0 + C(J,K)
      P(J,K) = P(J,K)*V
    8 CONTINUE
    9 CONTINUE
      C(J,K) = C(J,K)*TRIALS/10.0
      PRINT 1, J, K, P(J,K), C(J,K), B(J), SO, TR,TRIALS
      RETURN
      END
```

APPENDIX B

3. MAGNITUDE ADJUSTMENT (SIZE)

A. IDENTIFICATION

Title:	Size
Category:	Curve Fitting
Programmer:	Jay D. Rynbrandt
Date:	July 29, 1966

B. PURPOSE

Given a spectrum as a series of X - Y coordinates, a shape function capable of fitting the curve and a set of parameters other than magnitude, adjust the magnitude to give the lowest sum of squares of the deviation from the observed spectra.

C. USAGE

See Least Squares Spectra Synthesizing (IR FIT).

Subroutine SIZE

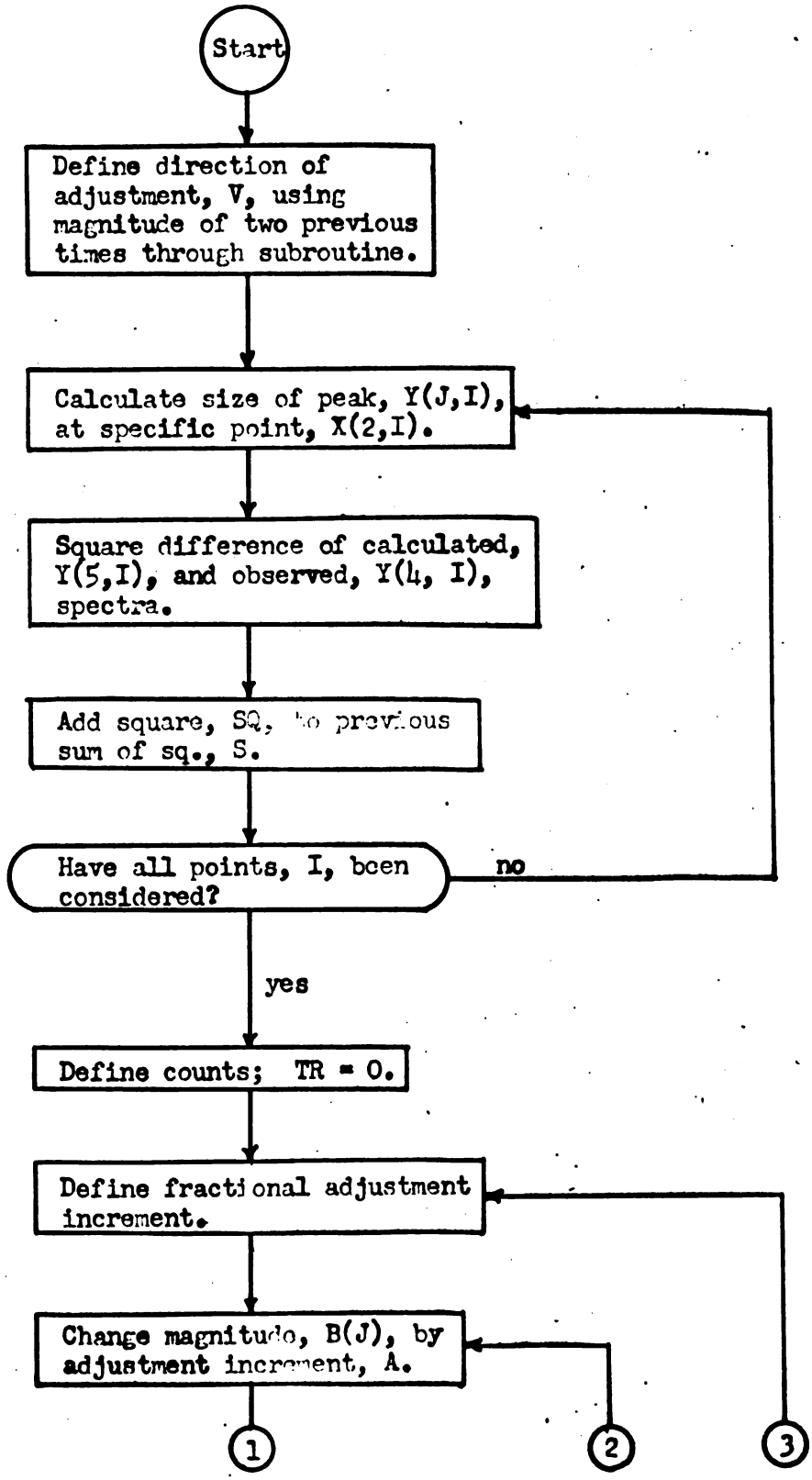

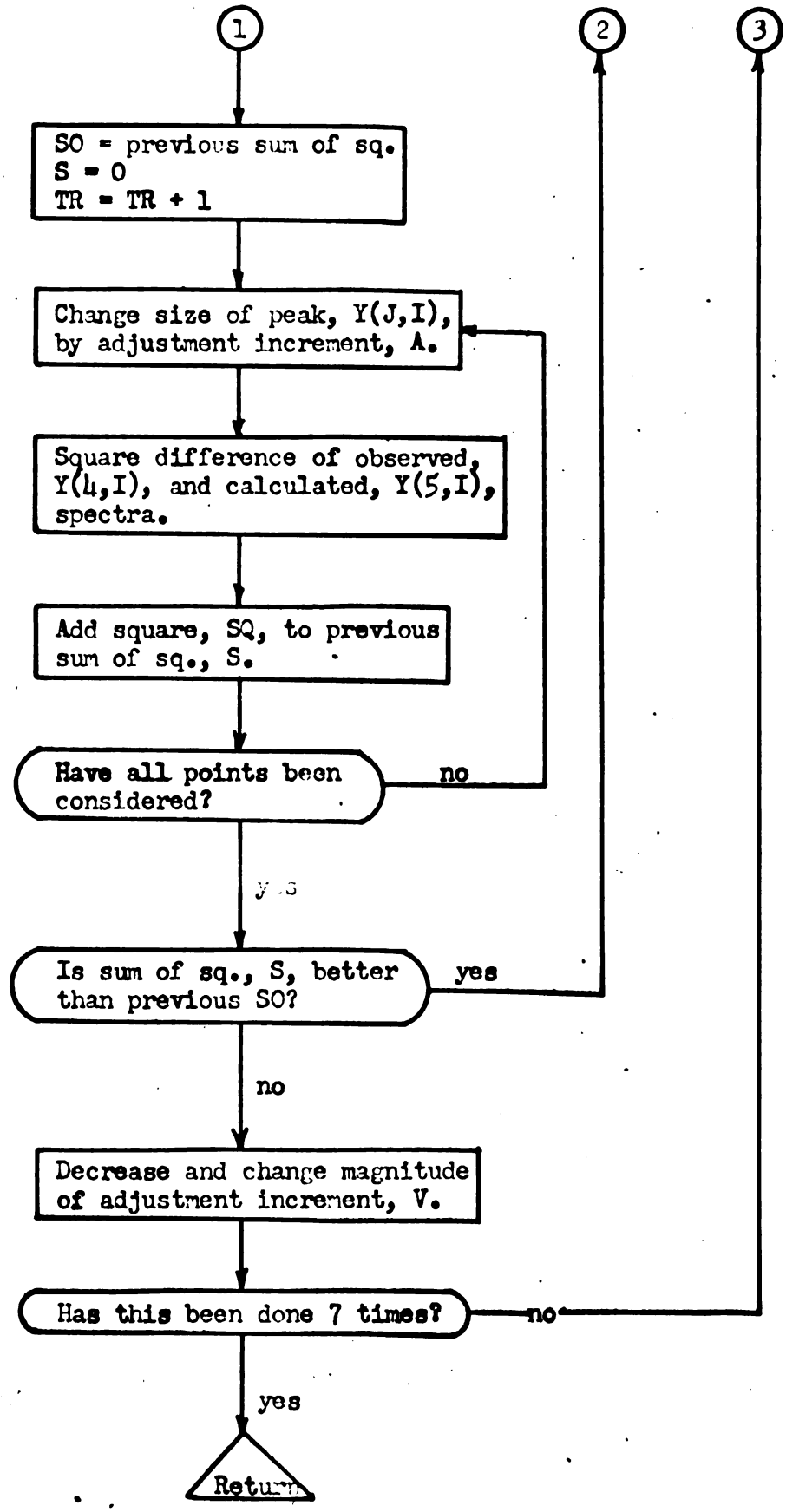
1
2
3
SO = previous sum of sq.
S = 0
TR = TR + 1
Change size of peak, Y(J,I), by adjustment increment, A.
Square difference of observed, Y(4,I), and calculated, Y(5,I), spectra.
Add square, SQ, to previous sum of sq., S.
Have all points been considered?
no
yes
Is sum of sq., S, better than previous SO?
yes
no
Decrease and change magnitude of adjustment increment, V.
Has this been done 7 times?
no
yes
Return

```
      SUBROUTINE SIZE
      DIMENSION X(3,100), Y(6,100), W(3,100), P(3,3), C(3,3), B(3)
      COMMON X, Y, W, P, C, B, SO, TRYS, N, J, K, L, TR, BO
      S = 0.0
      V = 0.025*(B(J)-BO)/ABSF(B(J)-BO)
      BO = B(J)
      GO TO (10,12,14,16,18,20,22,24) L
   10 CONTINUE
      DO 11 I = 1,N
      R = X(2,I) - P(J,3)
      PX = P(J,1)*X(2,I)
      Y(J,I) = B(J)*(1.+PX    )/(1.+(P(J,2)*R)**2)
      Y(5,I) = Y(1,I) + Y(2,I) + Y(3,I)
      Y(6,I) = Y(4,I) - Y(5,I)
      SQ = W(J,I)*Y(6,I)**2
      S = S + SQ
   11 CONTINUE
      GO TO 4
   12 CONTINUE
      DO 13 I = 1,N
      R = X(2,I) - P(J,3)
      PX = P(J,1)*X(2,I)
      Y(J,I) = B(J)*(1.+PX**2)/(1.+(P(J,2)*R)**2)
      Y(5,I) = Y(1,I) + Y(2,I) + Y(3,I)
      Y(6,I) = Y(4,I) - Y(5,I)
      SQ = W(J,I)*Y(6,I)**2
      S = S + SQ
   13 CONTINUE
      GO TO 4
   14 CONTINUE
      DO 15 I = 1,N
      R = X(2,I) - P(J,3)
      PX = P(J,1)*X(2,I)
      Y(J,I) = B(J)*(1.+PX**3)/(1.+(P(J,2)*R)**2)
      Y(5,I) = Y(1,I) + Y(2,I) + Y(3,I)
      Y(6,I) = Y(4,I) - Y(5,I)
      SQ = W(J,I)*Y(6,I)**2
      S = S + SQ
   15 CONTINUE
      GO TO 4
   16 CONTINUE
      DO 17 I = 1,N
      R = X(2,I) - P(J,3)
      PX = P(J,1)*X(2,I)
      Y(J,I) = B(J)*(1.+PX**4)/(1.+(P(J,2)*R)**2)
      Y(5,I) = Y(1,I) + Y(2,I) + Y(3,I)
      Y(6,I) = Y(4,I) - Y(5,I)
      SQ = W(J,I)*Y(6,I)**2
      S = S + SQ
```

```
17 CONTINUE
   GO TO 4
18 CONTINUE
   DO 19 I = 1,N
   R = X(2,I) - P(J,3)
   PR = P(J,1)*R
   Y(J,I) = B(J)*(1.+PR    )/(1.+(P(J,2)*R)**2)
   Y(5,I) = Y(1,I) + Y(2,I) + Y(3,I)
   Y(6,I) = Y(4,I) - Y(5,I)
   SQ = W(J,I)*Y(6,I)**2
   S = S + SQ
19 CONTINUE
   GO TO 4
20 CONTINUE
   DO 21 I = 1,N
   R = X(2,I) - P(J,3)
   PR = P(J,1)*R
   AR = ABSF(PR)
   Y(J,I) = B(J)*(1.+PR*AR)/(1.+(P(J,2)*R)**2)
   Y(5,I) = Y(1,I) + Y(2,I) + Y(3,I)
   Y(6,I) = Y(4,I) - Y(5,I)
   SQ = W(J,I)*Y(6,I)**2
   S = S + SQ
21 CONTINUE
   GO TO 4
22 CONTINUE
   DO 23 I = 1,N
   R = X(2,I) - P(J,3)
   PR =(P(J,1)*R)**3
   Y(J,I) = B(J)*(1.+PR    )/(1.+(P(J,2)*R)**2)
   Y(5,I) = Y(1,I) + Y(2,I) + Y(3,I)
   Y(6,I) = Y(4,I) - Y(5,I)
   SQ = W(J,I)*Y(6,I)**2
   S = S + SQ
23 CONTINUE
   GO TO 4
24 CONTINUE
   DO 25 I = 1,N
   R = X(2,I) - P(J,3)
   PR =(P(J,1)*R)**3
   AR = ABSF(P(J,1)*R)
   Y(J,I) = B(J)*(1.+PR*AR)/(1.+(P(J,2)*R)**2)
   Y(5,I) = Y(1,I) + Y(2,I) + Y(3,I)
   Y(6,I) = Y(4,I) - Y(5,I)
   SQ = W(J,I)*Y(6,I)**2
   S = S + SQ
25 CONTINUE
   GO TO 4
```

```
4 CONTINUE
  TR = 0.0
  DO 8 N2 = 1.7
  A = 1.0 + V
5 CONTINUE
  B(J) = B(J) *A
  SO = S
  S = 0.0
  TR = TR+1.0
  DO 6 I = 1.N
  Y(J.I) = Y(J.I)*A
  Y(5.I) = Y(1.I) + Y(2.I) + Y(3.I)
  Y(6.I) = Y(4.I) - Y(5.I)
  SQ = W(J.I)*Y(6.I)**2
  S = S + SQ
6 CONTINUE
  IF (S - SO) 5.7.7
7 CONTINUE
  V = -V*0.25
8 CONTINUE
  RETURN
  END
```

APPENDIX B

4. INFORMATION PRINTOUT (DRAW)

A. IDENTIFICATION

Title:	Information Printout
Programmer:	Jay D. Rynbrandt
Date:	July 29, 1966

B. PURPOSE

Printout information obtained previously.

```
      SUBROUTINE DRAW
      DIMENSION X(3,100), Y(6,100), W(3,100), P(3,3), C(3,3), B(3)
      COMMON X, Y, W, P, C, B, SO, TRYS, N, J, K, L, TR, BO
    1 FORMAT (*1    X OBS      LAMDA      CM-1     ABS CALC  ABS OBS  RESIDU
     1E      Y IR      WT IR        Y R       WT R        Y V       WT V*/)
    2 FORMAT (3F10.1,9F10.5)
      PRINT 1
      DO 12 I = 1,N
      PRINT 2,X(3,I),X(1,I),X(2,I),Y(5,I),Y(4,I),Y(6,I),Y(1,I),W(1,I),
     1Y(2,I),W(2,I),Y(3,I),W(3,I)
   12 CONTINUE
      RETURN
      END
```

APPENDIX C

1. GENERALIZED LEAST SQUARES

A. IDENTIFICATION

Title: Generalized Least Squares

Category: Parameter adjustment

Programmer: Jay D. Rynbrandt

Date: July 29, 1966

B. PURPOSE

Given F $(x_i, y_i, a^o, b^o, c^o)$, find the corrections to a^o, b^o, and c^o so as to minimize the weighted deviations,

$$D = \sum Wy_i (y_{obs} - y_{calc})^2 + Wx_i (x_{obs} - x_{calc})^2$$

C. USAGE

1. Arguments:

X is the array name of the independent variable.

Y is the array name of the dependent variable.

C is the array name of the parameters to be adjusted.

RECORD is the array name used to store and print the date set identification.

S is the array name for the nuclear spins.

P is the array name for the partial derivatives (partials) calculated at each point.

SB is the array name for some sums of partials going into subroutine SQRTMET and that for the corrections to the parameters which it calculates.

ST is the array name used to sum the products of partial derivatives calculated.

WY is the array name of the weights.

Y1, Y11 are the array names for the calculated single line contribution (Y11 being that obtained with weighing factors of 1).

Y4, Y14 are the array names for the calculated four line patterns.

YC, Y1C are the array names for the calculated spectrum.

YD, Y1D are the array names for the difference of the observed and calculated spectra.

N is the number of points in a particular data set.

2. Print Outs: All parameters with each adjustment and all observed and calculated spectra.

3. Input and Output Formats: See listing.

4. Timing: Less than one second for each complete adjustment with 50 data points.

5. Accuracy: Single precision, adjustment completed in three cycles.

6. References: W. E. Wentworth, J. Chem. Ed., 42, (2), 96 (1965)
W. E. Wentworth, J. Chem. Ed., 42, (3),162 (1965).

D. METHOD

Given:

$$F_i = F_i\ (\bar{x}_i, \bar{y}_i, a, b, c) = 0$$

a, b and c are the least squares estimate of these parameters.

$$F_i^o = F_i^o\ (x_i, y_i, a^o, b^o, c^o)$$

x_i, y_i, are the observed variables;

a^o, b^o, c^o are the estimated parameters.

If

$$A = a^o - a$$

$$B = b^o - b$$

$$C = c^o - c$$

then A, B and C can be found by solving the symmetric matrix:

$$\sum \frac{Fa_i Fa_i}{L_i} A + \sum \frac{Fa_i Fb_i}{L_i} B + \sum \frac{Fa_i Fc_i}{L_i} C = \sum \frac{Fa_i F_i^{\circ}}{L_i}$$

$$\sum \frac{Fb_i Fa_i}{L_i} A + \sum \frac{Fb_i Fb_i}{L_i} B + \sum \frac{Fb_i Fc_i}{L_i} C = \sum \frac{Fb_i F_i^{\circ}}{L_i}$$

$$\sum \frac{Fc_i Fa_i}{L_i} A + \sum \frac{Fc_i Fb_i}{L_i} B + \sum \frac{Fc_i Fc_i}{L_i} C = \sum \frac{Fc_i F_i^{\circ}}{L_i}$$

in which

$$L_i = \frac{Fx_i^2}{Wx_i} + \frac{Fy_i^2}{Wy_i}$$

and

Wx_i, Wy_i are the weighting factors of x_i and y_i,

and

$$Fx_i = \frac{\partial F_i}{\partial x}\Bigg|_{(x_i, y_i, a^{\circ}, b^{\circ}, c^{\circ}),\ \text{etc.}}$$

$$Fa_i = \frac{\partial F_i}{\partial a}\Bigg|_{(x_i, y_i, a^{\circ}, b^{\circ}, c^{\circ}),\ \text{etc.}}$$

Program GEN LS

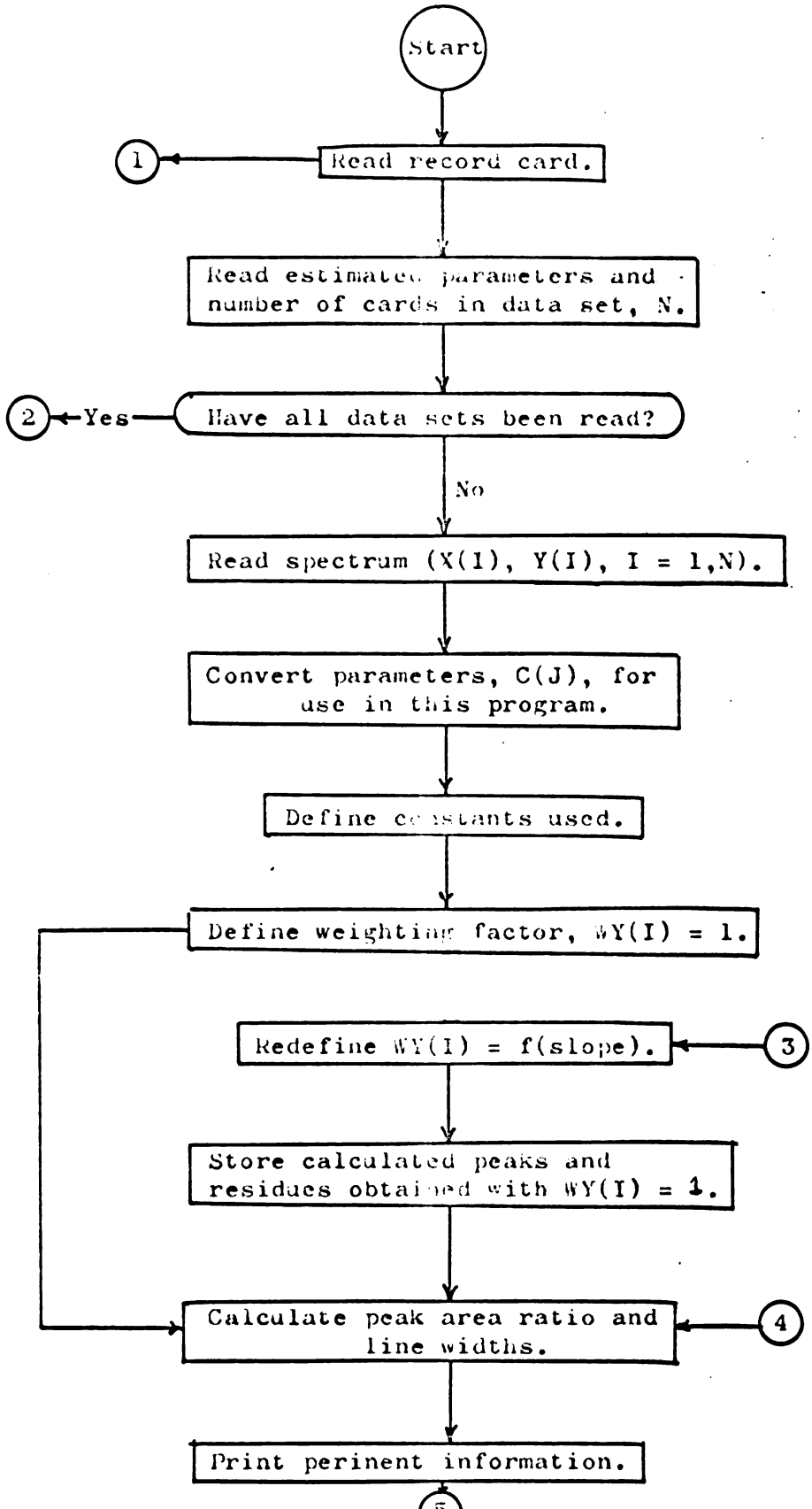

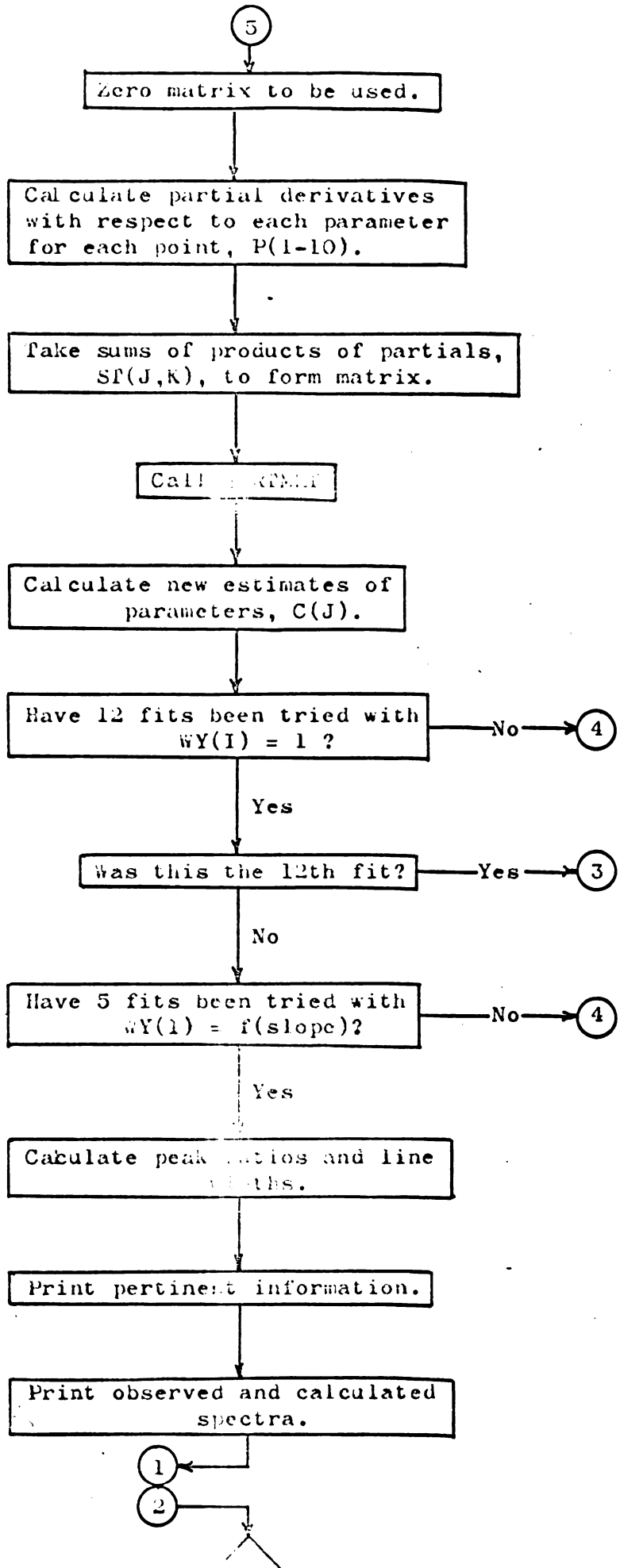
5
Zero matrix to be used.
Calculate partial derivatives with respect to each parameter for each point, P(1-10).
Take sums of products of partials, SF(J,K), to form matrix.
Call
Calculate new estimates of parameters, C(J).
Have 12 fits been tried with WY(I) = 1 ?
No
4
Yes
Was this the 12th fit?
Yes
3
No
Have 5 fits been tried with WY(1) = f(slope)?
No
4
Yes
Calculate peak ratios and line widths.
Print pertinent information.
Print observed and calculated spectra.
1
2

```
      PROGRAM GEN L S
      DIMENSION X(100),Y(100),C(10),RECORD(10),S(10),P(10),SB(10),
     1          ST(10,10),                    WY(100),       Y1(100),Y4(100),
     2           YD(100),YC(100),Y1C(100),Y11(100),Y14(100),Y1D(100)
    1 FORMAT (8E5.0,I5)
    2 FORMAT (2E10.0)
    3 FORMAT (    12F11.5)
    4 FORMAT (H1,10A8)
    5 FORMAT (*0    RI4/RI1        RI J       INT 4          A 4          W 4
     1     CEN 4        RI 1       INT 1         W 1       CEN 1          AVY
     2    SUM SQ*/)
    6 FORMAT (10A8)
    7 FORMAT (*0       X(I)      Y OBS     Y CALC      Y 4LN      Y 1LN     W
     1Y       RES         I RES WY=1      Y C         Y 1         Y 4*/)
    9 FORMAT (7F10.5,I5,4F10.5)
   10 FORMAT (9E14.4)
   18 CONTINUE
      READ 6, (RECORD(I), I = 1,10)
      READ  1,C(1),C(2),C(3),W4,W1,C(6),C(7),C(8),N
      IF (N-1)33,33,19
   19 CONTINUE
      READ  2, (X(I),Y(I),I=1,N)
      W4 = W4*2.0
      W1 = W1*2.0
      SRT = 1.414214
      C(3) = C(3)/3.0
      C(4) = SRT/W4
      C(5) = SRT/W1
      C(1)= C(1)/C(4)/C(4)
      C(7) = C(7)/C(5)/C(5)
      AR = 0.0691/0.9308
      SR = 9.07477/16.53766
      S(1)=-1.5$S(2)=-0.5$S(3)=0.5$S(4) = 1.5
      PRINT 4, (RECORD(I),I = 1,10)
      DO 99 L = 1,2
      GO TO (34,35) L
   34 CONTINUE
      NADJ = 12
      DO 20 I = 1,N
   20 WY(I) = 1.0
      GO TO 39
   35 CONTINUE
      NADJ = 5
      NM = N -1
      SW = 0.0
      DO 36 I = 2,NM
      IP = I + 1
      IM = I -1
      WY(I) = 1.0/(ABSF(Y(IP) -Y(IM)) + 1.0)
   36 SW = SW + WY(I)
```

```
      DO 37 I = 2,NM
   37 WY(I) =WY(I)*NM/SW
      WY(1) = 1.0
      WY(N) = 1.0
      DO 38 I = 1,N
      Y1C(I) = YC(I)
      Y11(I) = Y1(I)
      Y14(I) = Y4(I)
   38 Y1D(I) = YD(I)
   39 CONTINUE
      PRINT 5
      SQ = 0.0
      DO 99 NTIMES = 1,NADJ
      W4 = SRT/C(4)
      W1 = SRT/C(5)
      RI4 = 4.0*(1.0+AR)*C(1)/C(4)
      RI1 = C(7)/C(5)
       RAT = RI1 / RI4
      PRINT 3,RAT,RI4,C(1),C(3),W4,C(2),RI1,C(7),W1,C(6),C(8),SQ
      DO 22 J = 1,9
      DO 22 K = J,9
   22 ST(J,K) = 0.0
      SQ = 0.0
      DO 26 I = 1,N
      DO 23 J = 1,10
   23 P(J) = 0.0
      DO 24 M = 1,4
      RK = X(I) + S(M)*C(3) - C(2)
      RI = X(I) + S(M)*C(3)*SR - C(2)
      PK = C(1)*C(4)*C(4)*RK*EXPF(-(C(4)*RK)**2)
      PI = C(1)*C(4)*C(4)*RI*EXPF(-(C(4)*RI)**2)*AR
      P(1) = P(1) + (PK + PI)/C(1)
      PC = -PK/RK-PI/RI+PK*C(4)*C(4)*2.0*RK + PI*C(4)*C(4)*2.0*RI
      P(2) = P(2) + PC
      P(3) = P(3)+S(M)*(PK/RK+PI*SR/RI-PK*C(4)*C(4)*2.*RK-PI*SR*C(4)
     1        *C(4)*2.*RI)
      P(4) = P(4) + (PK +PI)*2.0/C(4) -PK*RK*RK*2.0*C(4)-PI*RI*RI*2*C(4)
      P(9) = P(9) + PK + PI
      P(10) = P(10) - PC
   24 CONTINUE
      RS = X(I) - C(6)
      PS = C(7)*C(5)*C(5)*RS*EXPF(-(C(5)*RS)**2)
      P(5) = PS*2.0/C(5) - PS*RS*RS*C(5)*2.0
      P(6) = -PS/RS + PS*C(5)*C(5)*RS*2.0
      P(7) = PS/C(7)
      P(8) = 1.0
      Y4(I) = P(9)
      P(9) = P(9) + PS + C(8) - Y(I)
      P(10) =(P(10) - P(6))**2  + 1.0/WY(I)
      YC(I) = P(9) + Y(I)
      Y1(I) = PS
      YD(I) = P(9)
      SQ = SQ + P(9)*P(9)
```

```
      DO 25 J = 1,9
      DO 25 K = J,9
   25 ST(J,K) = ST(J,K) + P(J)*P(K)/P(10)
   26 CONTINUE
      NX = 8
      DO 98 J = 1,NX
      SB(J) = ST(J,9)
   98 CONTINUE
      CALL SQRTMET(ST,SB,NX)
      DO 31 J = 1,NX
   31 C(J) = C(J)-SB(J)
   99 CONTINUE
      W4 = SRT/C(4)
      W1 = SRT/C(5)
      RI4 = 4.0*(1.0+AR)*C(1)/C(4)
      RI1 = C(7)/C(5)
       RAT = RI1 / RI4
      PRINT 3,RAT,RI4,C(1),C(3),W4,C(2),RI1,C(7),W1,C(6),C(8),SQ
      PRINT 4, (RECORD(I),I = 1,10)
      PRINT 7
      DO 32 I = 1,N
   32 PRINT 9, X(I),Y(I),YC(I),Y4(I),Y1(I),WY(I),YD(I),I,Y1D(I),Y1C(+),
     1          Y11(I),Y14(I)
      GO TO 18
   33 CONTINUE
      END
C     TWO BLANK CARDS SHOULD BE AT END OF DATA DECK
```

APPENDIX C

2. SQUARE-ROOT METHOD

A. IDENTIFICATION

Title: Square-Root Method

Category: Symmetric Linear Systems Solving

Programmer: Dr. R. H. Schwendenan, Department of Chemistry, Michigan State University

Date: January 1, 1966

B. PURPOSE

Given: AX = B in which A is a symmetric matrix and X and B are column matrices, find the values of X.

C. USAGE

1. Calling sequence:

   CALL SQRTMET (P, W, N)

2. Arguments:

   P is the array name of the symmetric matrix.

   W is the array name of the column matrix read in and the solutions to the linear system after execution.

   N is the order of the matrix.

3. Print-Outs: None.

4. Timing: Fast.

5. Accuracy: Single precision, to accuracy of input values.

6. Reference: V. N. Faddeeva, Computational Methods of Lineal Algebra, Translator C. D. Benster, Dover Publications Inc., New York.

D. METHOD

The symmetric matrix, A, is resolved into the product of a triangular matrix and its transpose

$$A = S'S$$

then

$$S'K = B$$

$$SX = K$$

This subroutine calculates the triangular matrix S. From the triangular matrix it is a simple matter to calculate K and from K to calculate X.

```
      SUBROUTINE SQRTMET (P,W,N)
      DIMENSION P(10,10), W(10)
      NN=N+1
      NM=N-1
   10 DO 50 I=1,N
      P(I,NN)=W(I)
      JM=I-1
      SUM=P(I,I)
      DO 20 J=1,JM
   20 SUM=SUM-W(J)*P(J,I)**2
      W(I)=SUM/ABSF(SUM)
      SUM    =SQRTF(ABSF(SUM))
      P(I,I)=SUM
      JP=I+1
      DO 40 J=JP,NN
      TUM=P(I,J)
      DO 30 K=1,JM
   30 TUM=TUM-P(K,I)*P(K,J)*W(K)
   40 P(I,J)=TUM/SUM
   50 CONTINUE
      W(N)=W(N)*P(N,NN)/P(N,N)
      DO 70 I=1,NM
      SUM=P(N-I,NN)
      JP=N-I+1
      DO 60 J=JP,N
   60 SUM=SUM-P(N-I,J)*W(J)
   70 W(N-I)=W(N-I)*SUM/P(N-I,N-I)
      END
```

APPENDIX D

1. LINEWIDTH ANALYSIS

A. IDENTIFICATION

Title: Polynomial Linewidth Fit

Category: Curve Fitting

Programmer: Jay D. Rynbrandt

Date: July 29, 1966

B. PURPOSE

Given the heights of a series of ESR hyperfine lines, obtain the linewidths and from them, the polynomial describing their dependency on the nuclear spin quantum number m_I.

C. USAGE

1. Calling sequence:

   Main program.

2. Arguments:

   S is the array name of the nuclear spins.

   W is the array name of the linewidths.

   WC is the array name of the linewidths calculated from the coefficients of the least squares polynomial.

   B is the array name of the coefficients.

   SB is the array representing the estimated errors in B.

   TT is the array name of the temperatures of all the samples.

   C is the array name of the coefficients calculated for all samples.

   EC is the array name of the estimated errors in C for all samples.

   TR is the array name of 1 / Kelvin temperature.

   H is the array name of the heights.

RE is the array name of the spectra identifications.

WS is the width of the standard line.

IS is the number of the standard line.

M is the number of data sets for a particular spectrum.

3. Output-Input Formats: See listing.

4. Timing: 1 minute for 100 spectra.

5. References: Jay D. Rynbrandt, MS Thesis, Michigan State University, (1966). Los Alamos Subroutine Description M-050.

D. METHOD

The heights, H(I), of the various hyperfine lines are read-in, along with the linewidths of a standard line, WS, which has been accurately determined. The linewidth of all of the lines are then determined from the expression

$$W(I) = WS\ (H\ (IS)\ /\ H\ (I)\ )^{\frac{1}{2}}$$

in which IS represents the number of the standard line. The polynomial describing the linewidth as a function of m_I is then calculated in subroutine LSQPOL.

```
      PROGRAM POLY LW
      DIMENSION S(100),W(100),WC(100),SB(10),B(10),TT(200),C(5,200),
     1          EC(5,200),TR(200),H(100),RE(200)
    1 FORMAT (A8,2X,2E10.2,2I5)
    2 FORMAT (8E 5.2)
    3 FORMAT (1H1,30X,* DATA OF SPECTRUM NO. *A8*   L =*I3)
    4 FORMAT (//* DEG CENT =*F9.4,5X,*STANDARD  L W   =*F8.3)
    5 FORMAT (*0SPINS    *8F10.3)
    6 FORMAT (* HEIGHTS *8F10.3)
    7 FORMAT (* WIDTHS  *8F10.3)
    8 FORMAT (*1  L    T     1/K        C 1          E 1          C 2
     1  E 2          C 3          E 3          C 4          E 4          C 5
     2         E 5*/)
    9 FORMAT (I4,F4.0,F9.6,2X,4(E12.4,E11.3),2X,A8)
   10 FORMAT (   * DEG KELV =*F9.4,5X, *NO OF STD L W   =*I4)
   11 FORMAT (   * 1/D KELV =*F9.6,5X, *NO OF DATA PTS  =*I4)
   12 FORMAT (*0  L    T     1/K        C 1          E 1          C 2
     1  E 2          C 3          E 3          C 4          E 4          C 5
     2         E 5*/)
   13 FORMAT (I5,F5.0,4E14.7,2X,A8)
      L = 0
  100 READ 1,REC,WS,T,IS,M
      IF(M)120,120,110
  110 READ 2, (H(I),I = 1,M)
      L = L+1
      SH = 4.5
      DO 20 I = 1,M
      SH = SH - 1.
   20 S(I) = SH
      DO 19 I = 1,M
      IF (H(I)) 17,17,19
   17 M = M-1
      IF (IS-I)15,15,16
   16 IS = IS-1
   15 CONTINUE
      DO 18 II = I,M
      IP = II+1
      H(II) = H(IP)
   18 S(II) = S(IP)
      I = I-1
   19 CONTINUE
```

```
      DO 21 I = 1,M
   21 W(I)= WS*SQRTF(H(IS)/H(I))
      PRINT 3,REC,L
      DK = 273.15+T
      RK = 1.0/DK
      PRINT 4,T ,WS
      PRINT 10,DK,IS
      PRINT 11,RK,M
      PRINT 5,(S(I),I = 1,M)
      PRINT 6,(H(I),I = 1,M)
      PRINT 7,(W(I),I = 1,M)
      KM = 4
      CALL LSQPOL (M,KM,S,W,WC,B,SB,SIG)
      PUNCH 13,L,T,B(1),B(2),B(3),B(4),REC
      DO 22 LP = 1,KM
      C(LP,L) = B(LP)
   22 EC(LP,L) = SB(LP)
      TT(L) = T
      TR(L) = RK
      RE(L) = REC
      PRINT 12
      PRINT 9,  L ,TT(L ),TR(L ),(C(LP,L ),EC(LP,L ),LP=1,KM),RE(L)
      GO TO 100
  120 CONTINUE
      PRINT 8
      PRINT 9, (LS,TT(LS),TR(LS),(C(LP,LS),EC(LP,LS),LP=1,KM),RE(LS),
     1          LS = 1,L)
      END
```

APPENDIX D

2. LEAST SQUARES POLYNOMIAL FITTING

A. IDENTIFICATION

Title:	Least Squares Polynomial Fitting
Co-op Ident.	E2 JCSD LSQPOL
Category:	Curve Fitting
Programmer:	T. L. Jordan and R. E. Vogel, Los Alamos Scientific Laboratory, New Mexico. Modified and tested on the CDC 1604 by George A. Baker, Jr. and E. Clark.
Date:	September 19, 1961

B. PURPOSE

Given X: $(X_1, X_2, \ldots X_m)$ and Y: $(Y_1, Y_2, \ldots Y_m)$ where Y is the observed dependent variable and X is the observed independent variable, the polynomial

$$Y = B_1 + B_2X + \ldots B_{km+1} X^{km}$$ is fitted to all degrees KM KM $_{max}$.

C. USAGE

1. Calling Sequence:

CALL LSQPOL (M, KM, X, Y, YCAL, DELM, B, SD, SIGMA)

2. Arguments:

M is the number of data points, M 100.

KM is the maximum degree of fit, KM 10.

X is the array name of observed independent variables.

Y is the array name of observed dependent variables.

YCAL is the output array name of the estimated dependent variable.

DELY is the output array name for the difference between Y and YCAL.

B is the output array name for the coefficients of the powers of X.

SB is the output array name of the estimates of the errors in B.

SIGMA is the standard deviation corrected for the order of fit used.

3. Output Formats: See listing.

4. Timing: Roughly 0.2 sec. per degree of fit for 30 data points.

5. Accuracy: Floating point, single precision.

6. References: Los Alamos Subroutine Description L-050.

D. METHOD

YCAL = $B_1 + B_2X + \ldots B_{KM+1} X^{KM}$ is obtained by collecting the powers of X in a set of orthogonal polynomials which are generated by this subroutine.

$$SIGMA = \sqrt{\frac{\sum^{M} (YCAL_i - Y_i)^2}{M - (KM + 1)}}$$

```
      SUBROUTINE LSQPOL(M,KM,X,Y,YCAL,B,SB,SIGMA)
      DIMENSION S(10),X(100),Y(100),ST(10),SB(10),P(100),B(10),
     1DELY(100),A(10,10),T(10),YCAL(100),PM(100)
      A(1,1)=1.0
      A(2,2)=1.0
      YBAR=0.0
      XBAR=0.0
      DO 10 I=1,M
      PM(I)=1.0
      YBAR=YBAR+Y(I)
   10 XBAR=XBAR+X(I)
      XBAR=XBAR/M
      T(1)=YBAR/M
      A(2,1)=-XBAR
      PXF=0.0
      PXP=0.0
      DO 20 I=1,M
      P(I)=X(I)-XBAR
      PXF=PXF+P(I)*Y(I)
   20 PXP=PXP+P(I)*P(I)
      T(2)=PXF/PXP
      PMXPM=M
      S(1)=PMXPM
      B(1)=T(1)*A(1,1)+T(2)*A(2,1)
      B(2)=T(2)*A(2,2)
   60 DO 190 K=2,KM
      L=K-1
      IF(K-2)190,165,65
   65 XPXP=0.0
      XPXPM=0.0
      B(K)=0.0
      DO 70 J=1,M
      XP=X(J)*P(J)
      XPXP=XPXP+XP*P(J)
   70 XPXPM=XPXPM+XP*PM(J)
      ALPHA=XPXP/PXP
      BETA=XPXPM/PMXPM
      PPXF=0.0
      PPXPP=0.0
      DO 90 I=1,M
   80 PT=P(I)
   81 P(I)=X(I)*PT-ALPHA*PT-BETA*PM(I)
   82 PPXF=PPXF+P(I)*Y(I)
   83 PPXPP=PPXPP+P(I)*P(I)
   90 PM(I)=PT
```

```
      T(K)=PPXF/PPXPP
      PMXPM=PXP
      PXP=PPXPP
      A(K,1)=-ALPHA*A(K-1,1)-BETA*A(K-2,1)
      A(K,K-1)=A(K-1,K-2)-A(K-1,K-1)*ALPHA
      A(K,K)=1.0
      IF(K-3)150,150,110
  110 K1=K-2
      DO 120 I=2,K1
  120 A(K,I)=A(K-1,I-1)-ALPHA*A(K-1,I)-BETA*A(K-2,I)
  150 DO 160 I=1,K
  160 B(I)=B(I)+T(K)*A(K,I)
  165 SIG2=0.0
      DO 180 I=1,M
      YCAL(I)=B(K)
      KK=K-1
      DO 40 J=1,KK
      IK=K-J
   40 YCAL(I)=X(I)*YCAL(I)+B(IK)
  175 DELY(I)=YCAL(I)-Y(I)
  180 SIG2=SIG2+DELY(I)*DELY(I)
      AMK=M-K
      IF(AMK)181,181,182
  181 AMK=1.0
  182 SIGMA=SQRTF(SIG2/AMK)
      S(K) = PXP
      DO 499 I=1,K
  499 ST(I)=SIGMA/SQRTF(S(I))
      DO 501 I=1,K
      SB(I)=0.0
      DO 500 J=1,K
  500 SB(I)=SB(I)+(A(J,I)*ST(J))**2
  501 SB(I)=SQRTF(SB(I))
      KJ = K
  190 CONTINUE
      WRITE OUTPUT TAPE 61,300,L
      DO 183 I=1,KJ
  183 WRITE OUTPUT TAPE 61,304,I,B(I),SB(I)
  195 WRITE OUTPUT TAPE 61,301,SIGMA
  670 WRITE OUTPUT TAPE 61,302,(I,X(I),Y(I),YCAL(I),DELY(I),I=1,M)
  300 FORMAT(51HOCOEFFICIENTS OF Y=B1+B2*X+ETC AND ERRORS FOR ORDER,I3,/
     1)
  301 FORMAT(8HOSIGMA =E16.8)
  302 FORMAT(4HO   I9X,4HX(I)14X,4HY(I)13X,7HYCAL(I)11X,7HDELY(I)//(I4,
     14E18.8))
  304 FORMAT(3X,2HB(I2,2H)=E15.8,5X,5HERRB=E10.3)
      RETURN
      END
```

APPENDIX E

SECOND ORDER CORRECTION (SEC OC)

A. IDENTIFICATION

Title:	Second Order Correction
Category:	Iterative Data Treatment
Programmer:	Jay D. Rynbrandt
Date:	January 1, 1966

B. PURPOSE

Given the chart position of ESR hyperfine absorption peaks, the nuclear spin quantum number of these peaks and the chart position of two frequency markers, calculate the field positions of the peaks, make second order corrections and calculate the g value.

C. USAGE

1. Calling Sequence:

Main program with no subroutines.

2. Arguments:

HA is the array name for the observed magnetic field positions.

S is the array name of the nuclear spin quantum number.

XM is the array name of the chart positions of the peaks.

HO is the array name of the field position calculated in the absence of interaction with nuclear moments.

HOB is the average value of HO.

SHO is the sum of HO.

FL, FH are the low and high field frequency markers.

FK is the klystron frequency.

XL, XH are the low and high field chart positions of the frequency markers.

SI is the nuclear spin.

SPECNO identifies the spectrum.

SL, C are the slope and intercept of the magnetic field as a function of chart position.

N is the number of peaks in a specific spectrum.

A is the hyperfine splitting.

A1, A2, A3 are the hyperfine splitting calculated between different pairs of ESR lines.

G is the g value.

3. Output and Input Formats: See listing.

4. Timing: 0.3 sec per spectra.

5. Accuracy: Consistent results after three iterations.

6. References: H. A. Kuska, Ph. D. dissertation, Michigan State University (1965), Jay D. Rynbrandt, MS dissertation, Michigan State University (1966).

D. METHOD

The magnetic field, HO (I), at which an electronic transition would occur in the absence of interaction with atomic nuclei is

$$HO(I) = HM(I) + A \cdot S(I) + A^2 / (2 \cdot HM(I)) \cdot (SI(SI+1) - S(I)^2) + A^3 / 4 \cdot HM(I)^2 \qquad (13)$$

in which the terms have been previously described. This program calculates the quantity $HO(I) - A \cdot S(I)$ by subtracting the

second and third order contributions from the observed field position. This calculation for various values of $\delta(I)$ can be used to evaluate $HO(I)$ and A. The process is repeated until constant values are obtained. The center of the spectrum, H_o, is taken as the average of values calculated for each peak using Equation (13). Finally the g value is calculated from the expression

$$g = h \cdot FK \; / \; \beta \cdot HOB$$

where h is Planck's constant, FK is the klystron frequency and β the electronic Bohr magneton.

Program SEC OC

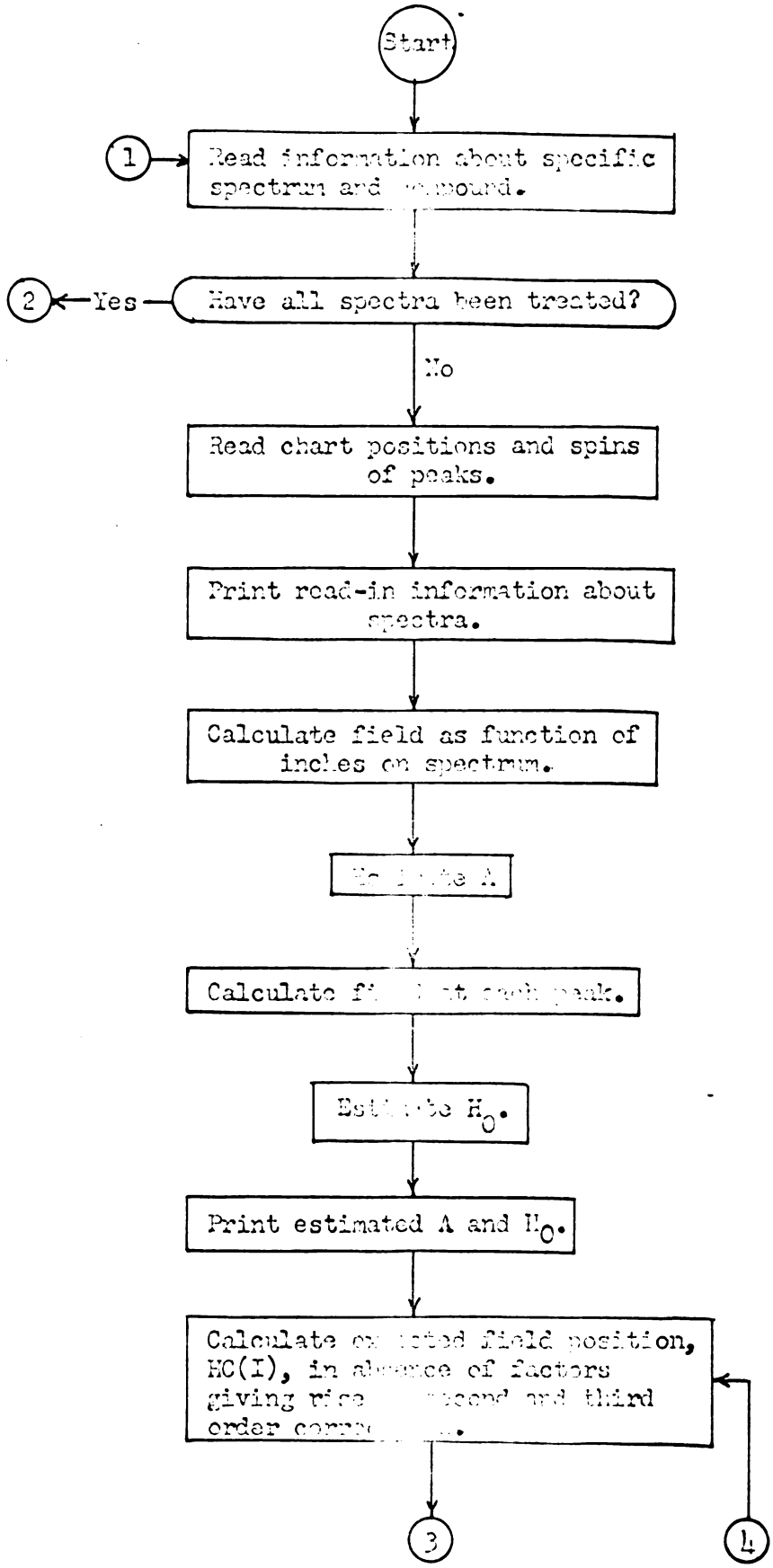

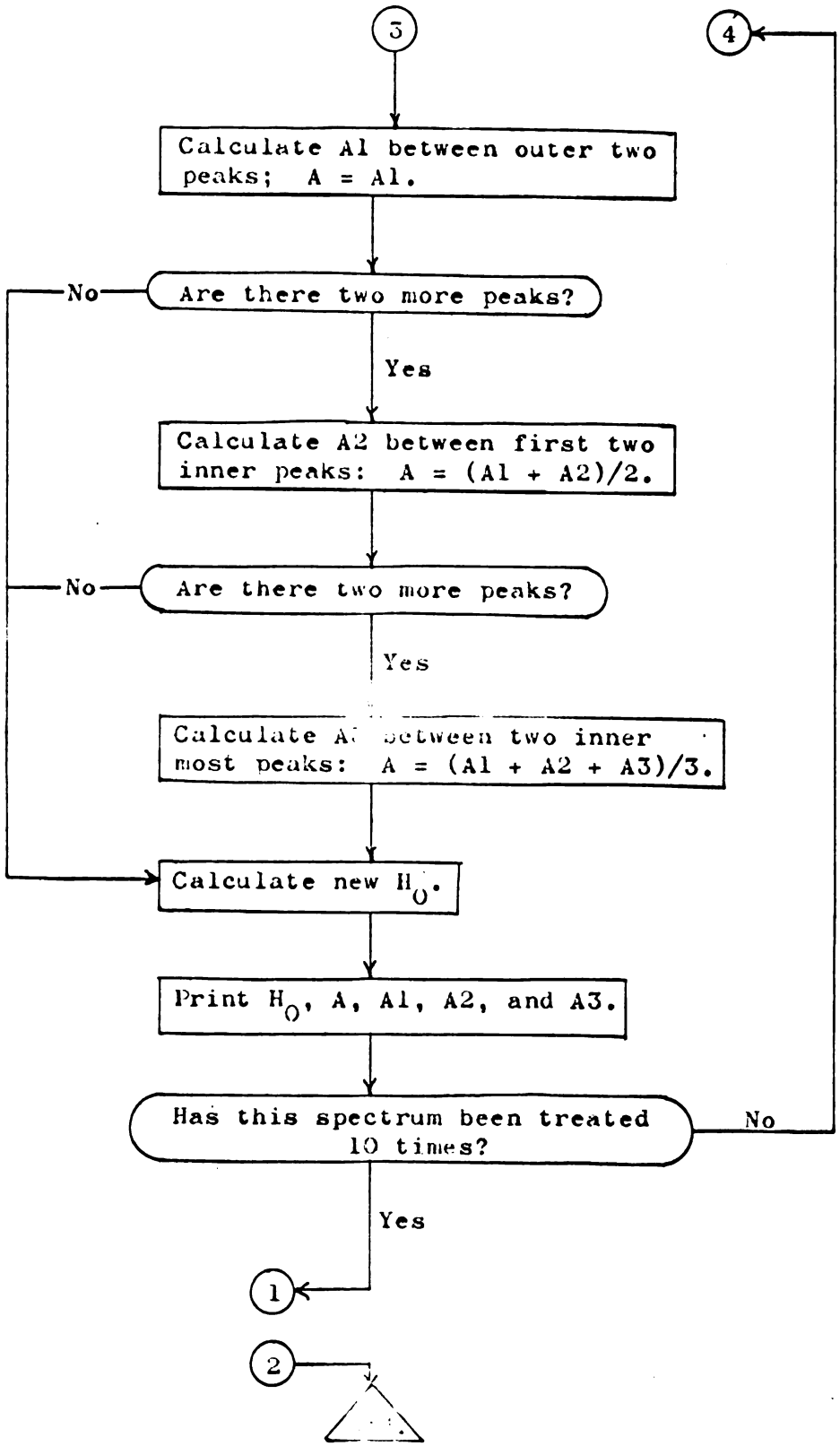
3
4
Calculate A1 between outer two peaks; A = A1.
No
Are there two more peaks?
Yes
Calculate A2 between first two inner peaks: A = (A1 + A2)/2.
No
Are there two more peaks?
Yes
Calculate A3 between two inner most peaks: A = (A1 + A2 + A3)/3.
Calculate new H_0.
Print H_0, A, A1, A2, and A3.
Has this spectrum been treated 10 times?
No
Yes
1
2

```
      PROGRAM SEC O C
      DIMENSION HM(20)• S(20)• HC(20)• XM(20)• HO(20)
    1 FORMAT (* G VALUE    =*F11•6)
    2 FORMAT (6E10•1•I10•A8)
    3 FORMAT (2E10•1)
    4 FORMAT(/*0       HO                A               A1              A2
     1        A3*/)
    5 FORMAT (5F14•7)
    6 FORMAT(/*0     SPIN     X VAL         H OBS          H CALC*/)
    7 FORMAT (2F9•2•2F14•6)
    8 FORMAT (*1                        DATA OF SPECTRUM NO• *•A8)
    9 FORMAT (*0SLOPE      =*F11•5/* INTERCEPT = *F10•3)
   50 FORMAT (3F12•4•3F9•3•I6)
   51 FORMAT(/*0     FREQ H       FREQ L       FREQ K   X VAL L   X VAL H
     1 SPIN    PEAKS*/)
   22 CONTINUE
      READ    2•FL•FH•FK•XL•XH•SI•    N•SPECNO
      IF   (FL) 20•20•21
   21 CONTINUE
      READ 3• (XM(I)•S(I)•I = 1•N)
      PRINT 8• SPECNO
      PRINT 51
      PRINT 50•FL•FH•FK•XL•XH•SI•    N
      PRINT 4
      A1=0•0 $ A2=0•0 $ A3=0•0
      BL = 2•3486855*FL
      BH = 2•3486855*FH
      SL = (BH-BL)/(XH-XL)
      C = BH -SL*XH
      A = SL*(XM(N)-XM(1))/(S(1)-S(N))
      A = ABSF(A)
      SHO = 0•0
      DO 10 I = 1•N
      HM(I) =SL*XM(I) + C
      HO(I) = HM(I) + S(I)*A
      SHO = SHO + HO(I)
   10 CONTINUE
      HOB = SHO / N
      A1 = A
      PRINT 5• HOB•A•A1•A2•A3
```

```
      DO 19 KB = 1.10
      DO 12 I = 1.N
      HC(I) = HM(I) + A**2/(2.0*HM(I))*(SI*(SI+1.0)-S(I)**2)  +A**3/(4*
     1          HM(I)**2)
   12 CONTINUE
      A1 = (HC(N) - HC(1))/(S(1) - S (N))
      A1 = ABSF(A1)
      A = A1
      IF  (N.GT.3) 13.15
   13 CONTINUE
      J = N - 1
      A2 = (HC(J) - HC(2))/(S(2) - S (J))
      A2 = ABSF(A2)
      A = (A1 + A2)/2.0
      IF  (N.GT.5) 14.15
   14 CONTINUE
      J = N - 2
      A3 = (HC(J) - HC(3))/(S(3) - S (J))
      A3 = ABSF(A3)
      A = (A1 + A2 + A3)/3.0
   15 CONTINUE
      SHO = 0.0
      DO 11 I = 1.N
      HO(I) = HM(I) + (A*S(I) + A**2/(2.0*HM(I))*(SI*(SI+1.0) -S(I)**2)
     1          + A**3/( 4.0*HM(I)**2))
      SHO = SHO + HO(I)
   11 CONTINUE
      HOB= SHO / N
      PRINT 5. HOB.A.A1.A2.A3
   19 CONTINUE
      PRINT 6
      DO 17 I = 1.N
      PRINT 7. S(I). XM(I). HM(I). HC(I)
   17 CONTINUE
      G = 0.714489*FK/HOB
      PRINT 9. SL.C
      PRINT 1. G
      GO TO 22
   20 CONTINUE
      END
'RUN.1.2000..M
```

APPENDIX F

LEAST SQUARES SPECTRA SYNTHESIZING (M ESR)

A. IDENTIFICATION

Title:	Least Squares Spectra Synthesizing
Category:	Curve Fitting
Programmer:	Jay D. Rynbrandt
Date:	August 1, 1965

B. PURPOSE

Adjust a set of parameters to synthesizing ESR spectra.

(Note: Program IR FIT uses this same method and is more general. This listing is presented for the sake of completeness.)

```
      PROGRAM K FSR
C   SAMPLE 5    TEMP. -41    SPLIT 4.82    LINE WD .603  CEN 9.75    CARDS 39
      COMMON  X,Y,JA,KA,A,B,T,AR,TR,AVX,AVY,AVXR,C,H,TRYS,P,PI,PIS,
     1 C2,C3,C4,C5,SW,TRIALS,TI,JB,CT,CB,CX,DT,DX
      DIMENSION X(9,100),Y(7,100)
    1 FORMAT  (2(F10.0))
      READ 1, ( X(1,I), Y(1,I), I = JA,KA)
      C = 1.0
      B = 4.71
      WL = 0.43
      AVX = 9.73
      AVXR = 9.8
      JA = 1
      KA = 39
      SUM Y = 0.0
      XJ = JA
      XK = KA
      TI = XK - XJ + 1.0
      DO 30 I = JA,KA
      SUM Y = SUM Y + Y(1,I)
      Y( 3,I) = 0.0
   30 CONTINUE
      AVY  = SUM Y/ TI
      A = C
      AR = C
      AVXR = AVX
      C2 = - 1.0/2.0
      C3 = - 1.0/6.0
      C4 = + 1.0/6.0
      C5 = + 1.0/2.0
      T = 1.0 /(1.414214*WL)
      TR = 0.39
      PI = 3.1415926536
      PIS = (2.0*PI)**2
      JB = 4
      TRYS = 20.0
      CB =-10.0
      CT = 10.0
```

```
      CALL SEP4
      CALL WDTH4
      CB = 1.0
      CT = 1.0
      CX = 1.0
      CALL SEP4
      CALL WDTH4
      CALL CEN4
      DT = 10.0
      CALL WDTHEX
      DT = 1.0
      CALL WDTHEX
      DX = 1.0
      CALL CENEX
      CB = 2.0
      CT = 2.0
      CALL SEP4
      CALL WDTH4
      CALL CEN4
      DT = 2.0
      DO 7 LA = 1,6
      CALL WDTHEX
      CALL SEP4
      CALL WDTH4
      CALL WDTHEX
      CALL SEP4
      CALL WDTH4
      CALL WDTHEX
      CALL CENEX
      CALL SEP4
      CALL WDTH4
      CALL CEN4
    7 CONTINUE
      CALL WDTHEX
      CALL CENEX
      CALL SEP4
      CALL WDTH4
      CALL CEN4
      CALL PRINT4
      CALL WDTHEX
      CALL CENEX
      CALL PRINT1
      END
```

```
      SUBROUTINE WDTH4
      COMMON  X,Y,JA,KA,A,B,T,AR,TR,AVX,AVY,AVXR,C,H,TRYS,P,PI,PIS,
     1 C2,C3,C4,C5,SW,TRIALS,TI,JB,CT,CB,CX,DT,DX
      DIMENSION X(9,100),Y(7,100)
    5 FORMAT ( 9(F11.5))
    6 FORMAT (////*        T            A           ST            B           WL
     1         RI        TRIALS       TRYS          C */)
      PRINT 6
      TRIALS = 0.0
      ST = 9999999999.9
      DO 14 I = JA,KA
      X(2,I) = AVX + B*C2 - X(1,I)
      X(3,I) = AVX + B*C3 - X(1,I)
      X(4,I) = AVX + B*C4 - X(1,I)
      X(5,I) = AVX + B*C5 - X(1,I)
      X(6,I) = AVX +BI*C2 - X(1,I)
      X(7,I) = AVX +BI*C3 - X(1,I)
      X(8,I) = AVX +BI*C4 - X(1,I)
      X(9,I) = AVX +BI*C5 - X(1,I)
   14 CONTINUE
      DO 25 NT = 1,2
   26 CONTINUE
      STO = ST
      AB = A
      A = C
      BI = B * (9.07477 / 16.53766)
      H = A * (0.0691 / 0.9308)
      SA = 0.0
      V = C
      DO 31 I = JA,KA
      Y2 = -A*X(2,I)*EXPF(-(T*X(2,I))**2)
      Y3 = -A*X(3,I)*EXPF(-(T*X(3,I))**2)
      Y4 = -A*X(4,I)*EXPF(-(T*X(4,I))**2)
      Y5 = -A*X(5,I)*EXPF(-(T*X(5,I))**2)
      Y6 = -H*X(6,I)*EXPF(-(T*X(6,I))**2)
      Y7 = -H*X(7,I)*EXPF(-(T*X(7,I))**2)
      Y8 = -H*X(8,I)*EXPF(-(T*X(8,I))**2)
      Y9 = -H*X(9,I)*EXPF(-(T*X(9,I))**2)
      Y(4,I) = Y2+Y3+Y4+Y5+Y6+Y7+Y8+Y9
      Y(7,I) = Y(1,I) - Y(4,I) - AVY - Y(3,I)
      SQ = Y(7,I)**2
      SA = SA + SQ
   31 CONTINUE
```

```
      DO 18 MD = 1,JB
   27 CONTINUE
      SAO = SA
      SA = 0.0
      AA = A + V
      AC = AA/A
      A = AA
      DO 13 I = JA,KA
      Y(4,I) = Y(4,I)*AC
      Y(2,I) = Y(1,I) - Y(4,I) - AVY
      Y(7,I) = Y(1,I) - Y(4,I) - AVY - Y(3,I)
      SQ = Y(7,I)**2
      SA = SA + SQ
   13 CONTINUE
      IF (SA  - SAO ) 27,34,34
   34 CONTINUE
      V =-V*0.1
   18 CONTINUE
      ST = SAO
      TRIALS = TRIALS + 1.0
      IF (TRIALS - TRYS) 2,2,3
    2 CONTINUE
      RI = (A*4.0*1.7724539) * (1.0 + 0.0691/0.9308) / (2.0*T**3)
      WL = 1.0 / (1.414214*T)
      PRINT 5, T, A, ST , B, WL, RI, TRIALS, TRYS, CT
      IF (ST  - STO ) 23,24,24
   23 CONTINUE
      T = T + CT*0.01
      GO TO 26
   24 CONTINUE
      CT = -CT
      T = T + CT*0.01
   25 CONTINUE
      A = AB + V*10.0
    3 CONTINUE
      CT = TRIALS * CT/ 10.0
      PRINT 5, T, A, ST,  B, WL, RI, TRIALS, TRYS, CT
      RETURN
      END
```

```
      SUBROUTINE SEP4
      COMMON  X,Y,JA,KA,A,B,T,AR,TR,AVX,AVY,AVXR,C,H,TRYS,P,PI,PIS,
     1 C2,C3,C4,C5,SW,TRIALS,TI,JB,CT,CB,CX,DT,DX
      DIMENSION X(9,100),Y(7,100)
    5 FORMAT ( 9(F11.5))
    6 FORMAT (////*        B            A           ST            T           WL
     1         RI         TRIALS       TRYS          C */)
      PRINT 6
      TRIALS = 0.0
      SB = 9999999999.9
      DO 45 NB = 1,2
   47 CONTINUE
      SBO = SB
      AB = A
      A = C
      BI = B * (9.07477 / 16.53766)
      H = A * (0.0691 / 0.9308)
      SA = 0.0
      V = C
      DO 49 I = JA,KA
      X(2,I) = AVX + B*C2 - X(1,I)
      X(3,I) = AVX + B*C3 - X(1,I)
      X(4,I) = AVX + B*C4 - X(1,I)
      X(5,I) = AVX + B*C5 - X(1,I)
      X(6,I) = AVX +BI*C2 - X(1,I)
      X(7,I) = AVX +BI*C3 - X(1,I)
      X(8,I) = AVX +BI*C4 - X(1,I)
      X(9,I) = AVX +BI*C5 - X(1,I)
      Y2 = -A*X(2,I)*EXPF(-(T*X(2,I))**2)
      Y3 = -A*X(3,I)*EXPF(-(T*X(3,I))**2)
      Y4 = -A*X(4,I)*EXPF(-(T*X(4,I))**2)
      Y5 = -A*X(5,I)*EXPF(-(T*X(5,I))**2)
      Y6 = -H*X(6,I)*EXPF(-(T*X(6,I))**2)
      Y7 = -H*X(7,I)*EXPF(-(T*X(7,I))**2)
      Y8 = -H*X(8,I)*EXPF(-(T*X(8,I))**2)
      Y9 = -H*X(9,I)*EXPF(-(T*X(9,I))**2)
      Y(4,I) = Y2+Y3+Y4+Y5+Y6+Y7+Y8+Y9
      Y(7,I) = Y(1,I) - Y(4,I) - AVY - Y(3,I)
      SQ = Y(7,I)**2
      SA = SA + SQ
   49 CONTINUE
```

```
      DO 48 MD = 1,JB
   29 CONTINUE
      SAO = SA
      SA = 0.0
      AA = A + V
      AC = AA/A
      A = AA
      DO 57 I = JA,KA
      Y(4,I) = Y(4,I)*AC
      Y(2,I) = Y(1,I) - Y(4,I) - AVY
      Y(7,I) = Y(1,I) - Y(4,I) - AVY - Y(3,I)
      SQ = Y(7,I)**2
      SA = SA + SQ
   57 CONTINUE
      IF (SA  - SAO ) 29,58,58
   58 CONTINUE
      V =-V*0.1
   48 CONTINUE
      SB = SAO
      TRIALS = TRIALS + 1.0
      IF (TRIALS - TRYS) 2,2,3
    2 CONTINUE
      RI = (A*4.0*1.7724539) * (1.0 + 0.0691/0.9308) / (2.0*T**3)
      WL = 1.0 / (1.414214*T)
      PRINT 5, B, A, SB , T, WL, RI, TRIALS, TRYS, CB
      IF (SB  - SBO ) 43,44,44
   43 CONTINUE
      B = B + CB*0.01
      GO TO 47
   44 CONTINUE
      CB = -CB
      B = B + CB*0.01
   45 CONTINUE
      A = AB + V*10.0
    3 CONTINUE
      CB = TRIALS * CB/ 10.0
      PRINT 5, B, A, SB,  T, WL, RI, TRIALS, TRYS, CB
      RETURN
      END
```

```
      SUBROUTINE CEN4
      COMMON  X,Y,JA,KA,A,B,T,AR,TR,AVX,AVY,AVXR,C,H,TRYS,P,PI,PIS,
     1 C2,C3,C4,C5,SW,TRIALS,TI,JB,CT,CB,CX,DT,DX
      DIMENSION X(9,100),Y(7,100)
    4 FORMAT (*0AVY = *F9.6)
    5 FORMAT (10(F11.5))
    7 FORMAT(////*       AVX            T            B            A            SX
     1         WL            RI          TRYS       TRIALS         C*/)
      PRINT 7
      TRIALS = 0.0
      BI = B * (9.07477 / 16.53766)
      H = A * (0.0691 / 0.9308)
      SX = 9999999999.9
      DO 55 NX = 1,2
   66 CONTINUE
      SXO = SX
      SUMDY = 0.0
      SW = 0.0
      SX = 0.0
      DO 51 I = JA,KA
      X(2,I) = AVX + B*C2 - X(1,I)
      X(3,I) = AVX + B*C3 - X(1,I)
      X(4,I) = AVX + B*C4 - X(1,I)
      X(5,I) = AVX + B*C5 - X(1,I)
      X(6,I) = AVX +BI*C2 - X(1,I)
      X(7,I) = AVX +BI*C3 - X(1,I)
      X(8,I) = AVX +BI*C4 - X(1,I)
      X(9,I) = AVX +BI*C5 - X(1,I)
      Y2 = -A*X(2,I)*EXPF(-(T*X(2,I))**2)
      Y3 = -A*X(3,I)*EXPF(-(T*X(3,I))**2)
      Y4 = -A*X(4,I)*EXPF(-(T*X(4,I))**2)
      Y5 = -A*X(5,I)*EXPF(-(T*X(5,I))**2)
      Y6 = -H*X(6,I)*EXPF(-(T*X(6,I))**2)
      Y7 = -H*X(7,I)*EXPF(-(T*X(7,I))**2)
      Y8 = -H*X(8,I)*EXPF(-(T*X(8,I))**2)
      Y9 = -H*X(9,I)*EXPF(-(T*X(9,I))**2)
      Y(4,I) = Y2+Y3+Y4+Y5+Y6+Y7+Y8+Y9
      Y(2,I) = Y(1,I) - Y(4,I) - AVY
      Y(7,I) = Y(1,I) - Y(4,I) - AVY - Y(3,I)
      SQ = Y(7,I)**2
      SUMDY = SUMDY + Y(7,I)
      Y(5,I) = Y(4,I) + AVY
      Y(2,I) = Y(1,I) - Y(5,I)
      SQW = Y(2,I)**2
      SX = SX + SQ
      SW = SW + SQW
   51 CONTINUE
      AVY = AVY + SUMDY/TI
```

```
      RI = (A*4.0*1.7724539) * (1.0 + 0.0691/0.9308) / (2.0*T**3)
      WL = 1.0 / (1.414214*T)
      PRINT 5, AVX, T, B, A, SX,  WL, RI, TRYS, TRIALS, CX
      TRIALS = TRIALS + 1.0
      IF (TRIALS - TRYS) 2,2,3
    2 CONTINUE
      IF (SX  - SXO ) 53,54,54
   53 CONTINUE
      AVX = AVX + CX*0.001
      GO TO 66
   54 CONTINUE
      CX = -CX
      AVX = AVX + CX*0.001
   55 CONTINUE
    3 CONTINUE
      CX = TRIALS * CX/ 10.0
      PRINT 5, AVX, T, B, A, SXO, WL, RI, TRYS, TRIALS, CX
      PRINT 4, AVY
      RETURN
      END
```

```
      SUBROUTINE WDTHEX
      COMMON  X,Y,JA,KA,A,B,T,AR,TR,AVX,AVY,AVXR,C,H,TRYS,P,PI,PIS,
     1 C2,C3,C4,C5,SW,TRIALS,TI,JB,CT,CB,CX,DT,DX
      DIMENSION X(9,100),Y(7,100)
    5 FORMAT ( 9(F11.5))
    6 FORMAT (////*       TR           AR           STR         AVXR          WLR
     1         RIR       TRIALS       TRYS          C*/)
      PRINT 6
      TRIALS = 0.0
      STR= 9999999999.9
      DO 15 I = JA,KA
      X(6,I) = AVXR - X(1,I)
   15 CONTINUE
      DO  65 NTR = 1,2
   70 CONTINUE
      STOR = STR
      ABR = AR
      AR = C
      SAR= 0.0
      V = C
      DO 71 I = JA,KA
      Y(3,I) = -AR*X(6,I)*EXPF(-(TR*X(6,I))**2)
      Y(7,I) = Y(2,I) - Y(3,I)
      SQ = Y(7,I)**2
      SAR= SAR+ SQ
   71 CONTINUE
      DO 73 KK= 1,JB
   75 CONTINUE
      SAOR = SAR
      SAR = 0.0
      AA = AR + V
      AC = AA / AR
      AR= AA
      DO 16 I = JA,KA
      Y(3,I) = AC * Y(3,I)
      Y(7,I) = Y(2,I) - Y(3,I)
      SQ = Y(7,I)**2
      SAR = SAR + SQ
   16 CONTINUE
```

```
      IF (SAR - SAOR) 75,74,74
   74 CONTINUE
      V =-V*0.1
   73 CONTINUE
      STR = SAOR
      RIR = AR*1.7724539 / (2.0*TR**3)
      WLR= 1.0 / (1.414214*TR)
      PRINT 5, TR, AR, STR, AVXR, WLR, RIR, TRIALS, TRYS,DT
      TRIALS = TRIALS + 1.0
      IF (TRIALS - TRYS) 2,2,3
    2 CONTINUE
      IF (STR - STOR) 63,64,64
   63 CONTINUE
      TR = TR + DT*0.01
      GO TO 70
   64 CONTINUE
      DT = -DT
      TR = TR + DT*0.01
   65 CONTINUE
      AR = ABR + V*10.0
    3 CONTINUE
      DT = TRIALS * DT/ 12.0
      PRINT 5, TR, AR, STOR,AVXR, WLR, RIR, TRIALS, TRYS,DT
      RETURN
      END
```

```
      SUBROUTINE CENEX
      COMMON  X,Y,JA,KA,A,B,T,AR,TR,AVX,AVY,AVXR,C,H,TRYS,P=PI,PIS,
     1 C2,C3,C4,C5,SW,TRIALS,TI,JB,CT,CB,CX,DT,DX
      DIMENSION X(9,100),Y(7,100)
    5 FORMAT (10(F11.5))
    6 FORMAT (////*      AVXR          AR           STR          TR           WLR
     1         RIR       TRIALS       TRYS          C*/)
      PRINT 6
      TRIALS = 0.0
      SXR= 9999999999.9
      DO 85  NXR = 1,2
   80 CONTINUE
      SXOR = SXR
      SXR = 0.0
      DO 81 I = JA,KA
      X(6,I) = AVXR - X(1,I)
      Y(3,I) = -AR*X(6,I)*EXPF(-(TR*X(6,I))**2)
      Y(7,I) = Y(2,I) - Y(3,I)
      SQ = Y(7,I)**2
      SXR= SXR+ SQ
   81 CONTINUE
      RIR = AR*1.7724539 / (2.0*TR**3)
      WLR= 1.0 / (1.414214*TR)
      PRINT 5,AVXR, AR, SXR, TR, WLR, RIR, TRIALS, TRYS, DX
      TRIALS = TRIALS + 1.0
      IF (TRIALS - TRYS) 2,2,3
    2 CONTINUE
      IF (SXR - SXOR) 83,84,84
   83 CONTINUE
      AVXR = AVXR + DX*0.001
      GO TO 80
   84 CONTINUE
      DX = -DX
      AVXR = AVXR + DX*0.001
   85 CONTINUE
    3 CONTINUE
      DX = TRIALS * DX/ 10.0
      PRINT 5,AVXR, AR, SXOR,TR, WLR, RIR, TRIALS, TRYS,DX
      RETURN
      END
```

```
      SUBROUTINE PRINT4
      COMMON  X,Y,JA,KA,A,B,T,AR,TR,AVX,AVY,AVXR,C,H,TRYS,P,PI,PIS,
     1 C2,C3,C4,C5,SW,TRIALS,TI,JB,CT,CB,CX,DT,DX
      DIMENSION X(9,100),Y(7,100)
    6 FORMAT (*0  X AXIS     5 LINE       OBS SP       4 LINE         RES*/)
    9 FORMAT  (5F12.6)
      PRINT 6
      DO 10 I = JA,KA
      Y(6,I) = Y(4,I) + Y(3,I)
      PRINT 9, X(1,I),                Y(6,I), Y(1,I),  Y(5,I), Y(7,I)
   10 CONTINUE
      RETURN
      END




      SUBROUTINE PRINT1
      COMMON  X,Y,JA,KA,A,B,T,AR,TR,AVX,AVY,AVXR,C,H,TRYS,P,PI,PIS,
     1 C2,C3,C4,C5,SW,TRIALS,TI,JB,CT,CB,CX,DT,DX
      DIMENSION X(9,100),Y(7,100)
    4 FORMAT  (4F12.6)
    8 FORMAT (  *0  X AXIS      CALC EX PK  DIFF EX PK       RES*/)
      PRINT 8
      DO 91 I = JA,KA
      PRINT 4, X(1,I),Y(3,I),Y(2,I), Y(7,I)
   91 CONTINUE
      RETURN
      END
```

APPENDIX G

VARIABLE-TEMPERATURE SPECTROPHOTOMETER

1. Figures.
   a. Temperature-controlled cell compartment (Figure 12).
   b. Coolant delivery system (Figure 13).
   c. Cell holder (Figure 14).
2. Notes.
   a. Housing of cell compartment constructed of 1/4" aluminum (Figure 12).
   b. Polyurethane foam used as insulation.
   c. Aluminum cylinder supporting Dewar connected to housing by a threaded ring which presses against a shoulder at the end of the cylinder (Figure 12).
   d. Plexiglas used for light tubes and cell compartment (Figure 13).
   e. Quartz windows used in light tubes (Figure 13).
   f. Teflon washers used to prevent glass from touching metal.
   g. Teflon gaskets used to seal the Dewar to the glass T and to seal quartz flats to light tubes (Figure 13).
   h. Lower section of cell holder can be replaced with unit to hold standard 1 cm optical cells (Figure 14).
   i. Point, groove and plane locating system used for all componets of spectrophotometer requiring alignment.

j. A polyurethane plug with a thermocouple seals the bottoms of cell compartments (Figure 13).

h. Nitrogen blown through light tubes to prevent frosting of the windows (Figure 13).

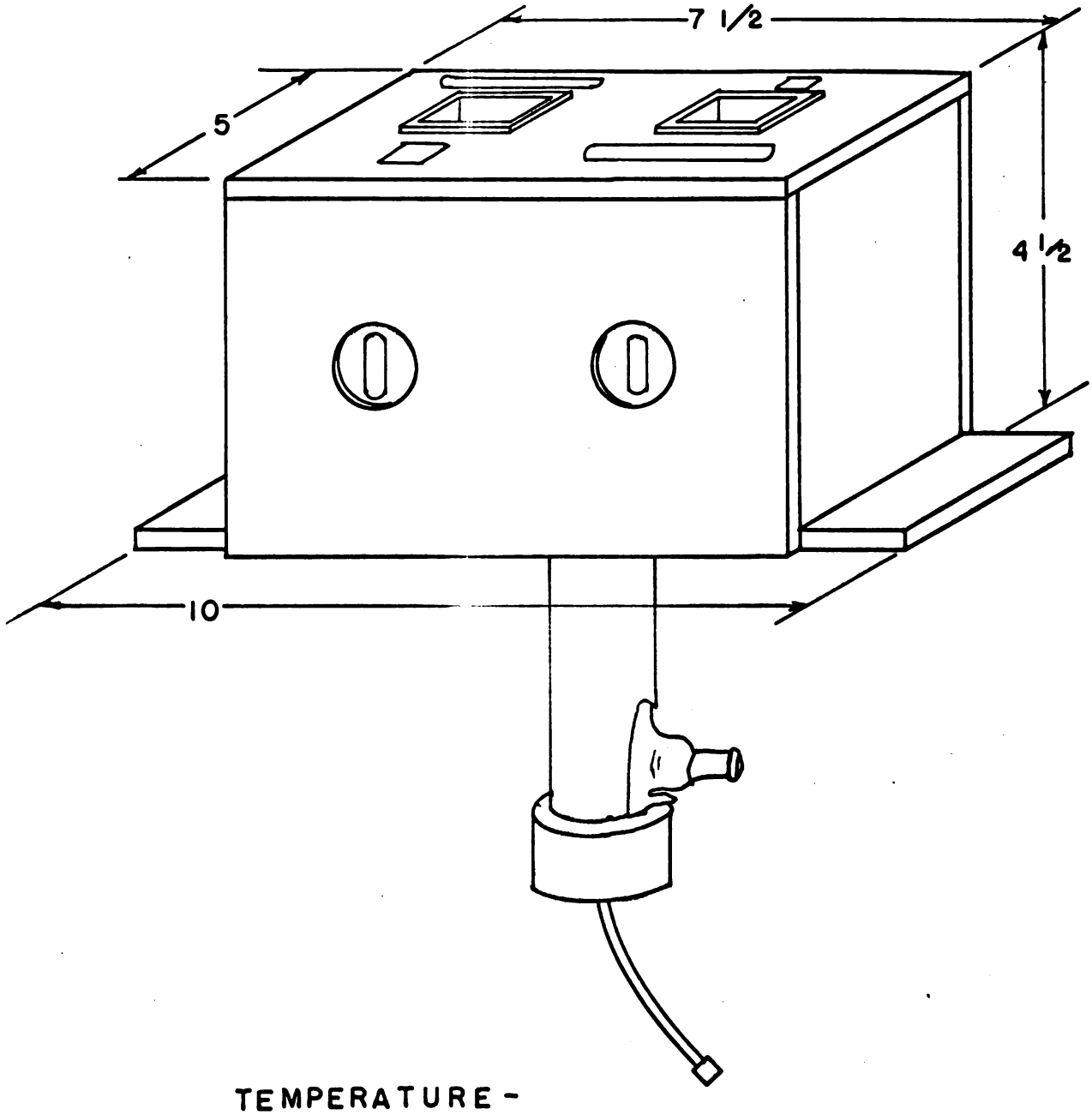

TEMPERATURE-
CONTROLLED
CELL COMPARTMENT

Figure 12.

COOLANT DELIVERY SYSTEM

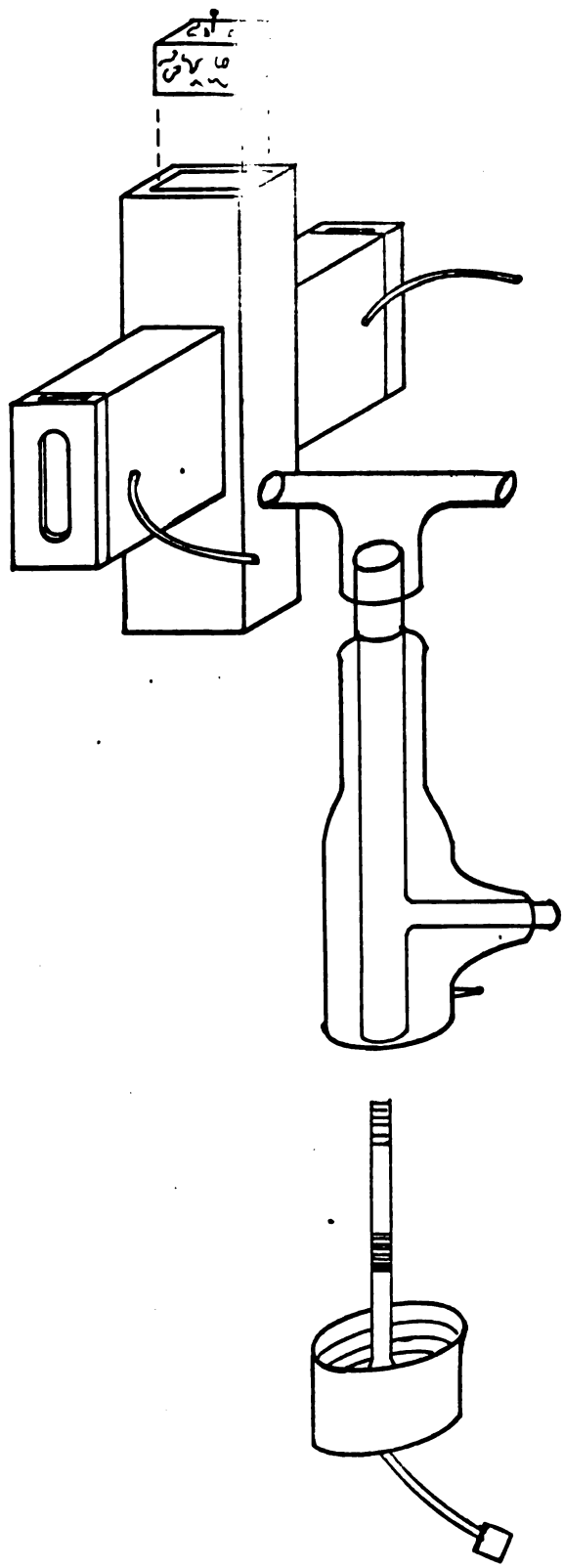

1"

Figure 13.

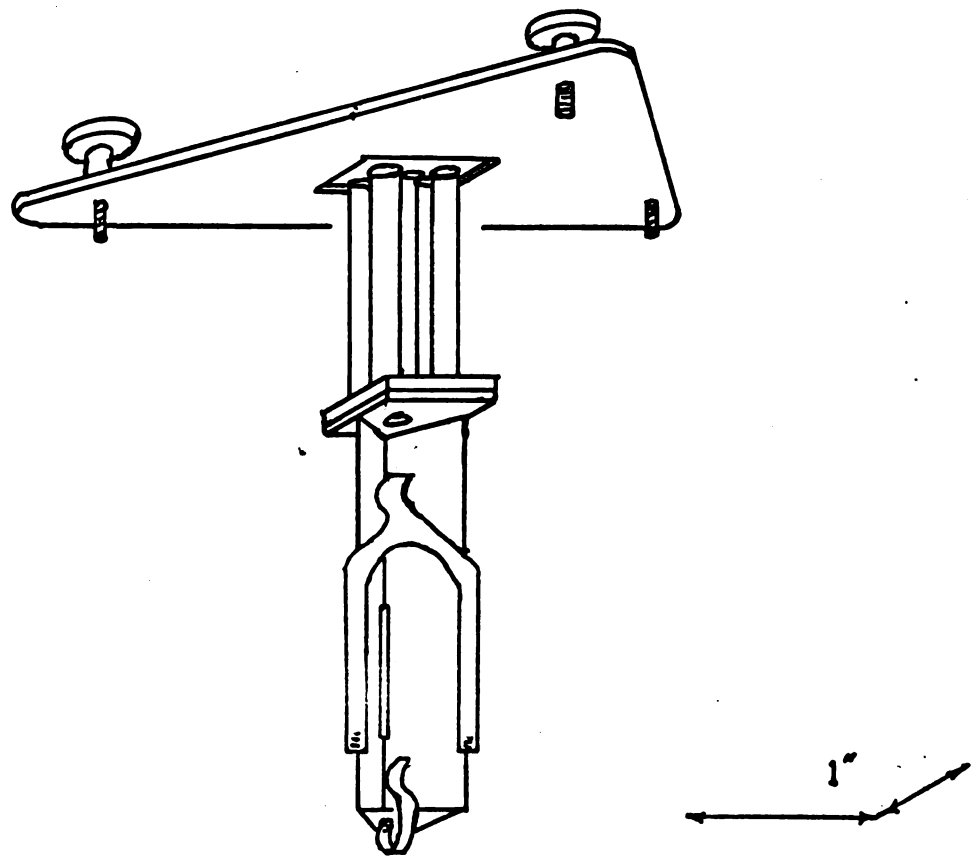

CELL HOLDER

Figure 14.